



UNIVERSIDAD DE  
SALAMANCA  
FACULTAD DE  
MEDICINA  
Departamento de Cirugía

**TESIS DOCTORAL**

Director: Dr. D. Alberto Albaladejo Martínez.

**ESTUDIO *IN VITRO* DEL EFECTO  
DE EMPLEO DEL LÁSER DE  
FEMTOSEGUNDO Y EL CICLADO  
MECÁNICO EN LA EFICACIA  
ADHESIVA DE LA INTERFASE  
CIRCONIO-RESINA.**

*Effect of femtosecond laser irradiation and  
cyclic loading on adhesive effectiveness of  
zirconia-resin interface:  
an in vitro study.*

**María Vicente Prieto  
Salamanca, 2016**



El Dr. D. FRANCISCO LOZANO SÁNCHEZ,

Director del Departamento de Cirugía de la Universidad de Salamanca,

**CERTIFICA:**

Que la presente Memoria, elaborada por **D<sup>a</sup> María Vicente Prieto** para optar a la Tesis Doctoral, con el título “Estudio *in vitro* del efecto del empleo del láser de femtosegundo y el ciclado mecánico en la eficacia adhesiva de la interfase circonio-resina”, ha sido realizada bajo la dirección **del Dr. D. Alberto Albaladejo Martínez** en el Departamento de Cirugía de la Universidad de Salamanca.

Y para que así conste, expide y firma la presente certificación en Salamanca a 23 de noviembre de 2015.

Fdo.: Dr. D. Francisco Lozano Sánchez



El profesor Dr. D. ALBERTO ALBALADEJO MARTINEZ,

Doctor del Departamento de Cirugía de la Universidad de Salamanca,

**CERTIFICA:**

Que el presente trabajo titulado “Estudio *in vitro* del efecto del empleo del láser de femtosegundo y el ciclado mecánico en la eficacia adhesiva de la interfase circonio-resina”, ha sido realizado bajo su dirección en el Departamento de Cirugía por la licenciada en Odontología **D<sup>a</sup> María Vicente Prieto** para optar a la tesis doctoral. Habiéndose concluido y reuniendo, a su juicio, las condiciones de originalidad y rigor científico necesarias, autorizan su presentación a fin de que pueda ser defendido ante el tribunal correspondiente.

Y para que así conste, expide y firma la presente certificación en Salamanca, a 23 de noviembre de 2015.

Fdo. Dr. D. Alberto Albaladejo Martínez



## Agradecimientos

La realización de esta tesis doctoral nunca hubiera sido posible sin la colaboración de todas aquellas personas que nunca han dudado en prestarme su ayuda de forma desinteresada, y a las que se lo quiero agradecer muy sinceramente:

A Dr. D. Alberto Albaladejo, por aceptar asumir la dirección de este trabajo siempre prestando sus más que necesarias orientaciones para la elaboración de este trabajo y su constante ánimo.

A la Dra. Dña. Ana Caseiro, por su incondicional ayuda en todo momento. Gracias por tener paciencia conmigo explicándome en qué consistía y como se realizaba cada tratamiento de superficie del circonio y cómo era el funcionamiento de cada una de las máquinas de la Clínica Odontológica de la Facultad de Medicina necesarias para el procesado y tratamiento de las muestras; así como por sus imprescindibles directrices y correcciones a la hora de elaborar los artículos.

Al D. Raúl Montero, por encargarse de la irradiación de las muestras de circonio con el láser de femtosegundo y por prestarme su ayuda en cualquier duda al respecto de cómo actúa el mismo.

Al Centro de Láseres Pulsados (CLPU), por la realización de las imágenes de microscopía electrónica de barrido.

A Dña. Marta Ortiz por acompañarme siempre a la obtención de las imágenes de microscopía garantizando siempre que tuvieran la mayor calidad posible, y sobre todo por estar a estar a mi disposición cada vez que lo necesitaba adaptándose a mis horarios y dándome ánimos para seguir adelante.

Al Dr. D. Javier Montero, por el asesoramiento en el análisis estadístico de los datos.

A mi hermana por hacerme de traductora en todo momento y ayudarme en la redacción de la tesis en inglés.

Y por supuesto, a toda mi familia y amigos, porque siempre han confiado en mí, en mi capacidad de trabajo y mi constancia para sacar las cosas adelante, y por hacerme todo este tiempo más llevadero al despejar de mi cabeza todas mis dudas, agobios y preocupaciones dandome su alegría y fuerza para seguir adelante.



# Contents

<b>TABLES .....</b>	14
<b>FIGURES .....</b>	16
<b>ACRONYMS .....</b>	19
<b>ABSTRACT .....</b>	22
<b>RESUMEN .....</b>	29
<b>I. INTRODUCTION .....</b>	37
<b>I.1Dental ceramics .....</b>	38
<i>I.1.1. Dental ceramics history .....</i>	39
<i>I.1.2. Dental ceramics properties .....</i>	42
<i>I.1.3 Dental ceramics classification .....</i>	42
<i>I.1.3.1 Chemical content .....</i>	43
<i>I.1.3.2 Processing method .....</i>	44
<i>I.1.3.3 Sintering temperature .....</i>	48
<i>I.1.3.4 Crystalline content .....</i>	50
<i>I.1.4 Zirconia ceramics .....</i>	53
<b>I.2 Adhesion in dental ceramics .....</b>	60
<i>I.2.1 Classical dental ceramics adhesion .....</i>	61

<b>I.2.2 Crystalline dental ceramics adhesion .....</b>	62
I.2.2.1 Luting cements mostly used with zirconia ceramics .....	62
<b>I.3 Surface conditioning to improve resin/zirconia adhesion.....</b>	64
I.3.1 <i>Grinding</i> .....	64
I.3.2 <i>Pyrochemical silica coating</i> .....	65
I.3.3 <i>Tribochemical silica coating</i> .....	66
I.3.4 <i>Selective Infiltration Etching (SIE)</i> .....	67
I.3.5 <i>Laser treatment</i> .....	68
<b>I.4 Femtosecond laser irradiation as treatment surface .....</b>	75
I.4.1 <i>Definition of laser and its introduction in dentistry ....</i>	75
I.4.2 <i>Parameters and classification of laser.....</i>	77
I.4.3 <i>Ultrashort lasers: femtosecond laser.....</i>	80
I.4.4 <i>Ti:Sapphire laser .....</i>	85
I.4.5 <i>Components of Ti:Sapphire laser .....</i>	88
I.4.6 <i>Ti:Sapphire laser applications .....</i>	90
<b>I.5 In vitro simulation oral conditions .....</b>	96
I.5.1 <i>Chemical complexity of oral environment .....</i>	96
I.5.2 <i>Mechanical complexity of oral environment .....</i>	97
I.5.2.1 Fatigue and fatigue crack growth .....	97
I.5.3 <i>Interfacial degradation by artificial aging .....</i>	98

I.5.3.1 Chemical degradation .....	98
I.5.3.2 Thermal degradation .....	99
I.5.3.3 Mechanical degradation .....	101
<b>I.6 Adhesive strength mechanical assay and microestrutural evaluation .....</b>	<b>106</b>
<b>II. OBJECTIVES AND JUSTIFICATION .....</b>	<b>110</b>
<b>III. MATERIAL AND METHODS .....</b>	<b>114</b>
<b>III.1 Preparation of zirconia samples .....</b>	<b>115</b>
<b>III.2 Experimental groups .....</b>	<b>117</b>
<i>III.2.1 Group 1: Control- No treatment (NT) .....</i>	118
<i>III.2.2 Group 2: Airborne particle abrasion with 25-<math>\mu</math>m alumina particles (APA 25) .....</i>	118
<i>III.2.3 Group 3: Tribocochemical silica coating (TSC) .....</i>	118
<i>III.2.4 Group 4: Femtosecond laser irradiation at step 20 (FS20) .....</i>	118
<i>III.2.5 Group 5: Femtosecond laser irradiation at step 40 (FS40) .....</i>	119
<b>III.3 Bonding procedure.....</b>	<b>119</b>
<b>III.4 Cyclic loading.....</b>	<b>120</b>
<b>III.5 Shear bond strength (SBS) test.....</b>	<b>122</b>

<b>III.6 Failure mode analysis .....</b>	123
<b>III.7 Scanning electron microscopy (SEM) examination .....</b>	123
<b>III.8 Statistical analysis .....</b>	124
<b>IV.RESULTS.....</b>	126
<b>IV.1 Shear bond strength (SBS) test .....</b>	127
<b>IV.2 SEM Observations .....</b>	129
<b>V. DISCUSSION .....</b>	135
<b>VI. CONCLUSIONS .....</b>	144
<b>VII. REFERENCES .....</b>	148
<b>VIII. APPENDIX.....</b>	185
<b>VIII.I Appendix 1. Original publications .....</b>	186
<b>VIII.2 Appendix 2. Tesis resumida en español .....</b>	230
<b>VIII.3 Appendix 3. Thematic index .....</b>	255



## Tables

Table 1 Dental ceramics classification by processing laboratorial technique.....	45
Table 2. Dental ceramics classification according to firing temperature and respective indications .....	49
Table 3. Chemical composition, physical, mechanical and thermal properties of Y-TZP.....	58
Table 4. Tables of most relevant and recent articles using zirconia surface treatment to enhance the adhesive effectiveness of the zirconia-resin interface.....	68
Table 5. Most common types of lasers with wavelength and time duration of the emission.....	78
Table 6. Summary table about application of femtosecond laser in Dentistry.....	91
Table 7. Summary of studies that using cyclic loading in zirconia ceramics.....	102
Table 8. Micro-testing advantages and drawbacks.....	107
Table 9. Materials and manufacturer's composition.....	116
Table 10. Comparison of the SBS among the zirconia surface treatment subgroups ANOVA with Bonferroni corrections.....	127
Table 11. Failure modes within the subgroups.....	128



# Figures

Figure 1. Dental ceramics history summary graphic.....	41
Figure 2. Zirconia crystal structure transitions with increasing temperaturas.....	54
Figure 3. Coulomb explosion.....	83
Figure 4. The absorption and emission rates of Ti:Sapphire laser.....	86
Figure 5: Schematic representation of the regenerative amplification technique of ultrashort pulses CPA (Chirped Pulse Amplification).....	87
Figure 6: Ti-sapphire oscillator-regenerative amplifier system.....	88
Figure 7. Variable neutral-density filter.....	89
Figure 8. Microprocessor team.....	90
Figure 9. Specimens of zirconia.....	115
Figure 10. Cutting machine.....	115
Figure 11. Samples of zirconia with cylinders of resin cement adhered over their surfaces.....	120
Figure 12. Cyclic loading of a sample.....	121
Figure 13. Chewing simulator.....	121
Figure 14. Universal SBS testing machine.....	122
Figure 15. Applying a shear load to a sample.....	122
Figure 16. SEM micrographs of zirconia surfaces after conditioning treatments.....	131
Figure 17. Representative zirconia surface SEM images (X30 and X700 magnification) of the most common failure type for the subgroups in which the cyclic loading was applied.....	132

Figure 18. Representative zirconia surface SEM images (X30 and X700 magnification) of the most common failure type for the subgroups in which the cyclic loading was not applied..... 133



## Acronyms

$\mu$ SBS	Micro-shear Bond Strength test
$\mu$ TBS	Micro-tensile Bond Strength test
10-MDP	10-methacryloxydecyl dihydrogenphosphate
3D	Three Dimensional
3-MPS	3-methacryloxypropyl trimethoxysilane
AFM	Atomic Force Microscope
APA	Airborne Particle Abrasion
C	Cubic crystalline zirconia form
CAD/CAM	Computer Aided Design/ Computer Aided Machining
CO <sub>2</sub>	Dióxido de Carbono
CPA	Chirped Pulse Amplification
Er: YAG	Erbium-doped Yttrium Aluminium Garnet
FEA	Finite Element Analysis
FPD	Fixed Partial Dentures
fs	femtosegundo
HF	Hydrofluoric Acid
hz	hertzio
ISO	International Standardization Organization
kV	kilovoltio
LASER	Light Amplification by Stimulated Emission of Radiation
LCTE	Linear Coefficient of Thermal Expansion
M	Monoclinic crystalline zirconia form
MASER	Microwave Amplification by Stimulated Emision of Radiation
MEB	Microscopía Electrónica de Barrido
MTBS	Micro-tensile Bond Strength test
MVD	Molecular Vapor Deposition
Nd: YAG	Neodymium -doped Yttrium Aluminium Garnet
nJ	nanojulio
ps	picosegundo

PSZ	Partially Stabilized Zirconia
SEM	Scanning Electronic Microscope
SBS	Shear Bond Strength test
SD	Standar Deviation
SP	Short Pulse
T	Tetragonal crystalline zirconia form
TBS	Tensile Bond Strength test
TC	Thermocycling
Ti:Zafiro	Titanium:Zafiro
TZP	Tetragonal Zirconia Polycrystal
VLP	Very Long Pulse
VSP	Very Short Pulse
XT	Adper Scotchbond 1 XT
Y- PSZ	Yttrium-oxide Partially Stabilized Zirconia





# *ABSTRACT*

In the field of orthodontics, adhesion of attachments on the ceramic surfaces, especially zirconia ceramics, remains one of the major problems with which clinicians routinely have to deal. Establishing a protocol to achieve proper adhesive effectiveness to prevent debonding of brackets, it is one of the priorities that should seek in research about adhesion in orthodontics, due to zirconia ceramics are widely used today in dentistry because they exhibit exceptional fundamental dental properties such as high strength, hardness, fracture toughness, and suitable aesthetics, among others. It is therefore essential to find an adhesion protocol that is available to all clinicians to get a resin-zirconia bond with high efficiency in restorative dentistry to cement zirconia on different biological substrates such as enamel or dentin; or in orthodontics to cement nonbiological substrates such as different orthodontic attachments on zirconia surface.

Regarding adhesion to zirconia, resin cements are the best that we can used, specifically self-adhesive resin cements. However, traditional chemical adhesion is ineffective on the zirconia surface so that their surfaces need conditioning techniques to improve adhesion of zirconia-resin interface. In such a way that zirconia is a relatively new and innovative material there is a lot of controversy, from the scientific point of view, about the best method for optimizing and promotes an effective bonding to substrates used in dentistry. Over the past two decades they have been using different surface conditioning methods to enhance the adhesive effectiveness of zirconia-resin interface with the intention that, after, it can be possible the bonding of orthodontics attachments with resin cement on zirconia surface or the bonding of zirconia restorations as crowns on enamel or dentine. But still none of these surface treatments proved to be the ideal to provide adequate adhesion of zirconia-resin interface. It is therefore necessary to seek new alternatives that guarantee us a strong and durable

adhesion in restorative dentistry and in orthodontics to cement brackets and tubes.

The use of lasers is presented as the future of dentistry, specifically the femtosecond laser. The use of this in the field of orthodontics to adhesion of brackets can complement the use it will have on the various specialties of dentistry. Thus, research is now beginning to focus on the use of femtosecond lasers irradiation as surface treatments to perform the conditioning of zirconia surfaces to establish an adhesion protocol that is available to all clinicians to cement zirconia restorations on biological substrates such as enamel or dentine; or to cement orthodontic attachments on zirconia surface.

This study is one of the first that have been made in the zirconia-resin interface so we began investigating at the zirconia-resin interface due to it is the only surface that we can change, because the adhesion of resin-bracket interface come preset by the type of mesh that has the orthodontic attachment. This is the first step in a line of research, where once we observe if employment of femtolaser at the interface resin -zirconia is successfull, we continue the research with a protocol to be cemented directly the bracket with resin cements on the zirconia surface.

The objectives of this thesis were: 1) to investigate the effect of the zirconia surface treatment with airborne particle abrasion with 25- $\mu\text{m}$  alumina particles, tribochemical silica coating, and femtosecond laser irradiation on the zirconia-resin interface bond strength; 2) to assess if femtosecond laser irradiation influences on the bond strength to zirconia-resin cement interface and determine the better parameters of irradiation to provide a reliable resin/zirconia bonding; and 3) to evaluate how the cyclic loading affects on the adhesive effectiveness of zirconia/resin interface.

A *in vitro* study was performed to evaluate the effect of femtosecond laser treatment on the shear bond strength (SBS) of self-adhesive resin cements to zirconia surfaces and to compare such treatment with more conventional surface conditioning methods; and the influence of cyclic loading on the shear bond of zirconia-resin interface.

One hundred fifty square-shaped zirconia samples (measuring 6x6x1mm) were divided into five groups according their surface treatment: Group 1- no treatment (NT) no surface conditioning method; Group 2- Airborne particle abrasion with 25- $\mu\text{m}$  alumina particles (APA 25): sandblasting with 25- $\mu\text{m}$   $\text{Al}_2\text{O}_3$  particles; Group 3- Tribocochemical silica coating (TSC): silica coating followed by silanization; Group 4- Femtosecond laser step 20 (FS20): femtosecond laser irradiation (800 nm, 4 mJ, 40 fs/pulse, 1 kHz, step 20), and Group 5- Femtosecond laser step 40 (FS40): femtosecond laser irradiation (same parameters except step 40).

After performing the different surface treatments on the zirconia samples, a self-adhesive resin cement (Clearfil™ SA Cement, Kuraray, Osaka, Japan) was bonded at the zirconia surface using a cylindrical silicone mould with a 3 mm internal diameter, 1 mm thickness and 1 mm in height positioned at the centre of the samples. The cement was placed on them against the zirconia surface and polymerized for 40 s (XL 3000, 3M/ESPE; light intensity 500 mW/cm<sup>2</sup>, distance 0) from above and towards the contact area from a lateral position.

All experimental groups were divided into two subgroups according to whether cyclic loading was applied or not. Thus, half of the specimens of each group ( $n=15$ ) were mounted in acrylic resin moulds for cyclic loading under 90 N (50.000 cycles, 3 cycles/sec) with the force applied perpendicularly to the zirconia surface opposite where the resin was cemented; and the rest of the specimens ( $n=15$ ) were stored in distilled

water at 37 ° C.

All subgroups were tested for SBS with a universal testing machine (AGS-X Autograph, Shimadzu Corporation, Kyoto, Japan), applying a shear load with a crosshead speed of 0.5 mm / min, until fracture.

After the SBS-test, each fractured specimen was examined under an Axio M1 (Carl Zeiss, Germany) light microscope at 40X magnification to determine the failure modes and representative fractured samples were examined with the scanning electron microscope (Zeiss EVO MA25; Carl Zeiss, Jena, Germany) in order to analyze the morphology of the debonded interfaces. Five zirconia surfaces from each experimental subgroup ( $n=5$ ) were prepared for surface morphology analysis with a variable pressure SEM.

The data were analyzed with SPSS v21 (Statistical Package for the Social Sciences, Chicago, IL). ANOVA, Student T, chi square tests and linear regressions were performed ( $p < 0.05$ ) to compare the SBS among the subgroups regarding the use of different zirconia surface treatments.

The main results to point out are the following:

- 1) When cyclic loading was not applied, the APA25 subgroup obtained higher SBS values than the control subgroup, but they were lower than the TSC, FS20 and FS40 SBS values, which were similar to each other.
- 2) When cyclic loading was applied, the four surface treatments afforded the same SBS values, which were higher than those of the control subgroup values.
- 3) In the control group most of the failures were adhesive, while in the treatment groups they were mostly mixed.

The results of our research allow us to conclude the following:

1) Femtosecond laser irradiation and tribochemical silica coating create a consistent and profound surface roughness, improving the adhesive effectiveness of the zirconia-resin cement interface. This is due to that the adhesion of the interface is influenced by the micromechanical retention, and this last is based more on the engraving depth created by conditioning method than on the engraving pattern become a fundamental requirement for establishing a strong and durable bond with zirconia-based materials.

2) Femtosecond laser treatment, both step 20 as step 40, might be a reliable way to achieve suitable adhesion between resins and zirconia due to creates a pattern of deep grooves on the zirconia surface that are filled by resin cement. The difference between the different steps is that the time of irradiation at step 40 is half , and it is an important clinical factor to be taken into consideration. The surface conditioning method must produce a pattern of engraving in order to ensure stable and durable bonding, but it must also be carried out as fast as possible. In this sense, since femtosecond laser irradiation at step 40 produced fewer and more widely spaced grooves, the irradiation time was substantially reduced (indeed, by half). Accordingly, for practical purposes, and since efficiency is preferred over effectiveness, to achieve the best results in the shortest time possible it is best to use femtosecond laser in this step.

3) When cyclic loading is applied, the adhesive effectiveness of the zirconia-resin interface decreases when any of the zirconia surface treatments are applied previously, except alumina particle abrasion, which is not affected by cyclic loading.





# *RESVMEN*

En la actualidad, existe un creciente número de restauraciones prostodónticas de circonio que, unido al hecho que cada vez son más los pacientes adultos que desean realizarse un tratamiento ortodóntico y muchos de ellos son portadores de este tipo de rehabilitaciones, hacen que los ortodoncistas tengan que enfrentarse, casi de forma rutinaria, al problema de tener que cementar distintos tipos de aditamientos sobre estas superficies prostodónticas. Por ello, el establecimiento de un protocolo para lograr una eficacia adhesiva adecuada para evitar el descementado de los *brackets* es una de las prioridades que se deben buscar en la investigación sobre la adhesión en ortodoncia.

A día de hoy, es esencial elaborar un protocolo de adhesión que nos proporcione, por un lado, en odontología restauradora, una adhesión correcta entre el cemento de resina y la superficie de circonio para cementar cualquier restauración prostodóntica de circonio en diferentes sustratos biológicos tales como el esmalte o la dentina; y por otro, en ortodoncia, para cementar sustratos no biológicos tales como diferentes aditamientos ortodónticos sobre la superficie del circonio.

En lo referente a qué cementos emplear con este tipo de cerámicas, los de resina son los mejores, y más en concreto, los cementos de resina autoadhesivos. La adhesión química tradicional es ineficaz en la superficie del circonio haciendo que sea necesario realizar alguna de las distintas técnicas de acondicionamiento de su superficie. Esto implica que, aunque el circonio se trate de un material nuevo e innovador que se encuentra en auge, es también objeto de mucha controversia, desde el punto de vista científico, sobre el mejor método para optimizar y promover una unión eficaz en odontología. En las dos últimas décadas, se han estado utilizando diferentes tratamientos de superficies a fin de poder mejorar la eficacia adhesiva de la interfase circonio-resina con la intención de que, después, pueda ser posible cementar

aditamientos de ortodoncia sobre su superficie o bien para pegar cualquier tipo restauración prostodóntica de circonio en el esmalte o la dentina. Sin embargo, ninguno de ellos ha resultado ser el ideal para proporcionar una adhesión adecuada y por tanto, es necesario buscar nuevas alternativas que nos garanticen una fuerte y duradera adhesión.

El uso del láser se presenta como el futuro de la odontología, específicamente el láser de femtosegundo, el cual se empieza a estudiar y a utilizar no sólo en el campo de la ortodoncia para mejorar la adhesión de *brackets*, sino también en las distintas especialidades odontológicas. Actualmente, la investigación está centrada en la irradiación con láseres de femtosegundo como tratamientos de superficie para llevar a cabo el acondicionamiento de superficies de circonio para establecer el protocolo de adhesión necesario que esté disponible para todos los clínicos tanto en odontología restaurativa como en ortodoncia para cementar *brackets* y tubos.

Este estudio es uno de los primeros que se han hecho en la interfase de la superficie de circonio con el cemento de resina, y el hecho de que comencemos con la investigación de esta interfase se encuentra en que es la única que podemos modificar ya que la adhesión de la interfase del cemento de resina con los *brackets* viene preestablecido por el tipo de malla que presenten estos últimos. Por tanto, este estudio se trataría del primer paso de una línea de investigación, donde, una vez que observemos si el empleo de femtoláser en la interfase circonio-resina es exitosa, continuaremos con un nuevo protocolo para cementar directamente los *brackets* con cementos de resina en la superficie de circonio.

Los objetivos de esta tesis fueron: 1) investigar el efecto de diferentes métodos de acondicionamiento de la superficie del circonio (la abrasión con partículas de alúmina

de 25- $\mu\text{m}$ , el revestimiento con sílice triboquímico, y la irradiación con el láser de femtosegundos) a fin de evaluar la eficacia adhesiva de la interfase circonio-resina; 2) evaluar si la irradiación con láser de femtosegundos influye en la resistencia a la fuerza de la cizalla de la interfase de circonio con el cemento de resina y determinar cuáles son los mejores parámetros de irradiación para proporcionar una adhesión adecuada; y 3) evaluar cómo afecta el ciclado mecánico en la eficacia adhesiva de la interfase circonio-resina.

Se realizó un estudio *in vitro* para evaluar el efecto del tratamiento con láser de femtosegundo en la resistencia a la fuerza de cizallamiento (SBS) de cementos de resina autoadhesivos en la superficie del circonio y comparar dicho tratamiento con métodos de acondicionamiento de superficies más convencionales; así como la influencia del ciclado mecánico sobre la eficacia adhesiva de la interfase circonio-resina.

Ciento cincuenta muestras, de forma cuadrada, de circonio (que medían 6x6x1mm) se dividieron en cinco grupos de acuerdo a su tratamiento de superficie: Grupo 1- no tratamiento (NT): ningún método de acondicionamiento de superficies; Grupo 2- abrasión con partículas de alúmina de 25 micras (APA 25): arenado con partículas de  $\text{Al}_2\text{O}_3$ ; Grupo 3- recubrimiento de sílice triboquímico (TSC): recubrimiento de sílice seguido por silanización; Grupo 4- láser de femtosegundo a *step 20* (FS20): irradiación láser de femtosegundo (800 nm, 4 mJ, 40 fs / pulso, 1 kHz, *step 20*), y el Grupo 5- láser de femtosegundo a *step 40* (FS40): irradiación láser de femtosegundo (misma los parámetros excepto *step 40*).

Después de realizar los diferentes tratamientos de superficie sobre las muestras de óxido de circonio, se adhirió un cemento de resina autoadhesivo (Clearfil <sup>TM</sup> SA Cemento, Kuraray, Osaka, Japón) a la de la superficie de circonio utilizando un molde

de silicona cilíndrico con un diámetro interno de 3 mm, 1 mm de espesor y de 1 mm de altura situado en el centro de las muestras. Se colocó el cemento en estos moldes contra la superficie de circonio y se polimerizó durante 40 segundos (XL 3000, 3M / ESPE; intensidad de la luz 500 mW / cm<sup>2</sup>, la distancia 0) desde arriba y hacia el área de contacto desde una posición lateral.

Todos los grupos experimentales se dividieron en dos subgrupos en función de si se aplicó o no el ciclado mecánico. Por lo tanto, la mitad de los especímenes de cada grupo ( $n=15$ ) fueron montadas en moldes de resina acrílica para realizar el ciclado mecánico bajo 90 N (50.000 ciclos, 3 ciclos/segundo) con la fuerza aplicada perpendicularmente a la superficie opuesta donde se unió la resina. El resto de las muestras ( $n=15$ ) se almacenaron en agua destilada a 37 ° C.

Todos los subgrupos se ensayaron para el test de SBS con una máquina de ensayo universal (AGS-X autógrafo, Shimadzu Corporation, Kyoto, Japón). Se aplicó una carga de cizallamiento con una velocidad de cruceta de 0,5 mm / min, hasta la fractura de la interfase del circonio con el cemento de resina.

Después de la prueba de SBS, cada muestra fracturada se examinó bajo un microscopio de luz M1 Axio (Carl Zeiss, Alemania) a 40 aumentos para determinar los modos de fractura y varias muestras fracturadas representativas fueron examinadas con el microscopio electrónico de barrido (Zeiss EVO MA25; Carl Zeiss, Jena, Alemania) con el fin de analizar la morfología de las interfaces desligada. Cinco superficies de circonio de cada subgrupo experimental ( $n =5$ ) se prepararon para el análisis de morfología de la superficie con el microscopio electrónico.

Los datos fueron analizados con SPSS v21. ANOVA, t de Student, pruebas de chi

cuadrado y regresiones lineales se realizaron ( $p <0,05$ ) para comparar los valores del SBS entre los subgrupos para analizar las diferencias existentes de los diversos tratamientos de superficie del circonio.

Los principales resultados a señalar son los siguientes:

- 1) Cuando no se aplicó el ciclado mecánico, el subgrupo APA25 obtuvo valores de SBS más altos que el subgrupo control, pero eran menores que los valores del TSC, FS20 y FS40 que fueron similares entre sí.
- 2) Cuando se aplicó el ciclado mecánico, los cuatro tratamientos de superficie mostraron los mismos valores de SBS que eran más altos que los del subgrupo control.
- 3) En el grupo control la mayor parte de los fallos de unión eran adhesivos, mientras que en los grupos de tratamiento eran en su mayoría mixtos.

Los resultados de nuestra investigación nos permiten concluir lo siguiente:

- 1) La irradiación con el láser de femtosegundo y el revestimiento con sílice triboquímico crean una rugosidad en la superficie consistente y profunda, mejorando la eficacia adhesiva de la interfase del circonio con el cemento de resina. Esto es debido a que la adhesión de la interfase se ve influenciada por la retención micromecánica, y esta última se basa más en la profundidad de grabado creado por el método de acondicionamiento que en el patrón de grabado convirtiéndose en un requisito fundamental para el establecimiento de una unión fuerte y duradera.
- 2) El tratamiento con láser de femtosegundo, tanto a *step* 20 como a 40, puede ser un método de acondicionamiento de superficie eficaz para lograr la adhesión

adecuada entre el circonio y los cementos de resina debido a que crea un patrón de surcos profundos en la superficie de circonio que son rellenados por el cemento de resina. La diferencia entre los diferentes *step* es que el tiempo de irradiación en el *step* 40 es la mitad, y el tiempo es un factor clínico importante para ser tomado en consideración. El método de acondicionamiento de superficies debe producir un patrón de grabado con el fin de asegurar una unión estable y duradera, pero también debe ser llevado a cabo lo más rápido posible. En este sentido, ya que la irradiación con láser de femtosegundo en el *step* 40 produce menos ranuras y que están más ampliamente espaciadas, el tiempo de irradiación se reduce sustancialmente (de hecho, a la mitad). En consecuencia, lo mejor es utilizar láser de femtosegundo a *step* 40 ya que se prefiere la eficiencia, a fines prácticos, más que la eficacia, para así lograr los mejores resultados en el menor tiempo posible.

3) Cuando se aplica el ciclado mecánico, la eficacia adhesiva de la interfase circonio-resina disminuye en cualquiera de los tratamientos de superficie realizados excepto en la abrasión con partículas de alúmina, que no se ve afectada por el ciclado.





# *i. INTRODUCTION*

## I.1 Dental ceramics

The word “ceramic” can be traced back to the Greek term “keramos” which Sanskrit roots mean “burn earth”. The American Ceramic Society has defined ceramic as inorganic, non metallic materials, which are typically crystalline in nature, and are compounds formed between metallic and non metallic elements such as: aluminium and oxygen (Alumina\_  $\text{Al}_2\text{O}_3$ ), calcium and oxygen (Calcia\_  $\text{CaO}$ ) or silicon and nitrogen (Nitride\_  $\text{Si}_3\text{N}_4$ ) (Sukumaran *et al.*, 2006).

They have usually crystalline structure, with regular and periodic arrangement of the component atoms, and may exhibit ionic or covalent bonding. Ceramics can be classified into four categories: (1) silicates, (2) oxides, (3) non-oxides, and (4) glass (Anusavice 2003). Silicate ceramics are characterized by an amorphous glass phase and can have a porous structure. The main component is  $\text{SiO}_2$  with small additions of crystalline  $\text{Al}_2\text{O}_3$ ,  $\text{MgO}$ ,  $\text{ZrO}_2$  and/or other oxides. Dental porcelain falls into this category (Anusavice 2003). Oxide ceramics contain a principal crystalline phase ( $\text{Al}_2\text{O}_3$ ,  $\text{MgO}$ ,  $\text{ZrO}_2$ ) with either no glass phase or a small amount of a glass phase (Anusavice 2003). Non-oxide ceramics are impractical for use in dentistry because of high processing temperatures, complex processing methods, and unaesthetic colour and opacity (Anusavice 2003). Glass-ceramics are partially crystallized glasses, which occur by nucleation and growth of crystals in the glass matrix (Anusavice 2003).

Ceramics can be very strong, but they are also extremely brittle. These materials are strong under compression yet weak submitted to tension and can catastrophically fail after minor flexure.

### *I.1.1 Dental ceramics history*

After decades of efforts Europeans mastered the porcelain manufacturing technique. By the 1720's the use of feldspar to replace lime (Calcium oxide) and high firing temperatures were crucial developments in the fine European porcelain which became comparable to the Chinese one. Porcelain is a high quality ceramic, less porous, harder with excellent properties and superficial look. The optical requisites demanded that in its production only the finest and purest components are to be used. Feldspathic dental ceramics were adapted from this porcelain simultaneously with their development.

Approximately in 1774, Alexis Duchateau, a Parisian apothecary, with the assistance of Nicholas Dubois de Chemant made the first porcelain denture at the Guerhard Porcelain factory, replacing the stained and malodorous ivory prosthesis of Duchateau (Kelly *et al.*, 1996). In 1791, Dubois de Chemant patented, in Britain, his idea and in 1792 he began selling his wares.

In the second half of the eighteenth century, Pierre Fauchard and others attempted to use porcelain in dentistry but their efforts were largely unsuccessful. In 1808, G. Fonzi, an Italian dentist invented the “terrometallic” porcelain tooth that used a platinum pin or frame to be held in place. Planteau, a French dentist, introduced porcelain teeth to the United States of America in 1817, and Peale, an artist in Philadelphia developed a baking process for them in 1822 (Anusavice 2003). Stockton began its commercial production in 1825. In 1844, the S.S. White Company was founded and this led to refinement of design and mass production of porcelain denture teeth.

Dr. Charles Land introduced the first successful fused feldspathic porcelain inlay and crowns to dentistry in 1886 (Kelly *et al.*, 1996). Land described a technique for fabricating ceramic crowns using a platinum foil, as a substructure, with the high controlled heat of a gas furnace. These crowns exhibited excellent aesthetics but the low flexural strength of porcelain resulted in a high incidence of failure. This was the first crown with esthetical aspirations for unitary use.

Dental ceramics production was highly impelled after, in the later 1950, Weinstein and Weinstein presented the metal-ceramic crown. They patented the formulation of feldspathic porcelain that allowed the control of the sintering temperature and thermal expansion, as well as the components that could be used to produce alloys that bonded chemically to and were compatible with feldspathic porcelains (Weinstein *et al.*, 1962; Weinstein *et al.*, 1962; Luthardt *et al.*, 1999).

In 1963, Vita Zahnfabrik, introduced the first commercial porcelain products which were known for their esthetic properties.

Significant improvement in the fracture resistance of porcelain crowns was introduced by McLean and Hughes, who developed the alumina reinforced feldspathic core 1965 (McLean *et al.*, 1965). The material consisted of a feldspathic glass containing 45-50%  $\text{Al}_2\text{O}_3$  (McLean 1967). The alumina ceramic is strengthened by dispersion of a crystalline phase in the glassy matrix (Craig *et al.*, 2002).

With the sudden dental ceramic development, in 1993, Procera All Ceram was invented in Sweden. This is a nucleus of highly sintered Alumina (99, 9%) that, because of the inadequate translucency of the aluminous porcelain core

material, a feldspathic porcelain veneer of was required to achieve acceptable aesthetics.

All ceramic crowns fulfill the esthetics expectations of both professional and patient. Since the 1960's, investigation developed new products with the aim of harder, stronger and with better marginal accuracy restorations. Recently, there has been development in both dental ceramic materials and fabrication techniques. For example, higher strength substructure materials such as lithium-disilicate, alumina, and zirconia have been used. Additionally, fabrication techniques such as slip-casting and copy milling techniques have been improved. Esthetic demand in dentistry influenced ceramic popularity as choice material used in crowns, veneers, inlays and onlays. In figure 1 are exposed the evolution of dental ceramics.

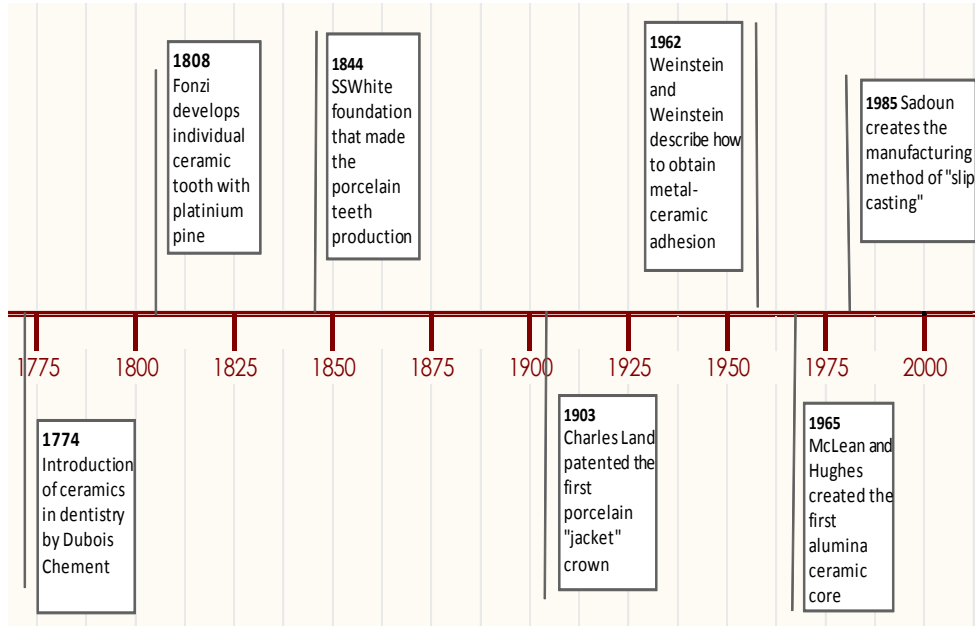


Figure 1. Dental ceramics history summary graphic.

### *I.1.2 Dental ceramics properties*

Dental ceramics present a properties set desirable as restorative materials (Álvarez-Fernandez *et al.*, 2003):

- ✓ Biocompatibility;
- ✓ Excellent optical characteristics such as translucency, transparency, color, brightness, high reflection and texture, which implies a variety of options to mimetizes natural teeth;
- ✓ Durability and time stability, due to high chemical stability in the oral environment;
- ✓ Compatibility with other material like metals and resins;
- ✓ Low thermal conductivity and elastic modulus similar to hard dental tissues;
- ✓ Radiopacity, that allows the marginal accuracy evaluation and secondary caries diagnosis;
- ✓ Hardness and high abrasion resistance;
- ✓ Mechanical strength;
- ✓ Easy production process and reasonable cost (Álvarez-Fernandez *et al.*, 2003).

### *I.1.3 Dental ceramics classification*

Dental ceramics are defined as inorganic materials predominantly formed by no-metallic elements, produced by firing several mineral at high temperature and which final structure is partial or totally crystalline (Denry *et al.*, 2010). Most

dental ceramics have a mixed structure with an amorphous glass matrix (with an atomically architecture disorganized without fixed angles or distances) where we find bigger or smaller mineral particles immersed (these particles have the atoms structured in a regular and periodic way with ionic or covalent connections) (Shenoy *et al.*, 2010). The crystalline phase improves the mechanical properties of the material. It can be said that the glass phase is responsible for the esthetics and the crystalline for the strength.

In the last decades, dental ceramics manufacturing methods had a big development directed towards the mechanical properties improvement, esthetic optimization and long term *in vivo* performance.

#### I.1.3.1 Dental ceramics classification according to chemical composition

Chemically ceramics can be grouped in (Fons-Font *et al.*, 2001; Álvarez-Fernandez *et al.*, 2003; Díaz-Romeral Bautista *et al.*, 2008):

❖ *Feldspathic ceramics:*

- **Classic or traditional:** used in veneering ceramic or metal cores.
- **Reinforced or high resistant:** leucite ( $K_2O$ ,  $Al_2O_3$ ,  $4SiO_2$ ) crystals or lithium-disilicate are used to strengthen feldspathic ceramic.

❖ *Alumina ceramic:*

Aluminous porcelain is composed of a glass matrix phase and at least 35 vol % of alumina. An aluminous core is stronger than feldspathic porcelain, the alumina particles are stronger than the glass and more effective at preventing crack propagation than quartz (van Noort 2002).

- **Classic**
- **Reinforced or high resistance**
- **Zirconia ceramic**

#### I.1.3.2. Dental ceramics classification by the laboratory

##### technique

Dental ceramics are produced using thermal processes, that involve high temperatures, like sinterization and ceramization. Processing method can be divided by (Álvarez-Fernandez *et al.*, 2003; Martínez-Rus *et al.*, 2007): pressing, powder condensation, casting, or machining (Table 1). Ceramics having similar composition may be fabricated by different laboratory techniques, and each method of forming results in a different distribution of flaws, opportunity for depth of translucency and fit accuracy.

<b>Classification by processing method</b>	<b>Presentation</b>	<b>Technique</b>
<b>Powder condensation</b>	Powder + Liquid	Mixing the component, build up by hand and fire in vacuum
<b>Pressing</b>	Pre fabricated ceramic ingots	Lost wax
<b>Casting</b>	Porous substrate + infiltrated glass	Slip casting
<b>Machining</b>	Pre fabricated ceramic ingots	CAD/CAM

Table 1. Dental ceramics classification by processing laboratorial technique.

#### Powder condensation

This is a traditional method of forming ceramic prostheses that involves applying a moist porcelain powder with an artist's brush and removing excess moisture to compact the powder particles. The porcelain is further compacted by viscous flow of the glassy component during firing under vacuum. The crystalline particles that strengthen the material on a microscopic scale aren't connected to each other but are separated by glassy regions. A large amount of residual porosity and the discontinuous nature of the crystalline phase lead to relatively low strength. Ceramics fabricated by powder condensation have greater translucency than can be achieved using other methods (Anthonsen *et al.*, 2001), so these materials are usually applied as the esthetic veneer layers on stronger cores and frameworks.

### Hot Pressing

The lost wax method is used to fabricate molds for pressable dental ceramics. A wax pattern of the restoration is invested in a phosphate-bonded investment material. Following the burn out procedure, a glass-ceramic prefabricated ingot is pressed into the mould at a temperature of 1050°C in a custom furnace. An example of the material used is leucite-reinforced feldspathic porcelains strengthened by incorporating leucite ( $K_2O$   $Al_2O_3$   $4SiO_2$ ) crystals, approximately 45% volume, in the glass matrix (Isgrø *et al.*, 2003). The microstructure is similar to powder porcelain, however, pressable ceramics do not contain much porosity and can have a higher crystalline content because the ingots are manufactured from non-porous glass ingots by applying a heat treatment that transforms some of the glass into crystals (Griggs 2007). Contrary to expected, the higher crystalline content and lack of porosity do not lead to increase fracture resistance or decrease strength variability (Tinschert *et al.*, 2000).

### Slip Casting

A slip is a low viscosity slurry or mixture of ceramic powder particles suspended in a fluid (usually water). Slip casting involves forming a negative replica of the desired framework geometry and pouring the slip into the mold. The mold is made

from a material (usually gypsum) that extracts some water from the slip into the walls of the mold through capillary action, and some of the powder particles become compacted against the walls of the mold forming a thin layer that is to become the framework. The remaining slurry is discarded, and the framework can be removed from the mold after partial sintering. This fired porous core is later glass infiltrated, a process by which molten lanthanum glass is drawn into the pores by capillary action at high temperatures. Materials processed this way exhibit less porosity, fewer defects from processing, greater strength and higher toughness than conventional feldspathic porcelains (Probster *et al.*, 1992) because the strengthening crystalline particles form a continuous network throughout the framework. This glass-infiltrated core is later veneered with a feldspathic ceramic for final restoration. The use of this method in dentistry has been limited to the series of In-Ceram<sup>®</sup>, Vita Zahnfabrik.

CAD-CAM (Computer Aided Design- Computer Aided Machinig)

Dental CAD-CAM systems have been available for 20 years. Recently, the increasing use of polycrystalline alumina and zirconia as framework materials and the expanding

popularity of informatic methods seem to be mutually accelerating trends. Like pressable ceramics, CAD-CAM ceramics are available as prefabricated ingots. These ingots are

machined or milled by computer-controlled tools. Glass infiltrated CAD-CAM ingots have similar composition to slip cast ceramics, but starting with a porous ingot eliminates the complicated steps of slip casting. After milling, the porosity is eliminated by molten glass infiltration.

In the case of pre-sintered ceramics, the ingots are porous, which enables a fast milling. The disadvantage of this called “Green Milling” method is the need for subsequent sintering treatment to eliminate the porosity. The computer software must calculate and compensate the shrinkage that occur during sintering to achieve a good fit accuracy.

Densely sintered ceramics are available in non-porous ingots, which are more difficult to mill, “Hard Machining”, but they do not require any further sintering.

#### I.1.3.3. Dental ceramics classification by sintering temperature.

According to the firing temperature, dental ceramics can be divided into high-fusing ( $1300^{\circ}\text{C}$ ), medium fusing ( $1101\text{-}1300^{\circ}\text{C}$ ), low fusing ( $850\text{-}1100^{\circ}\text{C}$ ), and ultra-low fusing ( $<850^{\circ}\text{C}$ ) ceramics (Anusavice 2003). This classification was employed more intensively with earlier dental ceramic compositions, which contained three major

ingredients: quartz, feldspar, and clay (or kaolin) (Craig *et al.*, 2002). The fusion temperature is dictated by the relative amount of these three ingredients.

The lower firing temperature the lower tendency to fracture and micro flaws, because there is less contraction during cooling; nevertheless the better properties are achieved when firing temperature is very high (Poujade *et al.*, 2004). Recently the classification was extended with the dental ceramics processed in very low temperature, even at room temperature. In table 2 are exposed the classification criteria and the main applications of different dental ceramics.

Classification	Firing temperature	Indications
<b>High fusing</b>	1300-1370°C	Industrial production tooth
<b>Medium fusing</b>	1101-1300°C	Jacket crowns cores
<b>Low fusing</b>	850-1100°C	Esthetical veneering aluminous or metal cores
<b>Very low fusing</b>	<850°C	Gold or titanium veneering. Small rectifications like contact point, oclusal anatomy, angles and details. Glazing.
<b>Room temperature</b>		Chair side processing avoiding the laboratorial technician

Table 2. Dental ceramics classification according to firing temperature and respective indications.

#### I.1.3.4 Dental ceramics classification by crystalline content

Nowadays dental ceramics classification by crystalline/glass content is one of the most accurate for comprehension and handling this material.

The glass phase is a binding matrix that keeps together the set and gives the ceramic translucency. The crystalline phase or charge consists in crystals that improve the mechanical properties and affect the ceramic optical behavior (opalescence, color and opacity) its influence depends on type, size and percentage they appear. Generally high esthetic porcelain are predominately vitreous and the high strength ceramics are highly crystalline.

The dental ceramics evolution was conducted in the way of increasing the crystalline phase to improve the mechanical properties and refine optical characteristics:

❖ *Glass based systems* (mainly silica)

Glass-based systems are made from materials that contain mainly silica which contains various amounts of alumina. These materials were the first used in dentistry to make porcelain dentures. Mechanical properties are low, with flexural strength from 60-70 MPa thus they tend to be employed as veneer materials for metal or ceramic frameworks as well as for laminate veneers.

❖ *Glass based systems with fillers* (usually crystalline, typically

leucite or a different high-fusing glass):

This category has a large range of glass-crystalline ratios and crystal types. The glass composition is basically the same as the glass-based systems the difference is that varying amounts of different types of crystals (leucite, lithium-disilicate) have either been added or grown in the glassy matrix. This category can be divided into three groups:

- **Low to moderate leucite-containing feldspathic glass:**

These materials have been called “feldspathic porcelains” by default; the glass phase is based on aluminosilicate glass.

- **High leucite-containing (approximately 50%) glass:**

Again, the glassy phase is based on an aluminosilicate glass. These materials have been developed in powder/liquid, machinable and pressable forms.

- **Lithium-disilicate glass ceramic:** This is a glass ceramic (introduced by Ivoclar IPS Empress<sup>®</sup> now called IPS e.max<sup>®</sup>) where the aluminosilicate glass has lithium oxide added.

Flexural strength for these materials has been reported to be 120 MPa (Isgro *et al.*, 2003). Conventional feldspathic porcelains designed for metal ceramic restorations contain 12 to 25% volume leucite and have a flexural strength in

the range of 60 MPa. The increase in strength has been achieved through a heat treatment that enhances the formation of a highly crystallized microstructure and resists crack propagation under stress (Isgro *et al.*, 2003). Also, large pore formation can be avoided due to the better distribution of the crystalline phase within the glass matrix (Isgro *et al.*, 2003). The final restoration can use either the leucite-reinforced core material alone or a 2-layer all-ceramic crown veneered with low fusing porcelain (Isgro *et al.*, 2003).

❖ *Crystalline-based systems with glass fillers*

Glass-infiltrated, partially sintered alumina was introduced in 1988 and marketed under the name In-Ceram. The system was developed as an alternative to conventional metal ceramics and has met with great clinical success. Examples of materials that have used this technique are In-Ceram Alumina, In-Ceram Spinell, In-Ceram Zirconia (Vita Zahnfabrik, Bad Säckingen, Germany). Infiltrated ceramics are made through the process called slip-casting described above. The limited application of this ceramics is probably because the fabrication method requires a complicated series of steps, which provide a challenge to achieve accurate fit and may result in internal defects that weaken the material from incomplete glass infiltration (Griggs 2007). To simplify the slip casting technique glass infiltrated CAD-CAM

ingots are available.

- **Polycrystalline solids**

Solid sintered, monophase ceramics are materials that are formed by directly sintering crystals together without any intervening matrix, forming a dense, air-free, glass-free, polycrystalline structure. Special processing techniques in combination with polycrystalline oxide ceramics has made it possible to fabricate FPD frameworks with a flexural strength and fracture toughness that are considerably higher than those of feldspathic, leucite or lithium disilicate ceramics that have been previously used.

There are several different processing techniques that allow the fabrication of either solid sintered alumina or zirconia frameworks. The esthetic and functional form are achieved by the use of conventional feldspathic dental ceramics.

#### *I.1.4 Zirconia ceramics*

Zirconium oxide ( $\text{ZrO}_2$ ) known as zirconia is a white crystalline oxide from the transition metal Zirconium (Zr). Pure zirconia is not spontaneous in nature but is founded in minerals: Baddeleyte ( $\text{ZrO}_2$ ) and Zircon ( $\text{ZrSiO}_4$ ) which contain a percentage of zirconia (80-90%) with traces of  $\text{TiO}_2$  and  $\text{Fe}_2\text{O}_3$ .

Zirconia is a polymorphic crystal, meaning it presents a different crystal

structure at different temperatures with no change in chemistry (figure 2).

Zirconia has three crystalline forms:

- 1) **Cubic (C):** prismatic form with square section, stable at temperatures above 2370° C until melting temperature (2680° C) with moderate mechanical properties;
- 2) **Tetragonal (T):** a prismatic form with rectangular section, stable between 1170-1370° C and with improve properties when compared with form C.
- 3) **Monoclinic (M):** irregular prismatic form with tetragonal section, stable under 1170° C with low mechanical properties.

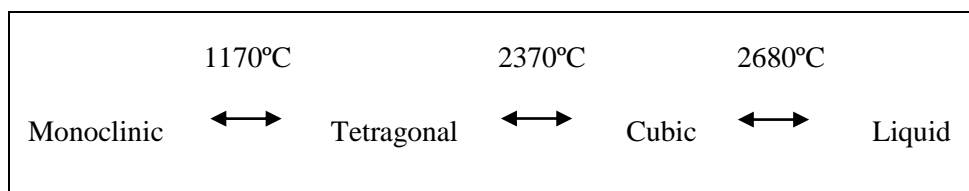


Figure 2. Zirconia crystal structure transitions with increasing temperatures.

Each crystal in M phase is 4.4% bigger in volume than T form, this implies a volume increase of 3-5% in the transformation T-M which occurs during cooling (for example after sinterization). This T-M transformation causes internal stress and fragmentation that, if not controlled, are capable of causing the material collapse (Piconi *et al.*, 1999; Vagkopoulou *et al.*, 2009).

In 1929 Ruff *et al* (Ruff *et al.*, 1929), described the zirconia stabilization in the cubic phase at room temperature with the addition of small amounts of

CaO, making it possible to use zirconia as an engineering material.

The addition of stabilizing oxides like CaO, MgO, CeO<sub>2</sub> and Y<sub>2</sub>O<sub>3</sub> to the pure zirconia allows the creation of multiphase materials known as Partially Stabilized Zirconia (PSZ). At room temperature PSZ generically consists in a primarily cubic zirconia phase with tetragonal and monoclinic precipitates in minor phase (Piconi *et al.*, 1999).

Garvie *et al* , in 1975 (Garvie *et al.*, 1975) found three similarities between PSZ and steel that allowed them to do the parallelism between both materials and call PSZ “the ceramic steel”: 1) presence of three allotropes; 2) martensitic transformation and 3) metastable phases. Also both materials have similar properties concerning the elasticity modulus and thermal expansion coefficient (Kelly *et al.*, 2008).

T-M transformation in PSZ can occur in order to enhance strength and hardness of zirconia ceramics (Garvie *et al.*, 1975). In their study, Garvie *et al* observed that finely dispersed, in the C matrix, metastable T precipitates can turn into M when the matrix pressure over them decreases, for example during a crack propagation. The hardness is improved, because there is a T-M transformation where the energy of the crack evolution is dispersed in the own transformation and in overcoming the volume expansion compressive stress. The excess of energy is now necessary for the crack to continue to propagate, thus increasing PSZ’s resistance to fracture. This mechanism known as transformation toughening is considered the basis of zirconia strength. However, it is noteworthy that this mechanism does not prevent the fracture progress it only makes it harder (Kosmac

*et al.*, 1999; Luthardt *et al.*, 1999; Piconi *et al.*, 1999; Kohal *et al.*, 2004; Raigrodski 2004).

PSZ can be obtained in the system ZrO<sub>2</sub>-Y<sub>2</sub>O<sub>3</sub>, with this combination it is possible to produce porcelain, that at room temperature, only presents T phase called TZP (Tetragonal Zirconia Polycrystal). TZP containing approximately 2-3% mol of Y<sub>2</sub>O<sub>3</sub> and are completely constituted by nanometric tetragonal zirconia grains. The tetragonal fraction present, at room temperature, depends on the grain size, the ytria content and the grade of constrain exerted on them by the matrix. The mechanical properties of these materials depend on such factors (Lange 1982).

As previously referred, zirconia properties depend on its granular metastable microstructure. Concerning the long term stability the low temperature degradation (LTD) phenomenon has to be considered, this degradation is due to a progressive and spontaneous transformation from T to M (Piconi *et al.*, 1999; Ban 2008; Vagkopoulou *et al.*, 2009) that is followed by a mechanical properties degradation.

Swab *et al* (Swab 1991) resumed the main steps of LTD on TZP:

- 1) The temperature range between 200-300° C is the most critical;
- 2) The LTD effects are the strength, toughness and density reduction as well as the increasing of M phase content;
- 3) The material degradation is due to the T- M transformations taking place with micro- and macro- cracking of the material;
- 4) The T-M transformation begins superficially and progresses into the

material bulk;

- 5) Reducing the grain size and/or increasing the stabilizing oxide concentration reduces the transformation rate;
- 6) The presence of water or vapor enhances the transformation T-M (Swab 1991).

Surface degradation during LTD involves roughening, increasing wear and micro-cracking, grains pullout and possible premature failure of the material (Chevalier 2006). Although LTD has been shown to be indirectly associated with a series of femoral head prostheses failures in 2001, and despite a well established definition of the conditions for which LTD is susceptible to occur, there seems to be no clear relationship between LTD and failure predictability when zirconia is used as bioceramic (Chevalier 2006; Denry *et al.*, 2008).

Y- PSZ (Yttrium-oxide partially stabilized zirconia) exhibits exceptional fundamental properties of great interest to biomedical appliances such as high strength, hardness, fracture toughness, wear resistance, low thermal conductivity, good frictional and non-magnetic behavior, modulus of elasticity similar to steel, corrosion resistance to acids and alkalis and coefficient of thermal expansion similar to iron (Vagkopoulou *et al.*, 2009), and they are exposed in table 3.

<i><b>Chemical composition (wt%)</b></i>	
<b>ZrO<sub>2</sub>- Y<sub>2</sub>O<sub>3</sub></b>	>99.0
<b>Y<sub>2</sub>O<sub>3</sub></b>	4.5-5.4
<b>Al<sub>2</sub>O<sub>3</sub></b>	<0.5
<b>Other oxides</b>	<0.5
<i><b>Physical properties</b></i>	
<b>Bulk Density (g/cm<sup>3</sup>)</b>	6.05
<b>Grain size (μm)</b>	0.2
<b>Monoclinic phase (%)</b>	1
<b>Porosity (%)</b>	< 0.1
<i><b>Mechanical Properties</b></i>	
<b>Flexural strength(4 points) (MPa)</b>	1666
<b>Elastic modulus (GPa)</b>	201
<b>Vickers Hardness (HV)</b>	1270
<b>Fracture toughness (Kgf/mm<sup>2/3</sup>)</b>	16.8
<b>Fracture toughness (MPa m<sup>-1</sup>)</b>	7-10
<b>Compressive strength (MPa)</b>	4900
<b>Impact strength (MPa)</b>	137
<i><b>Thermal properties</b></i>	
<b>Thermal expansion coefficient (x 10<sup>-6</sup>/°C)</b>	11x 10 <sup>-6</sup> K <sup>-1</sup>
<b>Thermal Conductivity (W/ m°K)</b>	2
<b>Specific Heat (J/kg°K)</b>	500

Table 3. Chemical composition, physical, mechanical and thermal properties of Y- PSZ.

Y-TZP cores have a radiopacity comparable to metal, which allows, via X-ray, a rigorous marginal integrity evaluation, the cement excesses presence observation and secondary caries diagnosis (Raigrodski 2004).

Zirconia can be milled in two main ways by CAD-CAM. First a core or framework increased in volume can be designed and milled from an homogeneous pre-sintered zirconia block (Sundh *et al.*, 2005). The framework suffers a linear contraction in the range of 20-25% during sintering until the desired dimension is achieved. This process known as green milling, not only reduces the working time but also diminishes the cutting instruments wear (Piwowarczyk *et al.*, 2005). On the other hand, Y-TZP cores can be milled, directly from a totally sintered zirconia block to the final dimensions, by a method called hard machining. Nevertheless this method can compromise the material microstructure and strength (Luthardt *et al.*, 2002; Luthardt *et al.*, 2004).

The spectrum of the contemporary clinical applications of zirconia includes the fabrication of veneers, full and partial coverage crowns or fixed partial dentures (FPDs), pods and/or cores, implants and implants abutments. In addition, different zirconia-based auxiliary components such as cutting burs and surgical drills, extracoronal attachments, and orthodontic brackets are also available as commercial dental products (Koutayas *et al.*, 2009).

## I.2 Adhesion in Dentistry

Adhesion is defined as the phenomenon in which of two surfaces that are held together by chemical or physical forces, or both, often with the aid of an adhesive (ISO/TR 11405: 1993) (International *et al.*, 1993). Adhesion implies a contact between adherent and adhesive by physical and chemical interactions. The adhesion conditions involve several mechanisms, compatibles and that can be observed simultaneously:

1. Mechanical adhesion depends on the adhesive penetration in the adherent micro or macroscopic irregularities.
2. Chemical adhesion, which is based in forces present in chemical bonds between the adherent and the adhesive. These can be primary and strong (ionic and covalent) or secondary or weak (Van der Waal's forces, Hydrogen bond, London dispersion forces).

In Prosthodontics, a strong adhesion provides high retention, improves marginal adaptation and prevents the micro infiltration, increases the fracture strength of the restored tooth and its restoration (Blatz *et al.*, 2003). This kind of bonding is based on micro-mechanical interconnections and chemical adhesion of the adhesive to the ceramics surface, which requires creation of roughness and have adequate cleaning to ensure the surface activation. Mechanical surface treatments such as sandblasting, sandblasting with alumina particles, abrasion with rotating tools, or chemical treatments such as acid etching and/or combinations of these are commonly accept.

### *I.2.1 Classical dental ceramics adhesion*

The adhesion to glass ceramics containing silica is a predictable process with lasting results when proceeding with the following protocol. Etching with hydrofluoric acid (HF) can achieve a favorable surface for bonding in the glass ceramics (Sorensen *et al.*, 1991; Blatz *et al.*, 2003). When the silica-based ceramics are treated with HF the glass matrix is dissolved and may be rinsed thereby obtaining a microscopically porous and micro-retentive surface with high energy. The acid treatment also increases the density of hydroxyl groups (-OH) on the surface, which potencies the connections between the surfaces with silica and the silanes (Matinlinna *et al.*, 2007).

The silanes are bifunctional molecules that bond to the silica dioxide ( $\text{SiO}_2$ ) through the -OH groups of the surface of the ceramics, on the other hand they have a functional group that co-polymerize with organic matrix resins. The silanization also increases the wettability of the ceramic surface. Thus we see that the bonding with the ceramic occurs by a condensation reaction between the silanol group (Si-OH) of the ceramic surface and the silanol groups of the hydrolyzed silane molecule, creating siloxanes joints (Si-O-Si) (with a water molecule as subproduct). The bonding occurs with the resin by the polymerization by addition reaction between methacrylate groups to the organic portion of the silane during the curing reaction of the resin used in the cementing (Söderholm *et al.*, 1993).

Mechanical engraving methods are sidelined since they can damage the ceramic and decrease its physical properties.

## *I.2.2 Crystalline dental ceramics adhesion*

The composition and mechanical properties of alumina and zirconia crystalline ceramics differ substantially from those of classical ceramics. The lack of silica makes the acid etching with HF useless and also removes the possibility of chemical bonding between silica-silane necessary for silanization, thus requiring the implementation of new techniques to achieve strong and durable adhesion (Kern *et al.*, 1998). Bonding to zirconia has become a topic of interest. Traditional adhesive chemistry is ineffective on zirconia surface, once it is non-polar and inert. The currently approaches for adhesive bonding to zirconia bioceramics are not suitable for all clinical applications, and long term durability is currently unknown (Blatz *et al.*, 2004).

### I.2.2.1 Luting cements mostly used with zirconia ceramics

Generally, the cements function is to establish a reliable retention between the indirect restorations inner surface and tooth structure irregularities, protecting the remaining tooth structure, providing a durable margins seal from oral fluid and/or bacteria micro-infiltration and adequate optical properties (Burke 2005).

Resin cements are active luting materials capable of bonding with enamel, dentin and indirect restorations surfaces. The difficulty associated with the use of resin cements lies in the application technique (Burke 2005). The use of resin cements requires a bonding procedure, in which becomes necessary the application of a series of complicated

bonding procedures to the dental substrate as to restoration surface (ceramic, composite, etc.). These cements application technique is critical, susceptible to factors related to the material and the operator that can lead to the occurrence of postoperative sensitivity and restorative treatment failure (Ferracane *et al.*, 2011).

Adhesive cements have been developed in order to combine the easy handling and self adhesion of conventional cements with the resin cements superior mechanical, adhesive and esthetic properties. Self-adhesive cements application is summarized as a clinical single step: after mixing base and catalyst pastes, the material is applied directly to the surfaces that will be bonded (Proença 2010).

There is a notable problem with chemical bonding a resin to Y-TZP as it is an inert, non-reactive and complex surface with Zr atoms on the surface. In contemporary dental research literature, there can be found several studies suggesting that the use of a phosphate monomer containing luting resin which provides higher bonding strength values to zirconia than conventional luting cements (Atsu *et al.*, 2006; Lüthy *et al.*, 2006; Wolfart *et al.*, 2007; Shahin *et al.*, 2010).

## I.3 Surface conditioning to improve resin/zirconia adhesion

In order to achieve good adhesion, the key requirement is that the substrate surface is clean, dry and degreased. The surface conditioning is a set of procedures that aims to increase the surface energy of the substrate to improve its affinity to the adhesive agent. Thereby it is intended that the surface energy of the substrate to be greater than the cohesive forces of the molecules of the adhesive agent so that the wettability is as high as possible.

Because of the difficulty in creating mechanical and chemical bonding in zirconia, alternative methods have been explored to bond zirconia using resin cements. In the following sections will be described some important techniques used in the conditioning of the surface of the zirconia used in dentistry (table 5).

### *I.3.1 Grinding*

Surface grinding is commonly used for roughening the zirconia surface. In dental laboratories, the usual procedure is blasting surfaces with alumina particles ( $\text{Al}_2\text{O}_3$ ) with an average size of 50 microns under a pressure of 380 kPa for about 10-15 s at a perpendicular distance of 10 mm from the holder (Blatz *et al.*, 2003). Some alumina particles can become embedded in the surface during blasting. Thus an alumina coated onto the substrate is formed after blasting. The amount of alumina increases with increasing blasting pressure (Darvell *et al.*, 1995). After silanization = Al-O-Si  $\equiv$  links can form, however they are

hydrolytically unstable (Lung *et al.*, 2012).

Other methods can be used for surface grinding: grinding using abrasive paper or wheels (SiC or Al<sub>2</sub>O<sub>3</sub>) and grinding using a diamond bur (Dérand *et al.*, 2000). These grinding methods are easy to apply in a dental environment. However research has concluded that these techniques, using traditional resin cements, have no significant effect on increasing the bond strength of zirconia to resin cements (Kern *et al.*, 1998; Dérand *et al.*, 2000; Wegner *et al.*, 2000; Piwowarczyk *et al.*, 2005; Atsu *et al.*, 2006; Blatz *et al.*, 2007; Akin *et al.*, 2011; Gomes *et al.*, 2013; Sarmento *et al.*, 2014).

### *I.3.2 Pyrochemical silica coating*

This process makes a pyrochemical and thermal silica coating application to the surface searching for obtain a durable covalent bonding  $\equiv\text{Si-O-Si}\equiv$ . The implementation systems of this method are the Silicoater® Classical, the Silicoater® MD and Siloc® (Heraus-Kulzer, Wehnheim, Germany) (Matinlinna *et al.*, 2007). Silicoater® system is composed by a serialization where the substrate, after blasting, passes through a flame. A silane solution is injected into the flame and a series of pyrochemical reactions occur, resulting in a silica coating on the surface (Matinlinna *et al.*, 2007). The gas is lit and the silane decomposed in the flame, coating the material with a layer of SiO<sub>x</sub>-C that bond adhesively to the surface of the material (Janda *et al.*, 2003). After cooling, to room temperature, layer of silane is applied on the newly formed silica layer and

allow it to proceed with adhesion (Kolodney *et al.*, 1992).

Silicoater® has been successful in improving the bond strength of resin cement to metals and decreasing the bond degeneration after thermocycling (Peutzfeldt *et al.*, 1988; Hummel *et al.*, 1994). Nevertheless, it was expensive and too complex to be commercially viable for standard dental applications.

Recent innovations in pyrolytical silica coating, the PyrosilPen-Technology (PyrosilPen, SurA Instruments, Jena, Germany) have made it easier to use for chair-side applications (Janda *et al.*, 2003). Only two studies were found about this technology application on ceramics (Janda *et al.*, 2003; Rüttermann *et al.*, 2008) so further investigation is required before it can be used as an acceptable method to enhance bonding of zirconia to resin cements (Thompson *et al.*, 2011).

### *I.3.3 Tribocochemical silica coating*

The basic principle of the tribocochemistry are the chemical and physicochemical changes of the matter during the application of mechanical energy (Fischer 1988). The Rocatec™ and CoJet™ (3M ESPE, Seefeld, Germany) systems using silica-coated alumina particles and compressed air for blasting the substrate surface. The impact of particles on the substrate results in kinetic energy transfer. The energy absorbed by the substrate surface cause its microscopic fusion, momentarily the surface temperature increases to 1200 °C. The particles of silica coated alumina penetrate the surface and become embedded in the substrate surface leaving the surface partially silica coated. This surface can

be subsequently primed by silanization, after which adhesive cement may be used.

The tribochemical silica coating is achieved using both the Rocatec™ Soft (with  $\text{Al}_2\text{O}_3$ - $\text{SiO}_2$  particles of 30  $\mu\text{m}$ ) or Rocatec™ Plus (with  $\text{Al}_2\text{O}_3$ - $\text{SiO}_2$  particles of 110  $\mu\text{m}$ ) blasting with a pressure of 280 kPa for 13 s/cm<sup>2</sup> at a perpendicular distance of 10 mm (Lung *et al.*, 2010).

#### *I.3.4 Selective Infiltration etching (SIE)*

With this surface conditioning method the surface of the zirconia is coated with a thin layer of a containing glass conditioning agent which is heated to a temperature above the glass transition temperature. The molten glass infiltrates the limits of micro-granular structure of the zirconia exerting capillary forces and surface tension. Finally, the glass is removed by an acid bath after cooling to room temperature, which creates a new 3D (Three Dimensional) network of inter-granular porosity that allows nano-mechanical interlocking of the resin cement (Aboushelib *et al.*, 2007; Aboushelib *et al.*, 2010). It was observed that the combination of SIE the use of silanes significantly improves the resin zirconia adhesion (Aboushelib *et al.*, 2008; May *et al.*, 2010; Aboushelib *et al.*, 2011; Queiroz *et al.*, 2013; Gomes *et al.*, 2015). Casucci *et al* (Casucci *et al.*, 2009) confirmed, with an AFM (Atomic Force Microscopes) work, that the surface roughness of zirconia after SIE is significantly greater when compared to APA (airborne particle abrasion) or HP etching (Casucci *et al.*, 2009).

### I.3.5 Laser treatment

The surfaces of the zirconia specimens can be treated with Nd: YAG or Er: YAG laser. After treating surfaces with laser is applied silane and proceed with the adhesive technique. It was reported that the adhesive strength of the laser-treated zirconia is superior when compared with the one that follows sandblasting (Spohr *et al.*, 2008). However the measured forces vary considerably depending on the type of laser used (Akyil *et al.*, 2010; Kasraei *et al.*, 2014; Kara *et al.*, 2015).

Currently, research is now beginning to focus on the use of femtosecond laser irradiation as surface treatments to perform the conditioning of zirconia surface (Akpinar *et al.*, 2015) encouraging results having been obtained in the sense of improvements in adhesive effectiveness.

<b>Title</b>	<b>Author</b>	<b>Year</b>	<b>Zirconia surface treatment.</b>	<b>Results and/or Conclusions.</b>
<i>Effect of various lasers on the bond strength of two zirconia ceramics.</i>	Kara O, Kara HB, Tobi ES, Ozturk AN, Kilic HS.	2015	72 ceramic discs of zirconia ceramics were divided into 2 groups according to the computer-aided design and manufacturing and then divided into three groups: <b>Group FS:</b> femtosecond laser. <b>Group NY:</b> Nd:YAG laser. <b>Group EY:</b> Er:YAG laser.	MPa and roughness were significantly affected by laser type being FS laser that had higher values.

<i>Efficacy of surface roughness and bond strength of Y-TZP zirconia after various pre-treatments.</i>	Kirmali O, Kustarci A, Kapdan A, Er K.	2015	80 discs of Y-TZP were divided into eight groups: <b>Group 1:</b> untreated (control). <b>Group 2:</b> air abrasion. <b>Group 3:</b> Er,Cr:YSGG laser irradiation-energy 1W. <b>Group 4:</b> Er,Cr:YSGG laser irradiation-energy 2W. <b>Group 5:</b> Er,Cr:YSGG laser irradiation-energy 3W. <b>Group 6:</b> Er,Cr:YSGG laser irradiation-energy 4W. <b>Group 7:</b> Er,Cr:YSGG laser irradiation-energy 5W. <b>Group 8:</b> Er,Cr:YSGG laser irradiation-energy 6W.	Surface treatment with air abrasion and high laser energy intensities (3-6W), can improve the bonding properties of Y-TZP zirconia.
<i>Effects of some chemical surface modifications on resin zirconia adhesion.</i>	Liu D, Tsoi JK, Matlinn a JP, Wong HM.	2015	Pre-sintered zirconia discs were randomly divided into: <b>Control group:</b> without any modification. <b>Group S:</b> fully sintered and sandblasted with silica coated alumina particles. <b>Group HN:</b> fully sintered and etched with a blend of mineral acid solution at 100 °C for 25 min. <b>Group HF:</b> fully sintered and etched with 48% hydrofluoric acid solution at 100 °C for 25 min. <b>Group Si:</b> silica coating and fully sintered.	Resin-zirconia adhesion could be effectively improved by both HF etching and silica coating on zirconia surface.
<i>Mechanical properties and bonding potential of partially stabilized zirconia treated with different chemomechanical treatments.</i>	El-Korashy DI, El-Refai DA.	2014	Pre-sintered yttrium-stabilized zirconium oxide blocks (in Coris ZI) were classified into: <b>Group 1:</b> air-borne particle abrasion (ABA). <b>Group 2:</b> silica coating. <b>Group 3:</b> hot etching solution. <b>Group 4:</b> hot etching solution followed by ABA. <b>Group 5:</b> hot etching solution followed by silica coating. <b>Group 6:</b> control.	Silica coating induced significant improvement in zirconia-resin interface, but its use of combined with treatment of hot etching solution did not provide an added advantage.
<i>Bond strength of resin cement to CO<sub>2</sub> and Er:YAG laser-treated zirconia ceramic.</i>	Kasraei S, Rezaei-Soufi L, Heidari B, Vafaei F.	2014	45 zirconia disks were assigned to 3 groups: <b>Group CNT:</b> control group. <b>Group COL:</b> CO <sub>2</sub> laser. <b>Group EYL:</b> Er:YAG laser. Composite resin disks were cemented on zirconia disk using dual-curing resin cement.	Treatment with CO <sub>2</sub> and Er:YAG laser improves the bond strength, being better than the CO <sub>2</sub> laser.

<i>Effects of surface treatment on bond strength between dental resin agent and zirconia ceramic.</i>	Moradabadi A, Roudsari SE, Yekta BE, Rahbar N.	2014	<p>Specimens of Y-PSZ blocks were divided into:</p> <p><b>Group SZ:</b> zirconia after airborne particle abrasion.</p> <p><b>Group ZH:</b> zirconia specimens after etching.</p> <p><b>Group HSZ:</b> zirconia specimens after airborne particle abrasion and simultaneous etching.</p> <p><b>Group GZ:</b> zirconia specimens coated with a layer of a fluorapatite-leucite glaze.</p> <p><b>Group HGZ:</b> GZ specimens with acid etching.</p> <p><b>Group SGZ:</b> zirconia coated with a layer of salt glaze.</p> <p><b>Group HSGZ :</b> SGZ specimens with 2% HCl etching.</p>	Micromechanical adhesion was a more effective mechanism than chemical adhesion and airborne particle abrasion significantly increased mean shear bond strengths values.
<i>Influence of air-particle deposition protocols on the surface topography and adhesion of resin cement to zirconia.</i>	Sarmento HR, Campos F, Sousa RS, Machado JP, Souza RO, Bottino MA, Ozcan M.	2014	115 sintered zirconia blocks (Lava, 3M ESPE) were divided according to the 'particle type': (Al: 110 µm Al <sub>2</sub> O <sub>3</sub> , and Si: 110 µm SiO <sub>2</sub> ), 'pressure' factors (2.5 or 3.5 bar) and 'thermocycling' (n = 10 per group): Control (no air-abrasion); Al2.5; Si2.5; Al3.5; Si3.5; ControlTC; Al2.5TC; Si2.5TC; Al3.5TC; Si3.5TC.	Air-abrasion with 110 µm Al <sub>2</sub> O <sub>3</sub> resulted in higher roughness, but air-abrasion protocols with SiO <sub>2</sub> promoted better adhesion.
<i>Effect of surface treatments on the bonding strength of self-adhesive resin cements to zirconia ceramics.</i>	Elsaka SE.	2013	<p>Specimens of Y-TZP were divided into four groups:</p> <p><b>Group A:</b> control; no treatment.</p> <p><b>Group B:</b> airborne-particle abrasion.</p> <p><b>Group C:</b> CH<sub>2</sub>Cl<sub>2</sub> for 60 min.</p> <p><b>Group D:</b> hot etching for 60 min.</p>	Adhesion between Y-TZP and resin cement can be improved by the use of CH <sub>2</sub> Cl <sub>2</sub> or hot etching surface treatments.
<i>Silica-based nano-coating on zirconia surfaces using reactive magnetron sputtering: effect on chemical adhesion of resin cements.</i>	Queiroz JR, Massi M, Nogueira L Jr, Sobrinho AS, Bottino MA, Ozcan M.	2013	<p>240 zirconia ceramic blocks (Cercon) were randomly divided into 24 groups according to 3 testing parameters:</p> <p>a) <b>resin cements</b> (Multilink, Panavia F, RelyX U100),</p> <p>b) <b>surface conditioning</b> (No conditioning- control group; Metal/Zirconia Primer; air abrasion + Metal/Zirconia Primer; Si-based nanofilm + Monobond ).</p> <p>c) <b>aging:</b> no aging / thermocycling at 5°C to 55°C, 6000 cs.</p> <p>Resin cements were bonded to zirconia surfaces.</p>	Surface conditioning method had a significant effect on the bond strength values, and chemical adhesion was similar after silica-based deposition and air abrasion.

<i>Bond strength of resin cement to zirconia ceramic with different surface treatments.</i>	Usumez A, Hamdemirci N, Koroglu BY, Simsek I, Parlar O, Sari T.	2013	<p>75 plates of Y-TZP ceramic were assigned to 5 groups:</p> <p><b>Group 1:</b> airborne particle abrasión</p> <p><b>Group 2:</b> Neodymium-doped yttrium aluminum garnet (Nd:YAG) laser irradiation (Fidelis Plus 3, Fotona; 2 W, 200 mJ, 10 Hz, with pulse durations of 180 µs)</p> <p><b>Group 3:</b> laser irradiation with pulse durations of 320 µs.</p> <p><b>Group 4:</b> glaze applied and 9.5 % HF acid gel conditioned.</p> <p><b>Group 5:</b> control.</p> <p>Clearfil Esthetic Cement was adhered onto the surfaces.</p>	<p>Surface treatment s modified the topography of the Y-TZP ceramic, and Nd:YAG laser increased surface roughness and SBS, specifically with short pulse duration.</p>
<i>Influence of sandblasting granulometry and resin cement composition on microtensile bond strength to zirconiacer amic for dental prosthetic frameworks.</i>	Gomes AL, Castillo-Oyagüe R, Lynch CD, Montero J, Albaladejo A.	2013	<p>40 zirconia blocks (Cercon, Dentsply) were divided into:</p> <p><b>Group NT:</b> no treatment.</p> <p><b>Group APA-I:</b> 25-µm Al<sub>2</sub>O<sub>3</sub> particles abrasion.</p> <p><b>Group APA-II:</b> 50-µm Al<sub>2</sub>O<sub>3</sub> particles abrasion.</p> <p><b>Group APA-III:</b> 110-µm Al<sub>2</sub>O<sub>3</sub> particles abrasion.</p> <p>Samples were divided into two subgroups depending on the resin cement used:</p> <p><b>Subgroup PAN:</b> used Clearfil Ceramic Primer Panavia.</p> <p><b>Subgroup BIF:</b> used Bifix SE self-adhesive cement.</p>	<p>PAN bonded to air-abraded surfaces attained the highest MTBS, and BIF recorded no significant differences depending on the conditioning method.</p>
<i>Microtensile bond strength evaluation of self-adhesive resin cement to zirconia ceramic after different pre-treatments.</i>	Casucci A, Goracci C, Chieffi N, Monticelli F, Giovannetti A, Juloski J, Ferrari M	2012	<p>40 cylinder-shaped of zirconia ceramic (Aadva Zirconia) were randomly divided into four groups:</p> <p><b>Group S:</b> Sandblasting with 125 µm Al<sub>2</sub>O<sub>3</sub> particles.</p> <p><b>Group SIE:</b> Selective infiltration etching.</p> <p><b>Group ST:</b> Heated etching solution for 30 min.</p> <p><b>Group C:</b> No treatment.</p> <p>Metal Primer II were applied to half of specimens, and 8 disks for each group were luted with self-adhesive resin cement to composite overlays.</p>	<p>Both surface treatments and Metal Primer II application improved BS values.</p> <p>When Metal Primer II was not applied ST achieve highest BS values.</p>
<i>Durable bonding to mechanically and/or chemically pre-treated dental zirconia.</i>	Inokoshi M, Kameyama A, De Munck J, Minakuchi S, Van Meerbeek B.	2012	<p>Fully sintered IPS e.max ZirCAD (Ivoclar Vivadent) blocks were subjected to tribochemical silica sandblasting (CoJet, 3M ESPE).</p> <p>The samples were additionally pre-treated using one of four zirconia primers/adhesives (Clearfil Ceramic Primer, Kuraray Noritake; Monobond Plus, Ivoclar Vivadent; Scotchbond Universal, 3M ESPE; Z-PRIME Plus, Bisco).</p>	<p>Combined mechanical/chemical pre-treatment resulted in the most durable bond to zirconia.</p>

<i>Influence of surface treatments and resin cement selection on bonding to zirconia.</i>	Subaşı MG, Inan O.	2012	<p>Sintered zirconia specimens were divided into five groups:</p> <ul style="list-style-type: none"> <li><b>Group 1:</b> control.</li> <li><b>Group 2:</b> air abrasión.</li> <li><b>Group 3:</b> silica coating.</li> <li><b>Group 4:</b> laser.</li> <li><b>Group 5:</b> air abrasion + laser.</li> </ul> <p>Composite were then bonded using RelyX U100 (RXU), Clearfil Esthetic Cement (CEC) and Panavia F (PF).</p>	There were no significant differences between the air abrasion and air abrasion + laser groups and the silica coating and laser groups.
<i>Shear bond strength of resin cement to zirconia ceramic after aluminum oxide sandblasting and various laser treatments.</i>	Akın H, Ozkurt Z, Kırmalı O, Kazazoglu E, Ozdemir AK.	2011	<p>120 zirconia specimens were assigned to six groups:</p> <ul style="list-style-type: none"> <li><b>Group 1:</b> untreated (control).</li> <li><b>Group 2:</b> sandblasted.</li> <li><b>Group 3:</b> Er:YAG laser irradiated.</li> <li><b>Group 4:</b> Nd:YAG laser irradiated with contact.</li> <li><b>Group 5:</b> Nd:YAG laser irradiated with non-contact.</li> <li><b>Group 6:</b> CO<sub>2</sub> laser irradiated.</li> </ul>	Er:YAG and Nd:YAG laser treatment increased the bond strength of zirconia compared to sandblasting and CO <sub>2</sub> laser treatment.
<i>Evaluation of zirconia/resin bond strength and interface quality using a new technique.</i>	Aboushelib MN.	2011	<p>Zirconia disks received one of these surface treatments: selective infiltration etching or airborne-particle abrasion with 50-μm Al<sub>2</sub>O<sub>3</sub> particles, while as-sintered surfaces served as control.</p> <p>The disks were bonded to pre-aged composite resin disks using a light-polymerized adhesive resin (Panavia F 2.0).</p>	Micromechanical retention and adhesion promoters are prerequisites for establishing a strong and durable bond to zirconia.
<i>Bond strength of three luting agents to zirconia ceramic - influence of surface treatment and thermocycling .</i>	Attia A.	2011	<p>18 blocks zirconia (ICE Zirkonia) were divided into:</p> <ul style="list-style-type: none"> <li><b>Group AA:</b> airborne-particle abrasion.</li> <li><b>Group SC:</b> silica-coating.</li> <li><b>Group SCSI:</b> silica coating followed by silane.</li> </ul> <p>After, they were divided into 3 subgroups according to the luting agents: Resin-modified glass-ionomer cement (Ketacem Plus), self-adhesive resin cement (RelyX Unicem) and adhesive resin cement (MultiLink Automix).</p>	Silica coating followed by silane application together with adhesive resin cements significantly increased μTBS, while thermocycling significantly decreased μTBS.

<i>Effect of surface pre-treatments on the zirconia ceramic-resin cement microtensile bond strength.</i>	Casucci A, Monticelli F, Goracci C, Mazzitelli C, Cantoro A, Papacchini F, Ferrari M.	2011	<p>12 cylinder-shaped blocks of a commercial zirconium-oxide ceramic (Cercon® Zirconia, DENTSPLY) were randomly divided into 4 groups (n=3):</p> <p><b>Group S:</b> Sandblasting with 125 µm Al<sub>2</sub>O<sub>3</sub> particles.</p> <p><b>Group SIE:</b> selective infiltration etching.</p> <p><b>Group 3 ST:</b> experimental hot etching solution for 30 min.</p> <p><b>Group C:</b> no treatment.</p> <p>Composite cylinders were bonded to conditioned ceramics using a resin cement (Calibra®, DENTSPLY).</p>	SIE and ST treatments had higher bond strengths than when zirconia ceramic was treated with airborne particle abrasion or left untreated.
<i>Evaluation of self-adhesive resin cement bond strength to yttria-stabilized zirconia ceramic (Y-TZP) using four surface treatments.</i>	Miragaya L, Maia LC, Sabrosa CE, de Goes MF, da Silva EM.	2011	<p>40 plates of a Y-TZP were divided into four groups:</p> <p><b>Group 1:</b> control, no treatment.</p> <p><b>Group 2:</b> airborne-particle abrasion with 50-µm Al<sub>2</sub>O<sub>3</sub>.</p> <p><b>Group 3:</b> coating with an MDP-based primer.</p> <p><b>Group 4:</b> conditioning with Rocatec System.</p> <p>The plates were divided according to the resin cement tested: RelyXTM ARC (ARC, conventional) and RelyXTM Unicem (Ucem, self-adhesive).</p>	Surface treatments significantly influenced the µSBS, and the highest µSBS values were presented by UCem on zirconia treated with the MDP-based primer and Rocatec system.
<i>Pilot evaluation of four experimental conditioning treatments to improve the bond strength between resin cement and Y-TZP.</i>	Monaco C, Cardelli P, Scotti R, Valandro LF.	2011	<p>50 Y-TZP ceramic discs were allocated into five groups:</p> <p><b>Gr1 (control):</b> no conditioning.</p> <p><b>Gr2:</b> silica coating (30-µm SiO<sub>2</sub>) before sintering.</p> <p><b>Gr3:</b> air abrasion with 50-µm Al<sub>2</sub>O<sub>3</sub> before sintering.</p> <p><b>Gr4:</b> air abrasion with 110-µ Al<sub>2</sub>O<sub>3</sub> before sintering.</p> <p><b>Gr5:</b> air abrasion with 50-µm Al<sub>2</sub>O<sub>3</sub> after sintering.</p> <p>After specimen preparation, cylinders of composite resin were prepared and immediately cemented onto the Y-TZP surface.</p>	Additional surface treatment with air abrasion before and after sintering provided a significant increase in bond strength.
<i>Effect Of Nd:YAG laser and CO<sub>2</sub> laser treatment on the resin bond strength to zirconia ceramic.</i>	Paranhos MP, Burnett LH Jr, Magne P.	2011	<p>80 Lava (3M ESPE) blocks were embedded in acrylic resin, polished, and randomly divided into three groups:</p> <p><b>Group 1:</b> no abrasión.</p> <p><b>Group 2:</b> Al<sub>2</sub>O<sub>3</sub> airborne-particle abrasion (50 µm).</p> <p><b>Group 3:</b> silica-coating (Cojet, 3M ESPE).</p> <p>Each group was divided into three subgroups that were treated with Nd:YAG laser, CO<sub>2</sub> laser, or not laser.</p> <p>Resin cement (Panavia F, Kuraray) were applied.</p>	Nd:YAG laser pretreatment created consistent roughness and significantly increased zirconia shear bond strength values to Panavia F.

<i>Bond strength of resin cement to yttrium-stabilized tetragonal zirconia ceramic treated with air abrasion, silica coating, and laser irradiation.</i>	Akyil MS, Uzun IH, Bayindir F.	2010	<p>141 Y-TZP discs were assigned to:</p> <ul style="list-style-type: none"> <li><b>Group 1:</b> C- no treatment.</li> <li><b>Group 2:</b> AA- air abrasión.</li> <li><b>Group 3:</b> CJ- silica coating.</li> <li><b>Group 4:</b> ER- Er:YAG laser.</li> <li><b>Group 5:</b> ND- Nd:YAG laser.</li> <li><b>Group 6:</b> CO- CO<sub>2</sub> laser.</li> <li><b>Group 7:</b> AA+ER- air abrasion + Er:YAG laser.</li> <li><b>Group 8:</b> AA+ND- air abrasion + Nd:YAG laser.</li> <li><b>Group 9:</b> AA+CO- air abrasion + CO<sub>2</sub> laser.</li> </ul> <p>Specimens were silanized and composite were cemented.</p>	Although air abrasion and silica coating were the most effective surface treatments, CO <sub>2</sub> and Er:YAG laser irradiation alone or Nd:YAG laser irradiation after air abrasion may be used as an alternative.
<i>Effect of silica coating combined to a MDP-based primer on the resin bond to Y-TZP ceramic.</i>	May LG, Passos SP, Capelli DB, Ozcan M, Bottino MA, Valandro LF.	2010	<p>96 Y-TZP tabs were randomly divided into four groups:</p> <ul style="list-style-type: none"> <li><b>Group 1:</b> cleaning with isopropanol (ALC).</li> <li><b>Group 2:</b> ALC + phosphoric acid etching + MDP-based primer application (MDP-primer).</li> <li><b>Group 3:</b> silica coating + 3-methacryloyloxypropyl trimethoxysilane (MPS)-based coupling agent application (SiO<sub>2</sub> + MPS-Sil).</li> <li><b>Group 4:</b> SiO<sub>2</sub> + MDP-primer.</li> </ul>	Bonding values were higher and more stable in the SiO <sub>2</sub> groups. The use of MDP-primer after silica coating increased the bond strength.
<i>The effect of zirconia surface treatment on flexural strength and shear bond strength to a resin cement.</i>	Qeblawi DM, Muñoz CA, Brewer JD, Monaco EA Jr.	2010	<p>Zirconia blocks were assigned into 16 groups. Each group underwent a combination of the following treatments.</p> <p><b>Mechanical treatment:</b> control (no treatment), airborne-particle abrasion, silica coating, or wet hand grinding.</p> <p><b>Chemical treatment:</b> control (no treatment), acid etching followed by silanation, silanation only, or application of zirconia primer.</p>	Mechanical and chemical conditioning was essential to develop a durable resin bond to zirconia.
<i>The effect of laser treatment on bonding between zirconia ceramic surface and resin cement.</i>	Ural Ç, Külänk T, Külänk S, Kurt M.	2010	<p>40 zirconia cores were produced and divided into:</p> <ul style="list-style-type: none"> <li><b>Group C:</b> no treatment applied (control).</li> <li><b>Group SB:</b> bonding surfaces of ceramic disks were airborne particle-abraded with 110-µm alumina oxide particles.</li> <li><b>Group HF:</b> bonding surfaces of ceramic disks were etched with 9.6% hydrofluoric acid.</li> <li><b>Group L:</b> bonding surfaces of ceramic disks were irradiated by a CO<sub>2</sub> laser.</li> </ul>	CO <sub>2</sub> laser may be an effective method for conditioning zirconia, enhancing micromechanical retention and improving the bond strength.

Table 4. Tables of most relevant and recent articles using zirconia surface treatment to enhance the adhesive effectiveness of the zirconia - resin interface.

## I.4 Femtosecond laser irradiation as treatment surface

### *I.4.1 Definition of laser and its introduction in dentistry*

The laser (Light Amplification by Stimulated Emission of Radiation) is a device that uses a quantum mechanical effect, induced or stimulated emission, to generate a beam of light (also called laser) consistent of a suitable medium and the size, the shape and the purity controlled. That is, a laser is a collimated, monochromatic and coherent light.

The laser appeared in 1916, when Albert Einstein laid the foundation for the development of lasers and their predecessors, the maser (microwave emitting) using the law of Max Planck radiation based on the concepts of spontaneous emission and induced radiation. This theory assumes the conceptual basis of the optical amplification (Sulewski, 2000).

In dentistry, the use of lasers has been a constant evolution and development; more and more dental specialties in which the different varieties of laser in either diagnostic or therapeutic procedures are applied (Oltra-Arimon *et al.*, 2004).

The application of lasers in dentistry must be based on knowledge of a number of physical and biological processes that depend on various factors, in particular, the phenomena of absorption depends mainly on two factors: the wavelength of the laser and the optical characteristics of tissue to be irradiated

(España-Tost *et al.*, 2004).

The oral cavity contains very different tissues from each other; therefore the optical tissues that form will not have the same behavior when they are irradiated with the same wavelength characteristics. That is, we may need a different wavelength of each of the tissues that are in the oral cavity. When the same laser irradiate two different tissues, the effects produced will also be different. Each laser will emit only a single wavelength and therefore can get different effects on the treated tissue (España-Tost *et al.*, 2004).

As for the use of laser in dental practice, some of its main indications in both dental therapeutic and cosmetic dentistry, prosthodontics, surgery, and orthodontics are, among others:

1. Preparation of cavities.
2. Removal of old fillings.
3. Sealing of pits and fissures.
4. Hyperesthesia dentin.
5. Endodontics.
6. Veneers and anterior fillings.
7. Teeth Whitening.

8. Dental carving.
9. Soft tissue injuries.
10. Premalignant lesions.
11. Conditioning of the dental and ceramic surfaces to increase adhesive effectiveness.

#### *I.4.2 Parameters and classification of laser*

The laser parameters can be classified into two groups:

1. NO can be modified by the operator:

- **Wavelength:** it is the spatial period and the distance from pulse to pulse.

Normally they considered two consecutive points having the same phase. The wavelength is a real distance traveled by the wave (which is not necessarily the distance traveled by the particles or wave propagating medium, as in the case of the waves , in which wave advances horizontally and particles move vertically ).

When the laser interacts with the target tissue produces a number of effects depends largely on the wavelength (**table**).

- **Energy distribution of beam laser:** the energy that carry the laser beam from the cavity resonance can be distributed in several ways:

1. Introducing a greater concentration of power in the central part (TEM00).
2. Distributing photons as mesta (TEM multimode).

- **Emission type of beam laser:** you can issue the energy beam in continuous

mode in which the laser beam emitted continuously while it is activated; or pulsed mode in which there are times that the beam emitted and others not.

## 2. YES can be modified by the operator:

- **Frequency:** it refers to the number of pulses produced in a second laser of pulsed type. It is measured in Hertz (Hz) which corresponds to one pulse per second (pps).
- **Energy and power:** the transmission power is the energy emitted in one second. It is measured in watts (W) or sub (mW).
- **Density Power and Energy:** Power density is the concentración of photons per unit area in the emission of a single pulse. It is the ratio of actual output power of the laser transmitter and the beam emitting surface of the same, not the total treatment área. The energy density or fluence is the relationship between the laser power and the surface where the beam hits per unit time in seconds (Velez *et al.*, 2000).

Type of laser	Wavelength	Duration of pulse emission
Argón	488/514 nm	CW
He-Ne	633 nm	CW
CO <sub>2</sub>	10. μm	CW o pulsado
Diodo	370-2200 nm	CW o pulsado
Rubí	694 nm	1-250 μs
Nd:YAG	1064 nm	100 ns-250 μs
Ho:YAG	2120 nm	100 ns-250 μs
Er,Cr:YSGG	2780 nm	100 ns-250 μs
Er:YAG	<b>2940 nm</b>	<b>100 ns-250 μs</b>
Nd:YAG	1064 nm	30-100 ps
Ti:Zafiro	<b>790 nm</b>	<b>10 fs-100 ps</b>

Table 5. Most common types of lasers with wavelength and time duration of the emission.

Lasers are likely to be classified in many ways. They can be classified in relation to:

1. **The active medium:** Gases (CO<sub>2</sub>), liquid (dyes), solid (Nd: YAG, Er: YAG) and diode semiconductors (AsGa).
2. **The emission spectrum:** ultraviolet (wavelength less than 400 nm), visible (wavelengths between 400 and 700 nm) and infrared (wavelength greater than 700 nm).
3. **The emission power:** high power (surgical lasers) and low power lasers (therapeutic lasers). The high power lasers available in the dental market are: Argon, Diodo, Nd:YAG, Nd:YAP, Ho:YAG, Er, Cr:YSGG, Er:YAG y CO<sub>2</sub> (España-Tost *et al.*, 2004).
4. **The power density:** high power density, low density or HLLT power or LLLT.
5. **The shape of issue:** continuous mode (CW) and pulsed mode (Q-switched).
6. **According to the pulse duration:** short (up to several hundred picoseconds), and ultra-short (less than one hundred picoseconds).

The duration of the laser pulse is a very important parameter to consider because the heat diffusion plays an important role in the mechanisms of interaction between light and tissue. Shorter pulses minimize these effects and introduce mechanisms of ablation mediated by plasma (Chen *et al.*, 1999). The type of interaction is a plasma-induced ablation, in which the tooth ablated of its components is a physical conversion. Generally, the longer pulses are less desirable because they produce more thermal damage due to the thermal energy penetrates and accumulates in target tissue enough to induce an undesirable thermo-mechanical effect.

Consequently irreversible damage is caused because the pulp tissues are especially sensitive to these thermal phenomena (Zach *et al.*, 1965).

Moreover the dental hard tissues suffer microfractures or cracks in response to increasing temperature (Boehm *et al.*, 1977; Anic *et al.*, 1992; Sandford *et al.*, 1994; Cox *et al.*, 1994).

Pulses of very short duration and sufficient energy, suitably focused, resulting in energy densities, are capables of producing direct ablation of solid materials (Pronko *et al.*, 1995; Momma *et al.*, 1996; Stuart *et al.*, 1996; Chichkov *et al.*, 1996; Varel *et al.*, 1997; Nolte *et al.*, 1997). Some studies have made a comparison between the effect of a nanosecond laser and one of PS on dental hard tissue, concluding that the morphology of the ablation shows better control with nanosecond and picosecond that there is less effect on surrounding areas (Niemz, 1995; Willims *et al.*, 1996; Lizarelli *et al.*, 1999; Marion *et al.*, 1999; Lizarelli *et al.*, 2000).

#### *I.4.3 Ultrashort lasers: femtosecond laser*

The femtolaser or femtosecond laser is a laser from the group of ultrashort pulse lasers, which are a pulse of laser light with an extremely short duration, namely, less than hundred picoseconds.

The spectacular advance of knowledge about nonlinear processes in materials, next to optoelectronics, have very recently enabled laser radiation sources are capable of emitting pulses of very short duration and enough power that, properly targeted, can produce direct ablation of both metallic and dielectric solids. The mechanism basically consists of nonlinear processes ionization of

atoms or molecules on the surface of the irradiated material, forming a dense plasma that expands the end of the pulse duration typically around 100 fs, with no time to be produce heat diffusion in the solid structure, which requires times of the order of tens of ps, resulting in material removal with little warming. This makes that ultrashort laser can be a very promising tool in producing high accuracy and machining quality with dimensions microns.

The mechanism of interaction of ultrashort pulses is radically different from conventional lasers such as Er:YAG, which allows the ablation of the materials and generates side effects that are also very different .

The interaction of these ultrashort pulses with different materials has been the subject of numerous studies (Bloembergen, 1974, Pronko *et al.*, 1995; Stuart *et al.*, 1995; Chichkov *et al.*, 1996; Momma *et al.*, 1996; Stuart *et al.*, 1996; Varel *et al.*, 1997; Nolte *et al.*, 1997; Gamaly *et al.*, 2002). . For this research, we will focus on describing the interaction process leading to the removal of material, which is known as ultrafast ablation. This phenomenon requires not only that the pulses are ultrashorts but also be able to deposit enough energy per unit area of the material.

For conventional lasers, the electrons absorb the energy of the pulses only if the frequency of the electromagnetic field (the inverse of wavelength) matches the energy difference between energy levels of the atom or molecule, It assumed here that the electron absorbs a light quantum, a photon. If not, it is not absorbed. This makes the crucial parameter to the linear absorption of radiation of, for example Er: YAG, is the wavelength. In that case, the intensity (power per unit

area) or fluence (energy deposited per unit area) only affect the amount of energy that can absorb these electrons, which determines the amplitude of the oscillating movement caused by the electromagnetic field, and then transmitted to the crystal lattice. Thus, the higher the intensity, the higher temperature is reached in the irradiated area or faster a given temperature is reached.

In the present case, when ultrashort pulses incident on the materials, energy is also absorbed by the electrons of the atoms and molecules of the surface layer of material. Linear absorption of radiation with the usual dependence of the wavelength is also produced; in the case of these pulses, if the intensity or fluence have a sufficiently high value (over what is known as the threshold) then the electrons can absorb more than one photon for promoted to higher energy levels. In this case, although there are also still dependence on wavelength, the fundamental factor for that the phenomenon occurs is the intensity that is it to be high enough, ie there are many photons available for absorption by the electrons. It occurs then that any material can absorb the energy of these ultrashort pulses and a more intense absorption the higher the intensity of the pulses, and all this taking place in a fraction of time less than the lower pulse duration.

Thus, if the intensity is high enough may occur that some of the electrons, that are performing oscillating movements of large amplitude within the electromagnetic field of the laser, end leaving be linked to the ions, and they become electrons free, in the process known as multiphoton ionization. These electrons continue to experience the action of the field duration of the pulse so that its oscillating movement can, by collision, cause that other electrons that are

weakly bonded to the ions, are be separated.

As the average time it takes an electron to give their energy to the lattice is greater than ps for any material (varies from a few to hundreds of ps, depending on material) is then that the process of absorption, ionization and ejection of the material It takes place without there has been practically energy transmission to the crystal lattice and therefore no temperature rise or heat transfer to the material surrounding the processed region occurs. This is a process of ablating thermal of inherent nature known as Coulomb explosion (Figure 3).

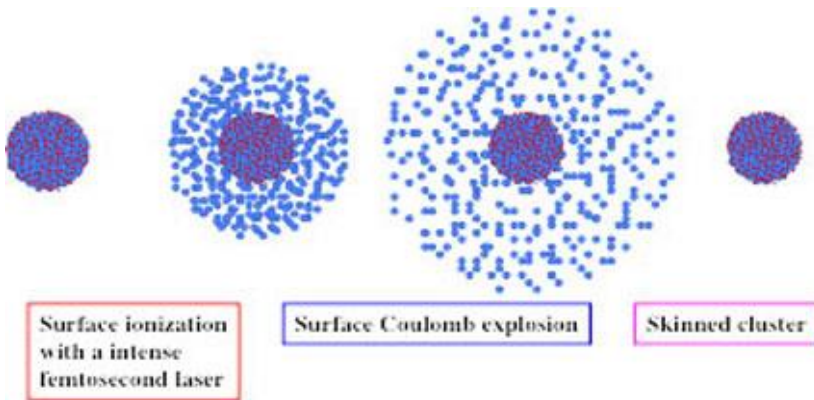


Figure 3. Coulomb explosion.

However, it should be noted that this process of thermal ablation is not the only way to remove material from the surface by these ultrashort pulses. In fact, as soon as the current exceeds the threshold for nonlinear ionization is triggered, this Coulomb process, which the material removal rate is very low, begins to compete with another that is of thermal nature, known as phase explosion. Indeed, when the intensity of the pulse rises, the number of free electrons generated is also very high and they continue to absorb more and more energy to

a point where they begin to radiate the energy in all directions and inconsistently.

Some of that radiation is directed towards the material surface where it is absorbed by it linearly, raising its temperature in a very tight spiral which causes melting and / or vaporization of the material almost immediate. In this case, the material is ejected without having been absorbed energy conducted beyond a few microns in the irradiated area. The result is that the material is removed in much larger quantities than in the Coulomb explosion process and thermal effects on surrounding areas, but not non-existent, are much more limited than in conventional spatial ablation

The ultrafast ablation process allows for eliminating, any material with a very high accuracy and with little side effects thermal or mechanical, not being the heat conducting a determining factor, because the absorbed laser energy is removed from the area process almost entirely of material transport.

According to all this we can say that the advantages may be summarized as follows: first , the minimum thermal and mechanical damage that occurs in the area adjacent to the processed material without observed residues neither resolidified melt or cracks or fissures; second , the universal applicability of the process , and which can be used for any type of material and not working environments with specific conditions are needed; and third , the ability to deposit on the material, the desired amounts of energy with great speed and accuracy, resulting in an enormous dimensional geometric precision and

machining quality, high reproducibility and no postprocessing. The biggest drawback of this technology lies in the low processing speed, overriding requirement in any industrial application, which, for now, prevents competition with other processes of less precision. Also, not being a mature technology, the cost of investment in equipment is still outrageously high relative to existing procedures.

Due to recent progress on the technology of ultrashort pulse laser, the femtosecond laser has been introduced in Dentistry (Kohns *et al.*, 1997; Momma *et al.*, 1997; Serbin *et al.*, 2002). And so, in the 90s, begin to appear publications on ultrashort pulse lasers in dentistry, and so, in 1993, MH Niemz (Niemz *et al.*, 1993), made the first proposal for the application of ultrashort pulse lasers to avoid thermal effects and the low rate of ablation.

Recently, it has begun to use femtosecond lasers in Dentistry as surface treatments to perform the conditioning of biological and non-biological surfaces (Luengo *et al.*, 2013; Lorenzo *et al.*, 2014; Lorenzo *et al.* 2015).

#### *I.4.4 Ti:Sapphire laser*

The Ti:Sapphire laser is a laser that belong to the group of ultrashort lasers, specifically to femtosecond laser group. It was introduced in 1986 by Moulton and it has subsequently been used in experimental studies of dental tissues in Dentistry (Kohns *et al.*, 1997; Serbin *et al.*, 2002) because is a highly

efficient laser material.

Its active medium is the sapphire and the amount of the titanium within the host material which is the sapphire ions is around 0.1% and are replacing these aluminum atoms in the crystal, because it has a hexagonal crystal structure. Its melting point is 2050 ° C and has a density of 3,98g / cm<sup>3</sup> and a hardness of 9 on the Mohs scale.

The absorption range is between 400 and 600nm with the peak at 488-490 nm, and the emission range, its wavelength, is 600 to 1050 nm with a peak located at 795 nm (Figure 4). Fluorescencua spectrum ranges from 600-1050 nm.

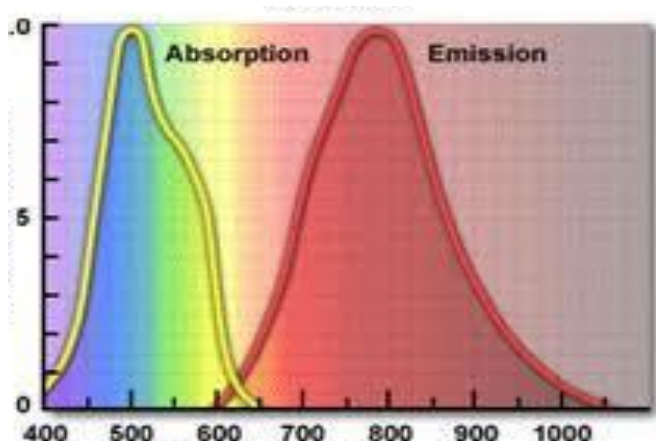


Figure 4. The absorption and emission rates of Ti:Sapphire laser.

Although the issuance of Ti: Sapphire is tunable in the spectral range between 650 and 1100 nm, most emission efficiency is obtained around 800 nm. Pumping power the Ti: Sapphire laser is 3 to 10 W and performed by other lasers emitting from 514 to 532 nm where the glass has the highest absorption coefficient, so Argon ion laser (514.5 nm) or solid-state lasers such as Nd:YAG, Nd: YLF or Nd: YVO (527-532 nm) are used.

The emission of a laser Ti: Sapphire is little energy, being the energy obtained by pulse of around nJ at a repetition rate of tens of MHz. Although useful for many other technological applications, these pulse energies are insufficient to cause the ablation of materials so that the pulsed output of these lasers is then subjected to amplification process energy of a fraction of the emitted pulses. It is what is known as regenerative amplification type CPA (Chirped Pulse Amplification) that was developed in the late eighties by Mourou et al. (Strickland and Mourou, 1985) (Figure 5) and it is a process in that are selected, in an optical cavity, a small number of pulses of the emission of the oscillator Ti: Sapphire (usually thousand per second), passed by a network of diffraction that stretches over time making them ns pulses and then, through a pump laser powerful, another glass Ti: Sapphire is radiated by where the energy pulses are passed increasing their energy to the order of the mJ. Finally, the amplified pulses pass by another grating that shortens the duration of the energy pulses of duration below ps.

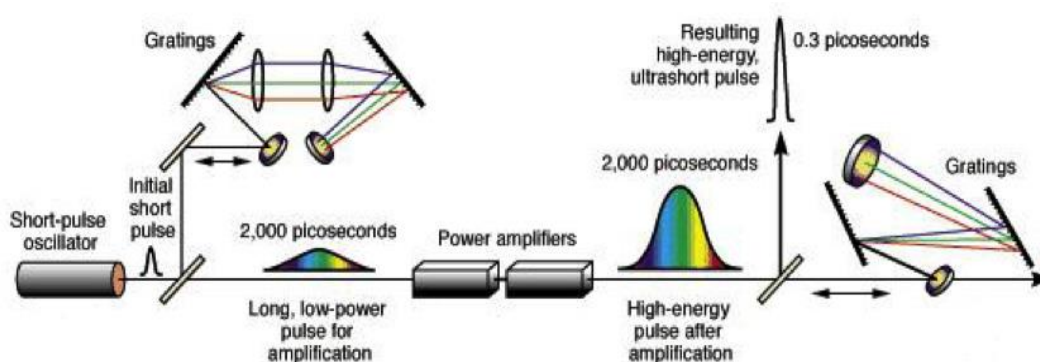


Figure 5. Schematic representation of the regenerative amplification technique of ultrashort pulses CPA (Chirped Pulse Amplification).

The fundamental rationale for following this strategy of

amplification is that optical elements required to drive ultrashort pulses in the amplifier cavity can be damaged or destroyed if those pulses are amplified directly, due to the high concentration of energy that would occur over time.

#### *I.4.5 Components of Ti: Sapphire laser*

In this thesis, a femtosecond laser that belongs to Laser Facility was used. The Laser Facility offers its services to researchers from the University of País Vasco (UPV/EHU), and also to external researchers. The equipment available at this SGIker unit consists of a complete set of nanosecond lasers (excimer lasers. Nd:YAG, different colouring systems that can be syntonized in the VIS-UV, etc.), and an ultrashort pulse system.

This femtosecond laser consists of a commercial Ti-sapphire oscillator-regenerative amplifier system, of the company Coherent Inc., Mantis-Legend model (figure 6) providing 1 kHz trains of pulses centered at 800 nm, with an energy of 4.0 mJ and a duration of 40 fs.

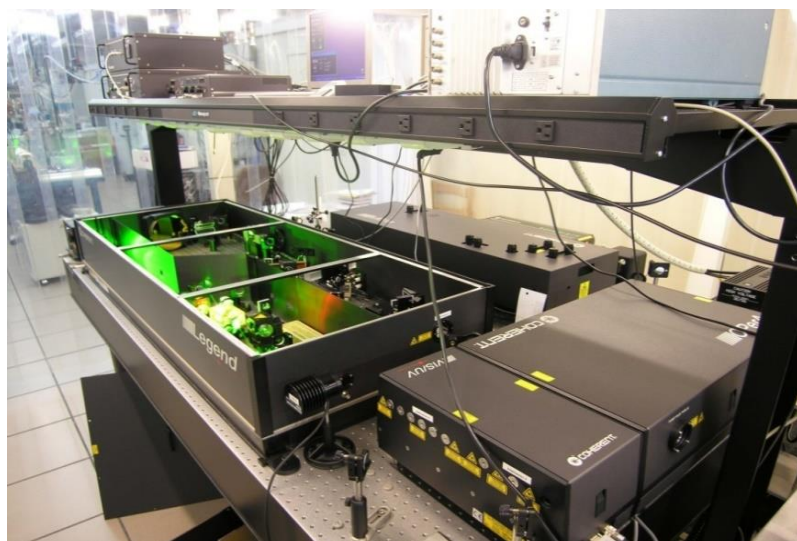


Figure 6. Ti-sapphire oscillator-regenerative amplifier system.

Since the energy of ultrashort pulses is excessive to ablate any material, two methods for reducing and accurately control the energy used . On one hand, sufficient reduction of energy occurs by employing using a variable neutral-density filter (figure 7) and measured with a thermal detector of the company Thorlabs Inc., S302C model and then use a combination of half-wave plate and linear polarizer to fine power adjustment. Only a fraction of the pulse energy of the amplifier output is used in the experiments.

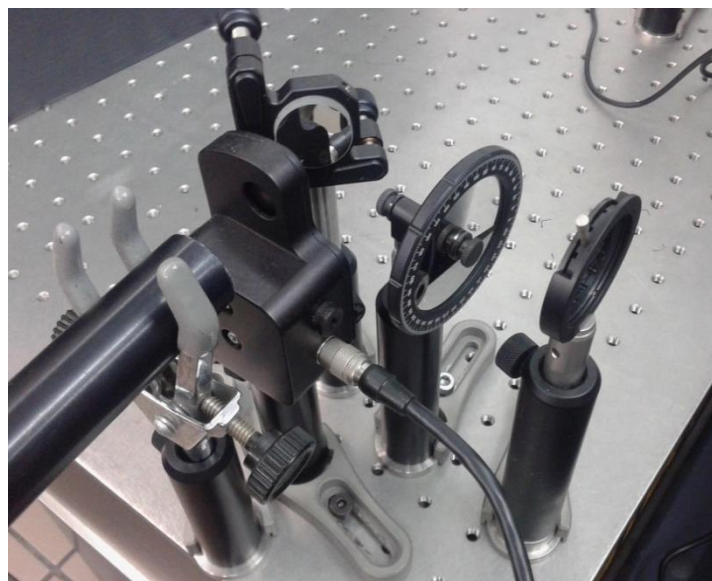


Figure 7. Variable neutral-density filter.

The laser pulses travel through the air and with the aid of mirrors with specific coatings for the intensity and the wavelength of these pulses, are conducted to the targeting system. In this case, the optical fiber transmission is prohibited because the high intensity pulses would damage the fiber.

The specimens were fixed on a computer-controlled XYZ-motorized stage (figure 8), of the company Thorlabs Inc, PT3-Z8 model, at atmospheric pressure, and the pulses impinge perpendicularly on the surface of the sample.

XY horizontal movement allows sweeping the surface while Z movement allows targeting of the pulses exactly on the surface of the samples. The experimental conditions were chosen to obtain a more uniform pattern across the surface, thus minimizing the depth of the grooves generated by laser ablation. Thus, the pulse energy was 0.015 mJ, the scanning velocity 0.25 mm/s, and the scanning step 20  $\mu\text{m}$ .

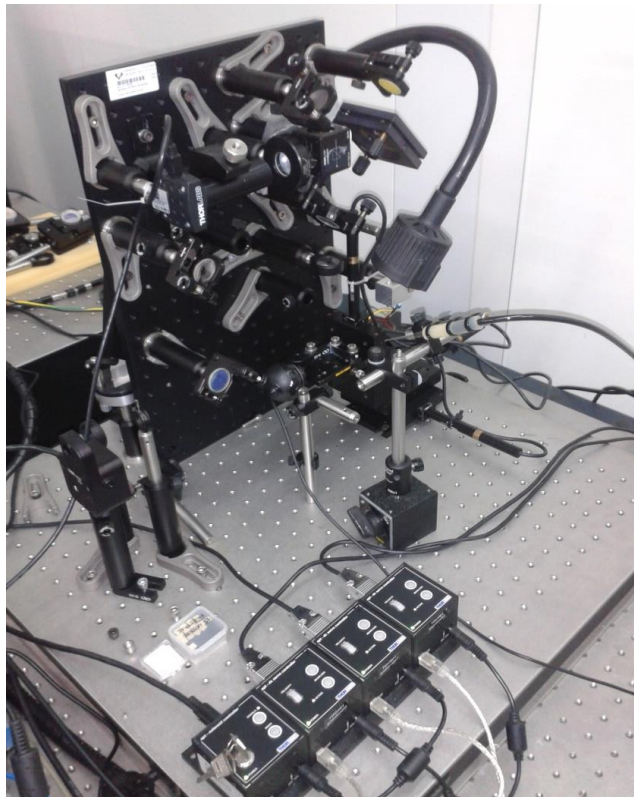


Figure 8. Microprocessor team.

#### *I.4.6 Femtosecond laser applications*

The ultrashort laser pulses have become popular primarily for medical applications since, fundamentally, its introduction in the field of Ophthalmology (femto-LASIK) in 2003 (Heisterkamp *et al.*, 2003; Ratkay-Traub *et al.*, 2003).

However, ultrafast ablation has been used extensively in biology (Tsai *et al.*, 2004), comprising cutting from subcellular organelles in cultured cells (Konig and Tirlapur., 2002, Watanabe *et al.*, 2004; Hoy *et al.*, 2008) and axonal regeneration processes in multicellular organisms (Yanik *et al.*, 2004; Bourgeois and Ben-Yakar, 2008; Gabel *et al.*, 2008;.. Guo *et al.*, 2008), ablation of bone, dentin and enamel (Neev *et al*, 1996; Perry *et al.*, 1999; Niemz, 2004; Nicolodelli *et al.*, 2011; Braun *et al.*, 2013;. Luengo *et al.*, 2013, Rego Filho *et al.*, 2013; Portillo *et al.*, 2015; Luengo *et al.*, 2015), cornea (Stern *et al.*, 1989; Kautek *et al.*, 1994; Juhasz *et al.*, 1999; Lubatschowski *et al.*, 2000; Maatz *et al.*, 2000; Odhner and Levis, 2014; Plötz *et al.*, 2014.) epithelia (Frederickson *et al.*, 1993), and neural tissues (Oraevsky *et al.*, 1996; Suhm *et al.*, 1996; Loesel *et al.*, 1998; Tsai *et al.*, 2003; Doronina *et al.*, 2009) Vascular (Nishimura *et al.*, 2006; Choi *et al.*, 2011.).

In the last years, femtosecond laser has begun to be used in Dentistry for ablation of different dental tissues and ceramics materials as a zirconia to enhance the adhesive effectiveness among other objectives (table 6).

<b>Title</b>	<b>Author</b>	<b>Year</b>	<b>Femtosecond laser irradiation as surface treatment.</b>	<b>Irradiated surface.</b>	<b>Results and/or Conclusions.</b>
<i>Effect of femtosecond laser beam angle on bond strength of zirconia-resin cement.</i>	Akpınar YZ, Kepçeoğlu A, Yavuz T, Aslan MA, Demirtag Z, Kılıç HS, Usumez A.	2015	A femtosecond amplifier laser pulse was applied on Y-TZP surface with different incidence angles (90°, 75°, 60°, 45°). The resin cement was adhered onto the zirconia surfaces.	Zirconia.	The degree of laser beam angle affects the SBS of resin cement to Y-TZP. The laser beam was applied to a surface with a 45° angle which resulted in significantly higher SBS.

<i>Ultrashort pulsed laser conditioning of human enamel: in vitro study of the influence of geometrical processing parameters on shear bond strength of orthodontic brackets.</i>	Lorenzo MC, Portillo M, Moreno P, Montero J, García A, Santos del Riego SE, Albaladejo A.	2015	<p>The surfaces of 63 premolar teeth were processed with intense ultrashort laser pulses (<math>\lambda = 795</math> nm; pulse duration, 120 fs; repetition rate, 1 kHz) to produce cross patterns with different pitches (s) in the micrometer range.</p> <p>The samples were classified in: control group and eight different laser-processed groups (cross patterns with s increasing from 15 to 180 <math>\mu\text{m}</math>).</p> <p>Brackets were luted with Transbond(TM) XT adhesive resin to all the samples.</p>	Enamel.	Enamel microstructuring with ultrashort laser pulses remarkably increase the bond strength of brackets. Dense cross patterns ( $s < 90 \mu\text{m}$ ) produce the highest increase of bond strengths.
<i>Influence of Er:YAG and Ti:Sapphire laser irradiation on the microtensile bond strength of several adhesives to dentin.</i>	Portillo M, Lorenzo MC, Moreno P, García A, Montero J, Ceballos L, Fuentes MV, Albaladejo A.	2015	<p>Flat dentin surfaces were divided into:</p> <p><b>Group 1:</b> control</p> <p><b>Group 2:</b> Er:YAG (2,940nm,100<math>\mu\text{s}</math>, 2.7W, 9 Hz)</p> <p><b>Group 3:</b> Ti:sapphire laser (795 nm,120 fs,1 W, 1 kHz).</p> <p>Each group was divided according to the adhesive system: two-step total-etching adhesive (XT), two-step self-etching adhesive (CSE), and all-in-one self-etching adhesive (OAO).</p>	Dentin.	The Er:YAG and ultrashort laser irradiation reduce the bonding effectiveness when a two-step total-etching adhesive or a two-step self-etching adhesive are used and do not affect their effectiveness when an all-in-one self-etching adhesive is applied.
<i>In vitro analysis of femtosecond laser as an alternative to acid etching for achieving suitable bond strength of brackets to human enamel.</i>	Lorenzo MC, Portillo M, Moreno P, Montero J, Castillo-Oyagüe R, García A, Albaladejo A.	2014	<p>Premolar teeth were divided depending on the laser treatment:</p> <p><b>Group 1:</b> no laser (control)</p> <p><b>Group 2:</b> Er:YAG laser (2,940nm, 0.8W, 100 <math>\mu\text{s}/pulse</math>, 10 Hz)</p> <p><b>Group 3:</b> Ti:Sapphire laser (795 nm, 1 W, 120 fs/pulse, 1 kHz).</p> <p>Each group was divided into two subgroups according to whether 37% orthophosphoric acid etching was made or not.</p> <p>Brackets were luted with Transbond XT.</p>	Enamel.	Femtosecond laser without acid seems to be the most suitable method to improve bond strengths at the bracket/enamel interface, thus avoiding the disadvantages inherent to acid etching.

<i>Evaluation of micro-morphological changes in tooth enamel after mechanical and ultrafast laser preparation of surface cavities.</i>	Luengo MC, Portillo M, Sánchez JM, Peix M, Moreno P, García A, Montero J, Albaladejo A.	2013	<p>12 third molars were collected and sectioned to provide several cut surfaces. These surfaces were exposed to infrared (<math>\lambda = 795</math> nm, 120 fs, 1-kHz repetition rate, maximum mean power 1 W) laser pulses and machined by means of a conventional mechanical technique.</p> <p>Two geometrical patterns were performed with FS laser: shallow rectangular cavities and deep cylindrical ones.</p>	Enamel.	Femtosecond laser have the ability to produce high-precision cavities in tooth enamel. No signs of collateral damage, burning, melting, or cracks were observed despite the far different laser pulse energies used (ranging from 7 to 400 $\mu$ J).
<i>Influence of the hydration state on the ultrashort laser ablation of dental hard tissues.</i>	Rego Filho Fde A, Dutra-Corvêa M, Nicolodelli G, Bagnato VS, de Araujo MT.	2013	<p>30 human teeth were split into 3 hydration groups and subdivided into dentin and enamel groups.</p> <p>The specimens were irradiated using a 70-fs Ti:sapphire laser (a 1-kHz repetition rate and a 801-nm wavelength). Ablation was performed using 5 different power levels and 3 exposure times.</p>	Enamel and dentin.	<p>There is an inversely proportional dependence of the ablation threshold to the hydration level.</p> <p>Thermal and mechanical damages were observed when a high repetition rate had been applied.</p>
<i>Influence of femtosecond laser treatment on shear bond strength of composite resin bonding to human dentin under simulated pulpal pressure.</i>	Gerhardt-Szep S, Werelius K, de Weerth F, Heidemann D, Weigl P.	2012	<p>3 test groups and a control group without laser treatment under pulpal pressure were investigated. Dentin discs of 800 nm thickness were cut from 60 extracted caries-free human molars.</p> <p>Clearfil SEBond/ Herculite XRV system was used and the samples were thermocycled. .</p>	Dentin.	Femtosecond laser treatment in a 160 $\mu$ m-sized enabled a simplified bonding procedure by dispensing the primer without affecting SBS.

<i>Ti:sapphire femtosecond laser ablation on dental enamel, dentine, and cementum.</i>	Ji L, Li L, Devlin H, Liu Z, Jiao J, Whitehead D.	2012	<p>A femtosecond laser (800nm wavelength) was used in the ablation of enamel, dentine, and cementum at various laser fluences from 0.2 to 3.68 J/cm<sup>2</sup> with single and multiple pulses.</p> <p>Ablation thresholds were determined to be 0.58, 0.44, and 0.51 J/cm<sup>2</sup> for enamel, dentine, and cementum, respectively.</p> <p>Laser fluence was found to influence the ablated diameter and depth, whereas under a certain fluence, pulse number only affects the depth, without affecting the diameter.</p>	Enamel, dentin and cementum.	<p>Under the average laser fluences of 1.13 to 3.68 J/cm<sup>2</sup> clean ablated surfaces without debris and microcracks.</p> <p>The low thermal loads of 0.708, 1.44, and 0.404 J/cm<sup>3</sup> required for ablating enamel, dentine, and cementum, are beneficial for minimizing the heat-affected zones and micro-damage.</p>
<i>Morphological alterations in dentine after mechanical treatment and ultrashort pulse laser irradiation.</i>	Portillo Muñoz M, Lorenzo Luengo MC, Sánchez Llorente JM, Peix Sánchez M, Albaladejo A, García A, Moreno Pedraz P.	2012	6 third molars were sectioned into 1 mm thick. The samples were randomly divided into two groups according to their cavity preparation: mechanical cavity preparation and laser cavity preparation.	Dentin.	<p>Cavities prepared with the laser with pulses of &lt;1 ps showed no microcracks, and the treated surface displayed a rough and irregular aspect with no smear layer and exhibited open dentinal tubules.</p> <p>Human dentine can be successfully ablated with the ultrashort pulse laser.</p>
<i>Femtosecond pulsed laser ablation of dental hard tissues with numerical control: a roughness and morphology study.</i>	Sun YC, Vorobyev A, Liu J, Guo C, Lü PJ.	2012	Enamel and dentin planes were prepared on human third molars. A universal motion controller was used to control the samples to do rectangle wave motion perpendicular to the incident direction of the laser at focus.	Enamel and dentin.	Precise ablation of the dental hard tissues can be achieved with femtosecond laser without micro-cracks or carbonization on enamel. But carbonization, cracks and a small amount of crystalline particles were observed on dentin.

<i>A new method for relative Sr determination in human teeth enamel.</i>	Alvira F, Ramirez Rozzi F, Torchia G, Roso L, Bilmes G.	2011	New method to determine Sr/Ca changes in hard dental tissues based on laser ablation and spectroscopic detection. By using femtosecond Laser Induced Breakdown Spectroscopy (fs-LIBS), we micro mapped the relative amount of strontium in the enamel of three human lower third molar. The method has a precision better than 95% and is sensitive enough to detect Sr/Ca ratio variations.	Enamel.	Fs-LIBS generates information in a fast and simple way that can be used to make inferences about diet or mobility in human populations and fossils.
<i>Femtosecond laser micro structuring of zirconia dental implants.</i>	Delgado-Ruiz RA, Calvo-Guirado JL, Moreno P, Guardia J, Gomez-Moreno G, Mate-Sánchez JE, Ramirez-Fernández P, Chiva F.	2011	66 cylindrical zirconia implants were divided into: <b>Control group:</b> with no laser modification. <b>Group A:</b> micropropored texture. <b>Group B:</b> microgrooved texture.  SEM observation was used to analyze the microgeometries X-ray diffraction and Raman spectra analysis were carried out to investigate any change in the crystalline structure induced by laser processing.	Zirconia.	Ultrafast laser ablation increased surface roughness and preserved the original tetragonal phase of zirconia but the traces of monoclinic phase were reduced.  There is minimal collateral damage of the original surface surrounding the treated areas.
<i>Effective laser ablation of enamel and dentine without thermal side effects.</i>	Kohns P, Zhou P, Störmann R.	1997	Laser treating dental materials by using femtosecond pulses generated by a titanium:sapphire laser system which consisted of an oscillator and a regenerative amplifier.  The pulse duration was varied between 200 fs and 2 ps. The observed energy thresholds for the ablation process of dentine and enamel were clearly smaller than those observed when longer pulse durations were used.	Enamel and dentine.	No thermal damage or mechanical damage, such as cracks, were produced during the laser treatment and it can produce ablation rates of 2 mm <sup>3</sup> per min in dental materials.

Table 6. Summary table of articles about application of femtosecond laser in Dentistry.

## I.5 In vitro simulation oral conditions

The oral environment is very complicated both chemically and mechanically and cause physicochemical alterations to the dental restorative materials as zirconia ceramics. The evaluation of fracture toughness and prediction of lifetime service under clinical situations have assumed important positions in dentistry (Drummond *et al.*, 2003).

### *I.5.1 Chemical complexity of oral environment*

When a restorative dental material is exposed to certain environments, it may absorb water and chemical from the environment and it may release components to its surrounding (Ferracane, 2006). Zirconia ceramics in the oral cavity are exposed to saliva which contains various molecules including numerous enzyme systems and they may have interactions with oral microbes, such as surface degradation (Willershausen *et al.*, 1999). In addition, they are exposed to exogenous substances that contain a variety of chemicals, including acids, bases, salts, alcohols, and oxygen (Ferracane, 2006). The chemical and the duration of exposure are important determinants (Ferracane, 2006).

There are two major concerns related solvent uptake from the surrounding environment, leaching and hydrolytic degradation of the dental materials:

- 1- Shortened service life of dental materials due to deleterious effect of solvents on the structure and function of them.

2- Possible biological effects caused by these molecules leached from restorative materials in the human body.

### *I.5.2 Mechanical complexity of oral environment*

In most instances, stress applied to zirconia ceramics is generally low and repeated (fatigue) rather than being single and impact in type. The normal occlusal loading of a filling is estimated at between 5 and 20 MPa (Braem *et al.*, 1994). It has been reported that the cyclic nature mastication forces is responsible for the wear, chipping, and generalized failure (Braem *et al.*, 1994). Occasionally, a higher peak stress may occur during parafunctional movement, such as during maximum clenching (Abe *et al.*, 2005). The stress may increase to 100 Mpa and higher in there occasions (Abe *et al.*, 2005).

#### I.5.2.1 Fatigue and fatigue crack growth

Fatigue failures can originate from existing inherent defects in a material that coalesce with cyclic loading and enable fracture through a reduction in load-bearing capacity. Alternatively, fatigue failures can originate from a well-defined flaw (or crack) that undergoes extension under cyclic loading until reaching a critical length. It recognition of the nature of mastication, the fatigue is a relevant concern.

Cyclic loading can also promote existing flaws and/or cracks to undergo extension through a process regarded as fatigue crack growth, and it may undergo cyclic extension under the forces of mastication, thereby

facilitating fracture (Aroa *et al.*, 1999).

### *I.5.3 Interfacial degradation by artificial aging*

The most common *in vitro* interfacial fatigue (fastened aging) techniques are water storage, thermocycling and cyclic loading. These aging methods, widely used and based on ISO standards for dental materials (ISO TR11450 standard, 1994) and can be used separately or combined.

There are many bonding procedure able to obtain a strong bond with Y-TZP initially. However, this bond must be adequate over years under the relatively aggressive circumstances of the oral environment: humidity, temperature shocks, pH fluctuation and mastication forces.

Several studies, using water storage, thermocycling and/or cyclic loading, observed that fatigue can take to a reduction of the zirconia-resin bond strength, which can deteriorate with time, causing loss of retention and increasing microleakage (Wegner *et al.*, 2000; Amaral *et al.*, 2006; Ghazy *et al.*, 2011).

#### I.5.3.1 Chemical degradation

The most usually used artificial aging technique is long term water storage (de Munck *et al.*, 2005). It was suggested that the decrease in bonding effectiveness reported after this aging method was caused by degradation of the interface component by hydrolysis (de Munck *et al.*,

2005). Hydrolytic degradation of the bonding interface is related to the diffusion of liquids. This diffusion is dependent on time, it takes time to

water penetrate the bonding interface and cause chemical breakdown (Ferracane *et al.*, 1995). Water can infiltrate and decrease the mechanical properties of the polymer matrix, by swelling and reducing the frictional forces between the polymer chains, a process known as “plasticization” (Ferracane *et al.*, 1998; Santerre *et al.*, 2001). Some interface components, such as uncured monomers and break-down products of previous reactions, can elute and weaken the bond (Hashimoto *et al.*, 2002).

To simulate more accurately the clinical situation, artificial saliva solutions can also be used, but bond strength reductions were very similar to those obtained with pure water degradation (Kitasako *et al.*, 2000).

### I.5.3.2 Thermal degradation

Another commonly used aging technique is thermocycling. The ISO TR 11450 standard (1994) determines that a thermocycling regimen comprised of 500 cycles in water between 5-55°C is an appropriate artificial aging method (de Munck *et al.*, 2005). A literature review (Gale *et al.*, 1999) concluded that 10000 cycles correspond approximately to one year of *in vivo* functioning, standing the proposition of 500 cycles as being very minimal in simulating long term bonding effectiveness.

Two main mechanisms of deterioration of the established bond strength have been proposed: a) hydrolytic degradation (as well as in long term water storage) and b) mechanical fatigue. The last results from

stresses affecting the bond, for example thermal expansion and contraction.

Different linear coefficient values of thermal expansion (LCTE) of resin and ceramic may have an effect on the failure mechanism at the bonding interface. Ceramic materials LCTEs are typically less than resin luting cements LCTEs. This difference causes thermal stresses at the bonding interface, generating unequal changes in dimensions, and eventually, the bond failure (Tezvergil *et al.*, 2003; Meric *et al.*, 2008).

These stresses may lead to cracks that propagate along bonded interfaces, once the gap is formed, changing the gap dimensions can cause an in- and outflow of fluids, known as “percolation” (Gale *et al.*, 1999). Percolation takes us to hydrolytic degradation.

In the light of the first aging effect (hydrolysis), thermocycling should be applied to very small specimens, and any further preparation after aging is to be avoided (de Munck *et al.*, 2005).

Thermocycling results in combined contraction/expansion stresses and accelerated chemical degradation. The contribution of each is highly dependent on the specific test setup.

### I.5.3.3 Mechanical degradation

Mechanical loading affects adhesion. To mimic the *in vivo* stress, is possible to “age” interfaces in a chewing simulator and measure the

bonding effectiveness afterward (Nikaido *et al.*, 2002; Frankenberger *et al.*, 2003). Thereby, to simulate occlusal masticatory forces *in vitro*, cyclic loading is used (Koyama *et al.*, 2012). Cyclic loading is the repeated or fluctuating application of stresses, strains or intensities to locations on structural components, and attempts to replicate the clinical conditions that zirconia restorations are subjected to due to masticatory forces (Attia and Kern, 2004). The technique is based on a computer-controlled masticatory simulator that produces a mechanical degradation of the zirconia-resin (Mirmohammadi *et al.*, 2010) interface through the continuous application of impact on it.

Under cyclic loading, zirconia fixed dental prostheses are subject to fracture during function, especially in the posterior area, and zirconia abutments exhibit a significantly lower fracture resistance (Foong *et al.*, 2013), with a significant reduction in preload (Butignon *et al.*, 2013). It has been reported that when cyclic loading is applied, there is a distribution of stresses generated around the bonding interface, with a progressive cone cracking surface (Zhou *et al.*, 2007) associated with low fracture strength (Aboushelib 2013). All these process are set out in table 7.

<i>Title</i>	<i>Author</i>	<i>Year</i>	<i>Cyclic loading.</i>	<i>Results and/or Conclusions.</i>
<b>ZIRCONIA FRAMEWORKS, IMPLANTS AND ABUTMENTS- Reduction of preload and/or torque and occurrence of cracks and fractures.</b>				
<i>Torque loss under mechanical cycling of long-span zirconia and titanium-cemented and screw-retained implant-supported CAD/CAM frameworks.</i>	Gomes ÉA, Tissi R, Faria AC, Rodrigues RC, Ribeiro RF.	2014	<p>Dry-pressed porcelain crowns were luted to 24 frameworks to standardize the specimens and were then divided into four groups according to framework material (titanium or zirconia) and retention method for the prosthesis (cement- or screw-retained).</p> <p>The specimens were submitted to a 200N cyclic load, at a frequency of 2 Hz, underwater in controlled temperature of 37°, and for <math>1 \times 10^6</math> cycles.</p>	<p>The screw removal torque was significantly reduced for all groups in this study after cyclic loading the specimens. Screw-retained zirconia specimens presented the highest torque loss before and after the cyclic loadings compared with the other specimens that were tested.</p>
<i>Influence of three types of abutments on preload values before and after cyclic loading with structural analysis by scanning electron microscopy.</i>	Butignon LE, Basilio Mde A, Pereira Rde P, Arioli Filho JN.	2013	<p>45 external-hex implants were embedded in epoxy resin, received their respective abutments, and were randomly divided into:</p> <p><b>Group Ti:</b> machined titanium abutments.</p> <p><b>Group Au:</b> pre-machined gold abutments.</p> <p><b>Group ZrO<sub>2</sub>:</b> machined zirconia abutments.</p> <p>10 specimens of each group were used to measure the reverse torque value (preload) of the abutment screw before and after loading.</p> <p>A cyclic loading (<math>0.5 \times 10^6</math> cycles; 15 Hz) between 11 and 211 N was applied at an angle of 30 degrees to the long axis of the implants.</p>	<p>The load application reduced the preload means significantly in all groups, and more significantly in the ZrO<sub>2</sub> group.</p>
<i>Fracture resistance of titanium and zirconia abutments: an in vitro study.</i>	Foong JK, Judge RB, Palamara JE, Swain MV.	2013	<p>22 specimens simulating implant-supported anterior single crowns were divided into:</p> <p><b>Group T:</b> with titanium abutments.</p> <p><b>Group Z:</b> with zirconia abutments.</p> <p>Abutments were attached to dental implants mounted in acrylic resin, and computer-aided design/computer-aided manufacturing (CAD/CAM) crowns were fabricated. Masticatory function was simulated by using cyclic loading in a stepped fatigue loading protocol until failure.</p>	<p>Zirconia abutments exhibited a significantly lower fracture resistance than titanium abutments.</p>

<i>Cyclic fatigue resistance of yttria-stabilized tetragonal zirconia polycrystals with hot isostatic press processing.</i>	Koyama T, Sato T, Yoshinari M.	2012	<p>50 Y-TZP cylinders were divided into:</p> <p><b>Group A:</b> (polished by centerless method; TZP-CP).</p> <p><b>Group B:</b> (blasted and acid-etched: TZP-SB150E).</p> <p>The cyclic fatigue test was performed in distilled water at 37°C. Surface morphology and roughness as well as crystal phase on the surfaces were also evaluated.</p>	<p>Fracture values under the cyclic test decreased to approximately 70% of those under the static tests.</p> <p>HIPed Y-TZP with a 3.0-mm diameter has sufficient durability for application to dental implants.</p>
<i>Effectiveness of screw surface coating on the stability of zirconia abutments after cyclic loading.</i>	Basílio Mde A, Butignon LE, Arioli Filho J.	2012	<p>20 prefabricated ZrO<sub>2</sub> ceramic abutments on their respective external-hex implants were divided into two groups according to the type of screw: <b>Group 1:</b> uncoated titanium alloy screw (Ti) <b>Group 2:</b> titanium alloy screw with W-DLC coating (W-DLC/Ti).</p> <p>The removal torque value (preload) of the abutment screw was measured before and after loading. Cyclic loading between 11 and 211 N was applied at an angle of 30 degrees to the long axis of the implants at a frequency of 15 Hz. A target of 0.5 x 10<sup>6</sup> cycles was defined.</p>	<p>After cyclic loading, both abutment screws presented a significant reduction in the mean retained preload and similar effectiveness in maintaining preload</p>
<i>The effects of cyclic loading and preparation on the fracture strength of zirconium-dioxide implants: an in vitro investigation.</i>	Kohal RJ, Wolkowitz M, Tsakona A.	2011	<p>48 one-piece implants were divided into:</p> <p><b>Group A:</b> without modification.</p> <p><b>Group B:</b> 1 mm chamfer preparation.</p> <p>They were divided into three subgroups:</p> <p><b>Subgroup 1:</b> no artificial load.</p> <p><b>Subgroup 2:</b> artificial load- 98 N; 1.2 million loading cycles.</p> <p><b>Subgroup 3:</b> artificial load-98 N; 5 million loading cycles.</p>	<p>Preparation as well as cyclic loading can decrease the fracture strength resistance of zirconia implants.</p>
<i>Contact damage in an yttria stabilized zirconia: implications.</i>	Zhou J, Mah J, Shrotriya P, Mercer C, Soboyejo WO.	2007	<p>His paper presents the results of a combined experimental and computational study of contact damage in a 3 mole% yttria partially stabilized zirconia (3-YSZ) that is relevant to hip implants and dental restorations.</p> <p>Contact-induced loading in real applications is idealized using Hertzian contact model to explain plasticity phenomena and failure mechanisms observed under monotonic and cyclic loading. Under monotonic loading, the elastic moduli increase with increasing loading levels.</p>	<p>Stress-induced phase transformation (tetragonal to monoclinic) occurs under cyclic contact loading above the critical load levels (8.5 kN), and when the cyclic loading level (5.0 kN) is less than a critical load levels (7.5 kN) occur surface cone cracks and plastic damage is observed in the subsurface zone underneath the contact area.</p>

**ZIRCONIA CROWNS- Reduction of bond strength and/or occurrence of structural damage.**

<i>Simulation of cumulative damage associated with long term cyclic loading using a multi-level strain accommodating load ing protocol.</i>	Abousheli b MN.	2013	<p>40 zirconia veneered crowns received thermal and cyclic loading (3.5 million cycles at maximum load of 25 kg representing 70% of the critical load of the veneer ceramic). Speed of load application and release was obtained from the chewing cycle of adult patients.</p> <p>Principles of fractographic analysis were used to study the behavior and origin of critical crack and associated structural damage.</p>	Cyclic loading using multi-level strain accommodating model can reproduce clinical failure. With exception to manufacturing errors, zirconia veneered restoration survived a simulated 7-year service time without fracture.
<i>Influence of fabrication techniques and artificial aging on the fracture resistance of different cantilever zirconia fixed dental prostheses.</i>	Ghazy MH, Madi na MM, Abo ushelib MN.	2012	<p>80 adhesive cantilever fixed dental prostheses (CFDP) were fabricated and assigned to:</p> <p><b>Group 1:</b> machine copy milling zirconia (Cercon).</p> <p><b>Group 2:</b> manual copy-milling technique (ZirkonZahn).</p> <p><b>Group 3:</b> slip casting technique (Vita In-ceram Zirconia).</p> <p><b>Group 4:</b> metal-ceramic CFDP.</p> <p>Specimens in groups 1 and 2 received selective infiltration-etching surface treatment, specimens in group 3 were acid etched with hydrofluoric acid and silanated, while those of group 4 were airborne particle abraded.</p> <p>Samples were bonded with resin cement (Panavia F2.0) and thermocycled (5000 cycles/ 5 to 55°C). Half of the specimens underwent dynamic loading (<math>10^6</math> cycles at alternating loads between 10 and 40 N in a water 37°C).</p>	The fatigue strength of adhesive zirconia restorations is influenced by cyclic loading.
<i>Effect of cyclic impact load on shear bond strength of zirconium dioxide ceramics.</i>	Kawai N, Shinya A, Yokoy ama D, Gomi H, Shinya A.	2011	<p>The following materials were used: Super Bond C&amp;B (SB) and Panavia Fluoro Cement (PF) as adhesive resin cements, Fuji Luting (FL) as a resin-modified glass-ionomer cement, and zirconia ceramics as adherend.</p> <p>Three different impact loading conditions (compressive direction, shear direction, and no impact) and the number of load cycles (1 to <math>10^6</math> cycles), were performed.</p> <p>A cyclic impact test was performed by applying a load of 98N at a distance of 40 mm with a frequency of 1 Hz.</p>	The shear bond strengths of SB, PF, and FL were greatest without cyclic impact, followed by compressive and then shear cyclic impact.

<i>The influence of rotating fatigue on the bond strength of zirconia-composite interfaces.</i>	Mirmohammadi H, Abousheli b MN, Klev erlaan CJ, de Jager N, Feilzer AJ.	2010	Bar shaped zirconia/composite specimens were prepared using three different resin cements and placed in a four-point bending test setup. Rotating fatigue resistance (RFR) was determined in a rotating bending cantilever test setup (104, 1.2 Hz) with the highest stress located at the interface.	After rotating fatigue testing there was a significant reduction in bond strength between 46 and 50% of resin cements. Zirconia-resin bond strength is liable to deterioration under the influence of fatigue.
<i>Mechanical strength and subcritical crack growth under wet cyclic loading of glass-infiltrated dental ceramics.</i>	Salazar Marocho SM, Studart AR, Bottino MA, Bona AD.	2010	Bar-shaped specimens of IA (In-Ceram Alumina) and IZ (In-Ceram Zirconia) were fabricated and loaded in three-point bending (3P) in 37°C artificial saliva and cyclic fatigued (F) in dry (D) and wet (W) conditions. The flexural strength ( $\sigma$ ) and subcritical crack growth (SCG) under cyclic loading were evaluated.	The lifetime of ceramics restorations is expected to increase by reducing their direct exposure to wet conditions and/or by using high content zirconia ceramics with higher strength.
<i>Fracture strength of two oxide ceramic crown systems after cyclic pre-loading and thermocycling</i>	Vult von Steyern P, Ebbesson S, Holmgren J, Haag P, Nilner K.	2006	60 crowns were made, 30 identical crowns of alumina and 30 of zirconia. Each group divided according to the different treatments: <b>Group 1:</b> water storage only. <b>Group 2:</b> pre-loading (10 000 cycles, 30-300 N, 1 Hz). <b>Group 3:</b> thermocycling (5-55 degrees , 5000 cycles) + pre-loading (10 000 cycles, 30-300 N, 1 Hz).	Crowns made with zirconia cores have significantly higher fracture strengths after pre-loading.

Table 7. Summary of studies that using cyclic loading in zirconia ceramics.

Accordingly, on performing cyclic loading in our research the results can be considered to be more clinically relevant because they represent the mechanical degradation process that zirconia restorations undergo due to masticatory forces more faithfully.

## I.6 Adhesive strength mechanical assay and microstructural evaluation

The bonding performance of the adhesive materials can be evaluated using various methods. In general, tensile bond test (TBS) and shear bond test (SBS) have been applied. The main purpose of bond strength tests is to do a comparative evaluation of the bonding fulfillment of the materials (Tagami *et al.*, 2010).

It is important to refer that a bond strength value cannot be considered as a material property (van Noort *et al.*, 1989) and the results depend on experimental factors and the test methodology (Sudsangiam *et al.*, 1999). For this reason, only relative study outcomes, in the comparative sense (for example: A is better than B) is a valid basis for the results interpretation. Bond strength values can reveal valuable clinical information when gathered in a well-controlled design (de Munck *et al.*, 2005).

These test methods are based on the application of a load in order to generate stress at the adhesive joints until fracture occurs (Valandro *et al.*, 2008). Therefore, for the test to measure accurately the bond strength value between an adherent and a substrate, it is crucial that the bonding interface should be the most stressed region, regardless the method used (De Hoff *et al.*, 1995; Della Bona *et al.*, 1995).

Bond strength testing has been predominantly accomplished by creating specimens which are loaded to failure in either shear (SBS) or micrtensile (MTBS) manner (table 7). Nowadays, a new approach is to load multiple test specimens from each sample.

	<b>Advantages</b>	<b>Drawbacks</b>
<b>MTBS</b>	<ul style="list-style-type: none"> <li>1. More adhesive failures.</li> <li>2. Less cohesive failures.</li> <li>3. Measurement of higher interfacial bond strengths.</li> <li>4. Means and variance can be evaluated for a single sample.</li> <li>5. Permits testing irregular surfaces.</li> <li>6. Permits testing of very small areas.</li> <li>7. Facilitates SEM examinations for the failed bonds.</li> </ul>	<ul style="list-style-type: none"> <li>1. Labor intensity</li> <li>2. Technical demand</li> <li>3. Dehydration potential of the smaller samples.</li> <li>4. Difficulty in measuring low adhesive values.</li> <li>5. Difficulty in removing the sample of the clamping device.</li> </ul>
<b>SBS</b>	<ul style="list-style-type: none"> <li>1. The specimen is only pre-stressed prior testing only by mold removal.</li> <li>2. Permits testing of very small areas.</li> <li>3. Means and variance can be evaluated for a single sample.</li> <li>4. Facilitates SEM examinations for the failed bonds.</li> </ul>	<ul style="list-style-type: none"> <li>1. Tensile stresses produced by the bending moment at load application are responsible for fracture initiation.</li> <li>2. Highly non-uniform stress distribution concentrated in the substrate.</li> <li>3. Measured bond strength underestimates the true stress the specimen resisted at fracture.</li> </ul>

Table 8. Micro-testing advantages and drawbacks (based in "Armstrong S, Geraldeli S, Maia R, Raposo LHA, Soares CJ, Yamagawa J (2009) Adhesion to tooth structure: a critical review of "micro" bond strength test methods. Dent Mater 26 (2):e50-e62").

Within the scientific community there is no agreement concerning the appropriate usage and interpretation of these tests, and the attempts of standardization of test methods have been difficult. Bond strength test remains useful and necessary for the screening of new products and study of experimental variable (Armstrong *et al.*, 2009).





## *ii. OBJECTIVES AND JVSTIFICATION.*

Currently, the number of adults who demand treatments orthodontics has increased and some of these patients usually carry some type of ceramic restoration in their mouths. This has caused that orthodontists have been exposed to problems such as having to cement orthodontic attachments on teeth restored with dental ceramics as zirconia. For this reason, it is necessary to establish an adhesion protocol in orthodontics to achieve proper adhesive effectiveness to prevent debonding of orthodontic attachments in zirconia surface seeking maximum bond strength to minimize the risk of failure during treatment period; and, on the other hand, in restorative dentistry, to get to cement zirconia restorations on different biological substrates such as enamel or dentin.

Zirconia ceramics are essential materials in dental restoration, and they have been used for oral rehabilitation for decades. The problem that present these ceramics is that traditional adhesive chemistry is ineffective and surface treatments are needed to improve the adhesive bonding between the resin cement and zirconia. Nevertheless, there is still no ideal zirconia surface conditioning method able to that provide sufficient effectiveness of adhesion on zirconia surfaces in restorative dentistry and in orthodontics to cement brackets and tubes and it is therefore necessary to seek new alternatives that guarantee us a strong and durable. Thus, research is now beginning to focus on the use of femtosecond lasers in dentistry as surface treatments to perform the conditioning of biological and non-biological surfaces encouraging results having been obtained in the sense of improvements in adhesive effectiveness.

It is also to note necessary that all zirconia restorations are subjected to cyclic forces ranging from 60 N to 250 N during masticatory function, and may even reach values of 800 N. Accordingly, it is crucial to investigate bond strength values obtained

under dynamic conditions using cyclic loading, in order to obtain more clinical results and hence make progress in attempts to validate femtosecond laser irradiation as an ideal surface-conditioning method.

In such a way that zirconia is a relatively new and innovative material there is a lot of controversy, from the scientific point of view, about the best method for optimizing and promotes an effective bonding to substrates used in dentistry.

The specific aims of this study were:

1. To investigate the effect of the zirconia surface treatment with airborne particle abrasion with 25- $\mu\text{m}$  alumina particles, tribochemical silica coating, and femtosecond laser irradiation on the zirconia-resin interface bond strength.
2. To assess if femtosecond laser irradiation influences on the bond strength to zirconia-resin cement interface and determine the better parameters of irradiation to provide a reliable resin-zirconia bonding.
3. To evaluate how the cyclic loading affects on the adhesive effectiveness of zirconia/resin interface.





### *iii. MATERIAL AND METHODS*

### III.1 Preparation of zirconia samples.

The study used one hundred fifty samples of densely sintered Y-TZP (Cercon®, DeguDent, Hanau, Germany). The specimens, which were square-shaped and measured 6x6x1mm (figure 9), were obtained using a precision cutting machine (Isomet 5000; Buehler, Lake Bluff, Illinois, USA) (figure 10). Each sample surface was wet-polished with 600-grit silicon carbide paper on a polishing machine (Phoenix Beta; Buehler, Lake Bluff, Illinois, USA).



Figure 9. Specimens of zirconia.

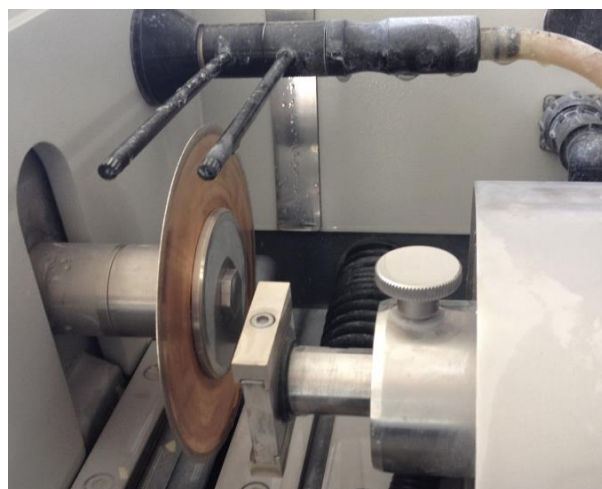


Figure 10. Cutting machine.

The manufacturer's composition and application mode of the materials used in the experiment are detailed in Table 9.

<i>Material</i>	<i>Manufacturer</i>	<i>Composition and/ or conditions.</i>
<b>Y-TZP.</b>	Cercon®, DeguDent, Hanau, Germany.	Zirconium oxide and yttrium oxide: 5%. Hafnium oxide: <2%. Aluminum oxide + silicon oxide: <1%.
<b>Polishing machine.</b>	Phoenix Beta; Buehler, Lake Bluff, Illinois, USA.	600-grit silicon carbide paper was used for the polishing.
<b>APA 25.</b>	Renfert GmbH, Hilzingen, Germany.	Alumina particles ( $\text{Al}_2\text{O}_3$ ) with an average size of 25 $\mu\text{m}$ .
<b>Rocatec™ Soft.</b>	3M Espe, Seefeld, Germany.	30 $\mu\text{m}$ silica with modified aluminium oxide.
<b>RelyX™ceramic primer.</b>	3M Espe, Seefeld, Germany.	Ethyl alcohol, water, methacryloxypropyltrimethoxysilane.
<b>Ti:Sapphire oscillator-regenerative amplifier system.</b>	Mantis-Legend, Coherent, USA.	$\lambda=800\text{nm}$ . Duration/pulse= 40 fs. Energies= 4mJ. Repetition rate= 1KHz.
<b>Thermal detector.</b>	S302C, Thorlabs Inc. Newton, New Jersey, USA.	Only a fraction of the pulse energy of the amplifier output is used in the experiments, using a variable neutral-density filter and measured with the thermal detector. Thus, the pulse energy was 0.015 mJ, the scanning velocity 0.25 mm/s, and the scanning step 20 or 40 $\mu\text{m}$ .
<b>Computer-controlled XYZ-motorized stage.</b>	PT3-Z8, Thorlabs Inc. Newton, New Jersey, USA.	The specimens were fixed on it.
<b>Clearfil™ SA Cement.</b>	Kuraray, Osaka, Japan.	MDP, hydrophobic aromatic dimethacrylate, hydrophobic aliphatic dimethacrylate, colloidal silica, barium glass.
<b>Curing light</b>	XL 3000, 3M/ESPE.	Light intensity was 500mW/cm <sup>2</sup> .

<b>Cyclic loading machine</b>	S-MMT-250NB; Shimadzu, Tokyo, Japan	The force is applied perpendicularly to the zirconia surface opposite where the resin was cemented. This compressive load was applied using a spherical stainless steel plunger, 5mm in diameter.
<b>Universal SBS testing machine.</b>	AGS-X Autograph, Shimadzu Corporation, Kyoto, Japan.	A shear load was applied with a crosshead speed of 0.5 mm/min, until fracture.
<b>Axio M1 light microscope.</b>	Carl Zeiss, Germany.	At $\times 40$ magnification.
<b>Scanning electron microscope.</b>	Zeiss EVO MA25; Carl Zeiss, Jena, Germany.	Specific regions across the zirconia surface were explored with the scanning electron microscope, focusing with different magnifications ( $\times 70$ and $\times 1000$ ) in order to obtain a panoramic view of the effect of laser processing and the effect of the other conditioning methods.
<b>Desiccator machine.</b>	Sample Dry Keeper Simulate Corp., Tokyo, Japan	Representative fractured samples were dehydrated for 48h in a desiccator before SEM analysis.
<b>SEM coating unit.</b>	Polaron Equipment Ltd., Hertfordshire, England, UK.	Representative fractures samples were sputter-coated with a 10-nm platinum layer before SEM analysis.
<b>SPSS v21</b>	Statistical Package for the Social Sciences, Chicago, IL.	The bond-strength values were measured in MPa and the data were analyzed with SPSS v21 using a p-value below 0.05 as the threshold for statistical significance.

Table 9. Materials and manufacturer's composition.

### III.2 Experimental groups.

Once the zirconia samples had been polished, they were randomly assigned to four

experimental groups (figure 9) according to the surface treatment to be applied ( $n=30$ ).

### *III.2.1 Group 1: Control- No treatment (NT).*

No surface treatment was applied.

### *III.2.2 Group 2: Airborne particle abrasion with 25- $\mu\text{m}$ alumina particles (APA 25).*

The zirconia surface was blasted with alumina particles ( $\text{Al}_2\text{O}_3$ ) with an average particle size of 25  $\mu\text{m}$  under a pressure of 0.25 MPa for 20 seconds at a perpendicular distance of 10 mm from the holder.

### *III.2.3 Group 3: Tribochemical silica coating (TSC).*

In this case, the zirconia surface was treated with a tribochemical silica coating (30- $\mu\text{m}$  alumina and silica particles) with the Rocatec system (Rocatec<sup>TM</sup> Soft, 3M Espe, Seefeld, Germany). Rocatec particles were applied under a pressure of 0.25 MPa for 20seconds at a perpendicular distance of 10 mm. Silica coating was followed by silanization, which was performed following manufacturer's instructions with a Rely X<sup>TM</sup> ceramic primer (3M Espe, Seefeld, Germany).

### *III.2.4 Group 4: Femtosecond laser irradiation at step 20 (FS20).*

The zirconia surface was irradiated with a femtosecond laser. The laser pulses were generated by a commercial Ti:Sapphire oscillator-regenerative amplifier system (Mantis-Legend, Coherent Inc. Santa Clara, CA, USA), providing 1 kHz trains of pulses centered at 800 nm, with an

energy of 4.0 mJ and a duration of 40 fs. Only a fraction of the pulse energy of the amplifier output is used in the experiments, using a variable neutral-density filter and measured with a thermal detector (S302C, Thorlabs Inc. Newton, New Jersey, USA). The laser pulses were focused by means of a fused silica singlet lens ( $f=100$  mm), yielding a spot diameter of approximately 20  $\mu\text{m}$ .

The specimens were fixed on a computer-controlled XYZ-motorized stage (PT3-Z8, Thorlabs Inc. Newton, New Jersey, USA) at atmospheric pressure. The experimental conditions were chosen to obtain a more uniform pattern across the surface, thus minimizing the depth of the grooves generated by laser ablation. Thus, the pulse energy was 0.015 mJ, the scanning velocity 0.25 mm/s, and the scanning step 20  $\mu\text{m}$ .

### *III.2.5 Group 5: Femtosecond laser irradiation at step 40 (FS40).*

In this group, the zirconia surface was irradiated with a femtosecond laser with the same parameters as the previous group except that the scanning step was 40  $\mu\text{m}$ .

## **III.3 Bonding procedure**

After performing the different surface treatments on the zirconia samples, all specimens were washed with ethanol and dried before that a self-adhesive resin cement was bonded to their surface according to manufacturer's recommendations:

Clearfil™ SA Cement (*CLE*) (Clearfil™ SA Cement, Kuraray, Osaka, Japan).

For application of the cement, a cylindrical silicone mould with a 3-mm internal diameter, 1 mm thickness and 1 mm in height was used (figure 11). It was positioned at the centre of the samples, and the cement was placed on them against the zirconia surface and polymerized for 40 s (XL 3000, 3M/ESPE; light intensity 500 mW/cm<sup>2</sup>, distance 0) from above and towards the contact area from a lateral position.

The mould was removed and the cylinder cement was light-cured for a further 40 seconds. Thus, a resin cement cylinder of 3 mm diameter and 1 mm in height bonded to the zirconia surface was obtained.



Figure 11. Samples of zirconia with cylinders of resin cement adhered over their surfaces.

### **III.4 Cyclic loading.**

All experimental groups were divided into two subgroups according to whether cyclic loading was applied or not. Thus, half of the specimens of each group ( $n=15$ ) were mounted in acrylic resin moulds for cyclic loading under 90 N (50.000 cycles, 3

cycles/sec) with the force applied perpendicularly to the zirconia surface opposite where the resin was cemented (figure 12).



Figure 12. Cyclic loading of a sample.

This compressive load was applied using a spherical stainless steel plunger, 5mm in diameter, attached to a cyclic loading machine (S-MMT-250NB; Shimadzu, Tokyo, Japan) (figure 13). The rest of the specimens from each group ( $n=15$ ), the other subgroup, were not subjected to cyclic loading and were stored in water until cyclic loading for the other zirconia samples had been completed.

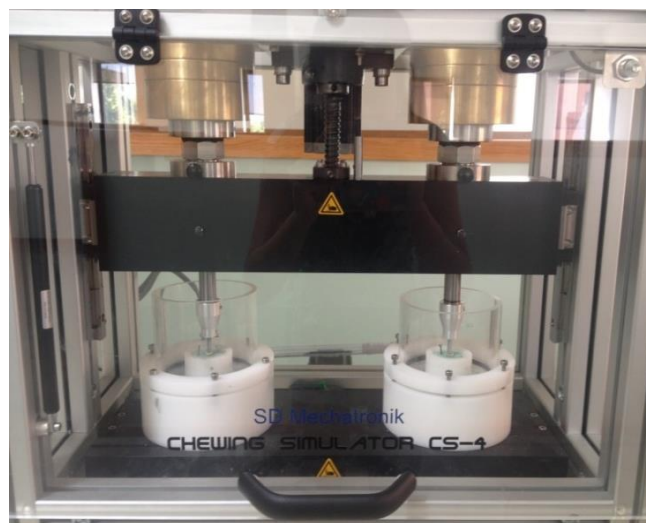


Figure 13. Chewing simulator.

### III.5 Shear Bond Strength (SBS) Test

With the cement cylinder on their surface, all subgroups were tested for SBS with a universal testing machine (AGS-X Autograph, Shimadzu Corporation, Kyoto, Japan) (figure 14), applying a shear load with a crosshead speed of 0.5 mm / min, until fracture (figure 15).



Figure 14. Universal SBS testing machine.

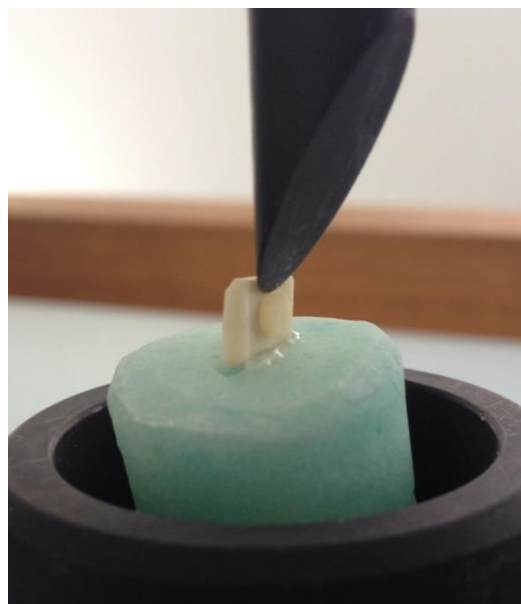


Figure 15. Applying a shear load to a sample.

To calculate the bond strength values in MPa, the maximum load recorded upon failure (in Newtons N) was divided by the bonding area (in square millimeters).

### **III.6 Failure mode analysis.**

After the SBS-test, each fractured specimen was examined under an Axio M1 (Carl Zeiss, Germany) light microscope at 40X magnification to determine the failure modes. These were classified according to the amount of cement deposited on the surface, or what it is the same, based on the percentage of zirconia surface appreciated: adhesive (more of 75 % of zirconia surface exposed, failure in adhesion), cohesive (less than 25%) or mixed- adhesive and cohesive failures simultaneously (between 25% and 75%, zirconia samples showing residual cement on their surfaces with both adhesive and cohesive failures).

### **III.7 Scanning electron microscopy (SEM) examination.**

Five zirconia surfaces from each experimental subgroup ( $n=5$ ) were prepared for surface morphology analysis with a variable pressure SEM (Zeiss EVO MA25; Carl Zeiss, Jena, Germany). Specific regions across the zirconia surface were explored with the scanning electron microscope, focusing with different magnifications ( $\times 70$  and  $\times 1000$ ) in order to obtain a panoramic view of the effect of laser processing and the

effect of the other conditioning methods.

In addition, representative fractured samples were dehydrated for 48h in a desiccator (Sample Dry Keeper Simulate Corp., Tokyo, Japan) and were sputter-coated with a 10-nm platinum layer in a Polaron E5100 SEM coating unit (Polaron Equipment Ltd., Hertfordshire, England, UK).

Specific zirconia surface areas were examined with the scanning electron microscope, focusing with different magnifications (from  $\times 30$  to  $\times 1000$ ) in order to analyze the morphology of the debonded interfaces and identify possible differences among the experimental groups with respect to the surface topography and morphology of the debonded interfaces.

### **III.8 Statistical analysis**

The bond-strength values were measured in MPa. The data were analyzed with SPSS v21 (Statistical Package for the Social Sciences, Chicago, IL), using a p-value below 0.05 as the threshold for statistical significance. ANOVA tests were applied to compare the SBS among the subgroups regarding the use of different zirconia surface treatments.

When the ANOVA test detected significant differences, Bonferroni post-hoc comparisons were performed to quantify the differences between two subgroups. The Chi-square test was used to detect differences in the types of failures among subgroups.





## *IV. RESVITS*

## IV.1 Shear Bond Strength (SBS) Test

The mean values and standard deviations (SD) of SBS for all the different surface treatment subgroups are shown in Table 10. The results obtained using one way ANOVA indicated that the SBS values varied according to the surface treatment method ( $p<0.001$ ) in both loaded and unloaded specimens.

The paired-T tests comparisons indicated that all surface method conditionings had significantly lower SBS values after the cyclic loading, except APA25, for which similar values were observed in both subgroups.

	<i>Control</i> <i>n=15</i>	<i>APA25</i> <i>n=15</i>	<i>TSC</i> <i>n=15</i>	<i>FS20</i> <i>n=15</i>	<i>FS40</i> <i>n=15</i>	
<b>Unloaded subgroups</b>	4.4(1.3)a*	8.1(3.6)b	9.5(2.3)bc*	10.8(1.9)c*	10.7(1.4)c*	F=20.4 $p<0.001$
<b>Loaded subgroups</b>	3.1(0.5)a*	7.2(3.4)b	7.0(1.7)b*	8.5(1.0)b*	7.7(0.4)b*	F=19.0; $p<0.001$

The different letters refer to significant inter-group comparisons after Bonferroni corrections ( $p<0.05$ ) and \* refers to significant differences ( $p<0.01$ ) between unloaded and loaded specimens within the same subgroup.

Table 10. Comparison of the SBS among the zirconia surface treatment subgroups. ANOVA with Bonferroni corrections.

The Bonferroni post-hoc inter-group comparisons found that among unloaded specimens, the APA25 subgroup obtained higher SBS values than the control subgroup, but they were significantly lower than the FS20 and FS40 SBS values ( $p<0.05$ ), which were similar to each other. However comparable values were observed within the

unloaded specimens of the APA25 and TSC subgroups ( $p=0.94$ ) after bonferroni post-hoc comparisons. By contrast, after cyclic loading as applied, the four surface treatments afforded the same SBS values, which were significantly higher than those of the control subgroup values ( $p<0.001$ ).

The bond failure-mode analyses are shown in Table 11. In the control group, most of the failures were adhesive, while in the treatment groups they were mostly mixed-adhesive and cohesive failures simultaneously, and none of the samples of either group had cohesive failure, this comparison being statistically significant ( $p<0.05$ ) except for the APA25 subgroup ( $p=0.14$ ) among the unloaded samples. Among the loaded samples there were not significant differences between subgroups (Chi= 8.2, df:4;  $p=0.08$ ), although mixed failures were clearly more common among the treated samples than in controls. In addition, the distribution of the adhesive failure rates was not significantly different after loading in any subgroups.

		<i>Control</i> <i>n=15</i> <i>N(%)a</i>	<i>APA25</i> <i>n=15</i> <i>N(%)b</i>	<i>TSC</i> <i>n=15</i> <i>N(%)b</i>	<i>FS20</i> <i>n=15</i> <i>N(%)b</i>	<i>FS40</i> <i>n=15</i> <i>N(%)b</i>	
<b>Failure mode of unloaded subgroups</b>	Adhesive	10(66.7)	5(33.3)	3(20.0)	4(26.7)	1(6.7)	Chi:14.2 (df=4); p-value: 0.007
	Cohesive	0	0	0	0	0	
	Mixed	5(33.3)	10(66.7)	12(80.0)	11(73.3)	14(93.3)	
<b>Failure mode of loaded subgroups</b>	Adhesive	9(60.0)	3(20.0)	3(20.0)	3(20.0)	4(26.7)	Chi:8.2 (df=4); p-value: 0.08
	Cohesive	0	0	0	0	0	
	Mixed	6(40.0)	12(80.0)	12(80.0)	12(80.0)	11(73.3)	
		Chi:0.1; p:1.0	Chi: 0.7; p:0.7	Chi:0.0; p:1.0	Chi:0.1; p:1.0	Chi:2.2; p:0.3	

**The different letters refer to significant inter-group comparisons after two-by-two Chi Square Tests taking the control as reference.**

Table 11. Failure modes within the subgroups.

## IV.2 SEM Observations.

The SEM micrographs in figure 16 show the zirconia surface morphology after the different surface treatment methods had been applied (magnification power, x 700). In image 16A, which represents the NT group, marked scratches running in the same direction on its surface as result of the polishing procedure can be seen. Image 16B corresponds to the APA25 group and reveals granule-shaped micro-retentions on the surface, due to the impact of the high-speed 25- $\mu$ m alumina particles. Image 16C represents the TSC group and reveals a rough appearance as a result of the coating and solidification of the tribochemical silica particles. Image 16D, which corresponds to the FS20 group, and image 16E, which represents the FS40 group, show a well-defined pattern of deep grooves, which are higher and wider apart in the FS40 group.

Figures 17 and 18 show representative SEM images of the debonded zirconia surfaces of all the subgroups after SBS, at magnification powers of x30 and x700.

Figure 17 shows the debonded zirconia surfaces of the subgroups to which cyclic loading were applied. Images 17A and 17B represent the control subgroup and show adhesive failure, with a very small amount of remains of the resin cement on the zirconia surface of which more than 75% was appreciated without resin. Images 17C and 17D (APA25 subgroup), images 17E and 17F (TSC subgroup), images 17G and 17H (FS20 subgroup) and images 17I and 17J (FS40 subgroup) exhibit mixed failures, that is adhesive and cohesive failures simultaneously, with residual cement on the zirconia surface exposed between 25 and 75 % of it.

Figure 18 shows the debonded zirconia surfaces of the other subgroups, to which

cyclic loading was not applied. As in figure 17, images 18A and 18B (Control subgroup) show adhesive failure, where there is a very small part of resin cement residual on the zirconia surface of which more than 75% was appreciated without resin. Images 18C and 18D (APA25 subgroup), images 18E and 18F (TSC subgroup), images G and H (FS20 subgroup), and images 18I and 18J (FS40 subgroup) exhibit mixed failures, adhesive and cohesive failures simultaneously, with a large cohesive phase and visible pores in the remaining residual cement.

In neither group cohesive failure, in which the zirconia surface is exposed at least 25%, is not observed.

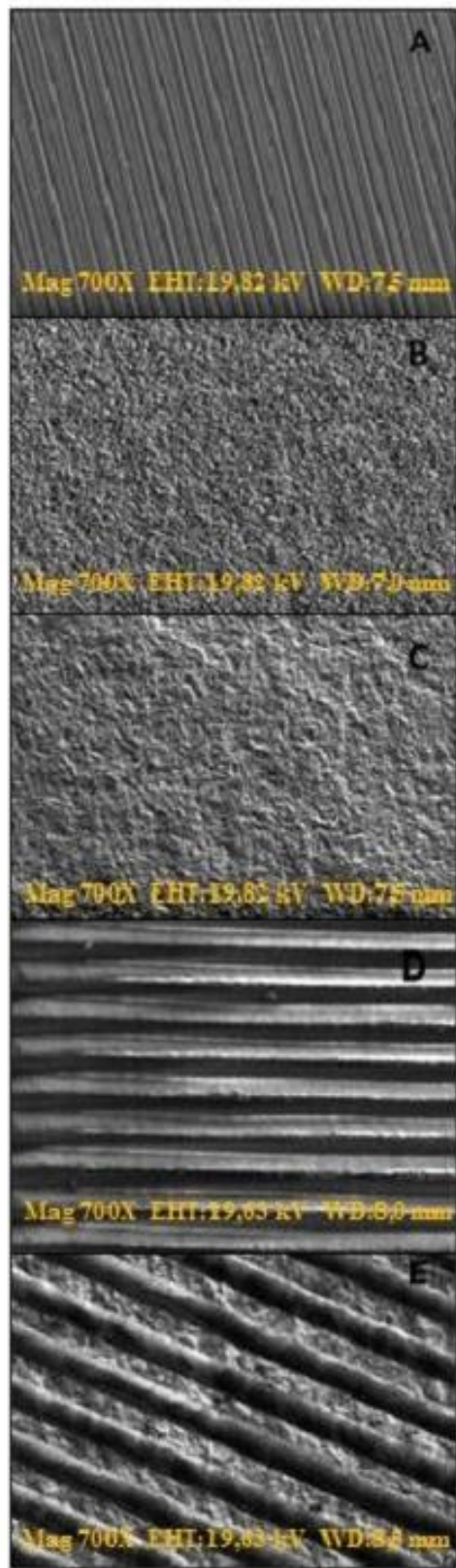


Figure 16. SEM micrographs of zirconia surfaces after conditioning treatments.

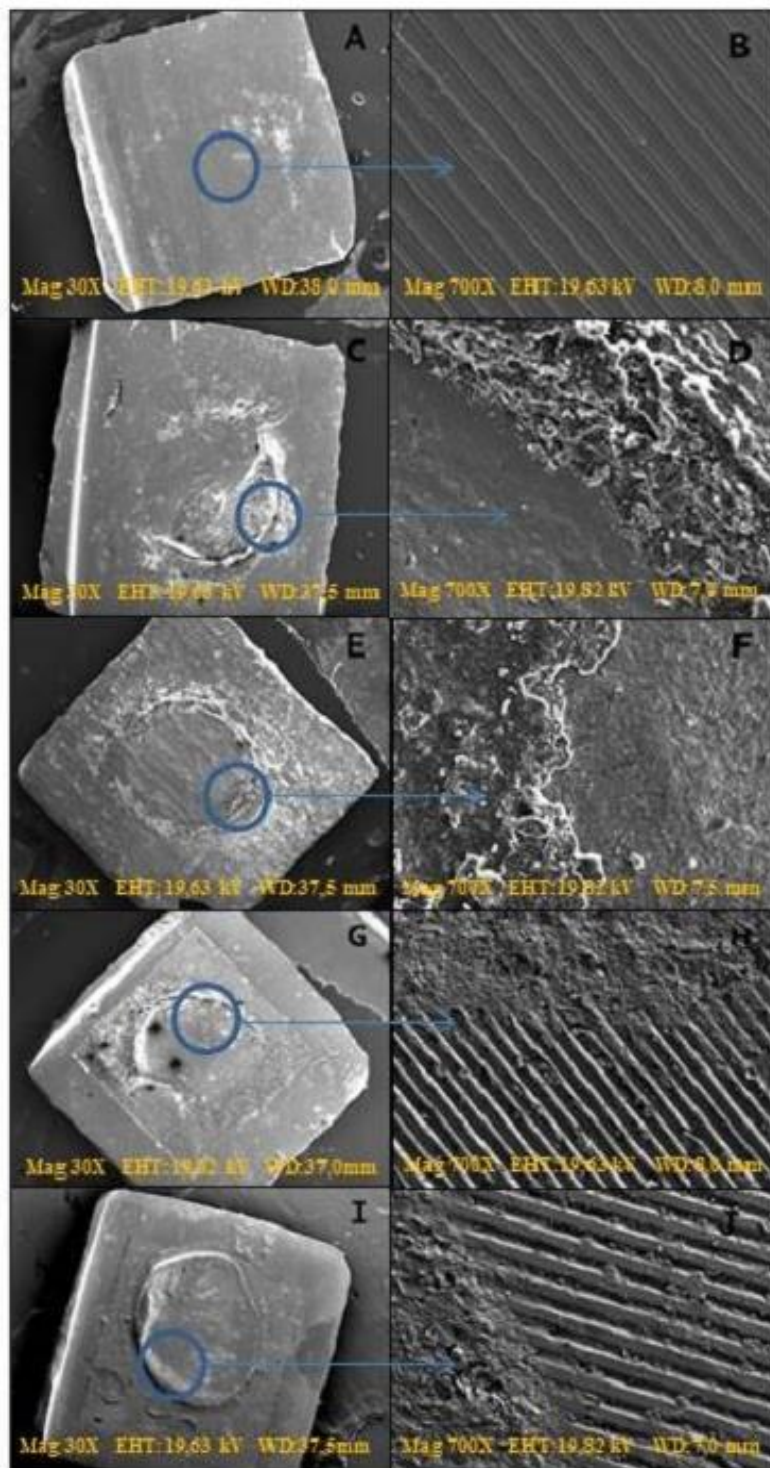


Fig 17. Representative zirconia surface SEM images (X30 and X700 magnification) of the most common failure type for the subgroups in which the cyclic loading was applied.

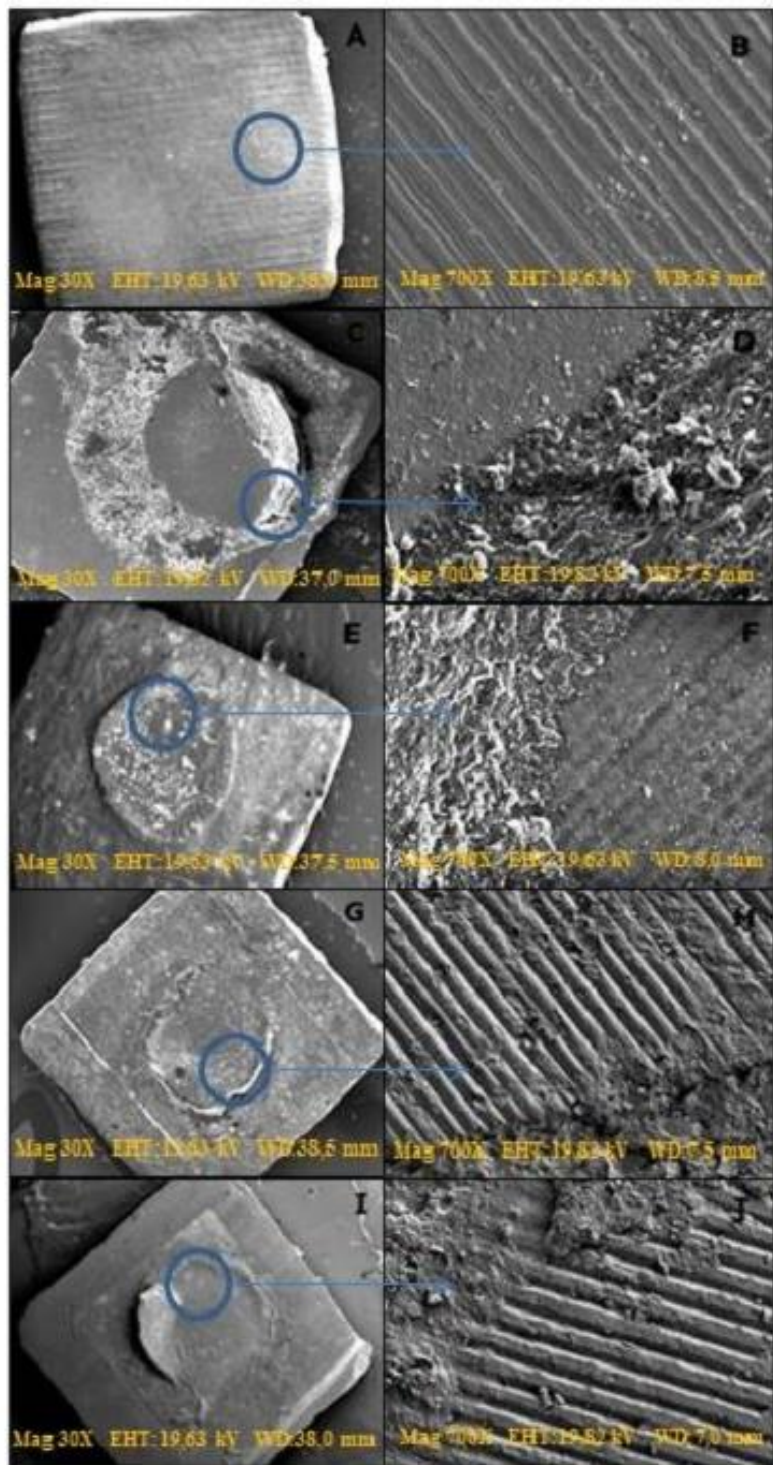


Fig 18. Representative zirconia surface SEM images (X30 and X700 magnification) of the most common failure type for the subgroups in which the cyclic loading was not applied.





## *V. DiSCVSSION*

Zirconia ceramics are widely used today in dentistry because they exhibit exceptional fundamental dental properties such as high strength, hardness, fracture toughness, and suitable aesthetics, among others [Camposilvan *et al.*, 2015] and this has made that, in the field of orthodontics, many patients that demand orthodontics treatments, carry some type of zirconia restoration in their mouths. However, there is still no an adhesion protocol that is available to all clinicians to get a resin-zirconia bond with high efficiency in restorative dentistry to cement zirconia on different biological substrates such as enamel or dentin; neither in orthodontics to cement nonbiological substrates such as different orthodontic attachments on zirconia surface, and it remains one of the major problems with which orthodontists routinely have to deal and they are exposed to problema such as debonding of brackets that increase the risk of failure during treatment period.

In our research, we began investigating at the zirconia-resin interface employing a self-adhesive resin cement (Clearfil) because, regarding adhesion to zirconia, self-adhesive resin cements are the best that we can used [Ferracane *et al.*, 2011; Casucci *et al.*, 2012; Maeda *et al.*, 2014]. This cement contain 10-MDP acidic functional monomer that enhance the ceramic surface wettability, protect against moisture, and create an acid environment that may support the bonding reaction. As a result, the 10-MDP monomers form cross-linkages with the 10-MDP groups dispersed in the cement resin matrix and with the -OH radicals of the zirconium-oxide surfaces [Kern *et al.*, 1998; Yoshida *et al.*, 2006; Wolfart *et al.*, 2007].

The long-term success of zirconia ceramics depends on the type of cement [Passos *et al.*, 2010], the cementing procedure [Inokoshi *et al.*, 2014] and, especially, the surface roughness, because the surface conditioning procedure seems to be a more relevant

factor in bonding to zirconia surfaces [Abousheib, 2011; Usumez *et al.*, 2013]. The results regarding bond strength demonstrated that femtosecond laser irradiation was more effective in improving bond strength than airborne-particle abrasion with 25- $\mu\text{m}$  alumina particles and no surface treatment (Table 10). The SEM observations suggested considerable quality differences in the zirconia ceramic architecture after femtosecond laser irradiation (Figure 16) as compared with the other conditioning methods, and this could be related to these higher values. A recent study reported that femtosecond laser irradiation is an effective surface treatment for roughening the surfaces of zirconia ceramics [Kara *et al.*, 2015]. It produces a pattern of deep horizontal furrows on the zirconia surface (Figures 16D and 16E), allowing greater retention of resin cements, which become intertwined within these grooves to form a single bonded structure, thereby increasing bond strength. By contrast, in the control group (Figure 16A) there is no abrasion or irregularities on the surface that provide micromechanical retention, only the effect of wet-polished with 600-grit silicon carbide paper. Also, in the APA25 group, alumina particle sandblasting created a rough surface (Figure 16B), but the surface irregularities have insufficient micro depth and therefore both groups exert less mechanical retention than the FS20 group (Figures 16D), FS40 group (Figure 16E) and TSC group (Figure 16C).

In recent studies [Lorenzo *et al.*, 2014; Lorenzo *et al.*, 2015] an abrasion pattern similar to that obtained in our study when applying femtosecond laser on the enamel surface, also showing increased adhesive efficiency, has been reported. Thus, the use of a femtosecond laser may be valid for conditioning on enamel and zirconia, as we show here. Thus, the use of femtosecond lasers is increasingly supported as an alternative in the field of adhesion in dentistry, replacing drills in conservation

dentistry [Luengo *et al.*, 2013] and also serving as both a conditioning agent and for the ablation of different types of surfaces -whether they are biological, such as the enamel [Lorenzo *et al.*, 2014; Lorenzo *et al.*, 2015] or dentine [Portillo *et al.*, 2012], with a minimum amount of thermal and mechanical damage to the surfaces [Pike *et al.*, 2007; Girard *et al.*, 2007]. In addition, in a recent study [Akpinar *et al.*, 2015] applied femtosecond laser irradiation to zirconia surfaces and obtained an abrasion similar to that obtained in our study, with a gentle, precise and clear zirconia surface and an increase in the adhesive efficiency of the zirconia-resin interface. Thus, the use of a femtosecond laser may be valid for the conditioning of non-biological surfaces with minimum damage to the surfaces [Kara *et al.*, 2015]. These clinical findings, together with those obtained here, support the use of femtosecond laser irradiation as a future alternative for the treatment of dental cavities and the conditioning of different surfaces on which elements are to be cemented in dentistry, replacing the traditional methods employed currently.

The FS20 and FS40 groups had similar bond strength values, which were higher than those obtained with the other conditioning methods (Table 10). The SEM observations suggest considerable quality differences in the zirconia ceramic architecture after femtosecond laser irradiation as compared with the other conditioning methods, but also differences between the FS20 (Figure 16D) and FS40 (Figure 16E) groups. In the FS40 group, although the same pattern of grooves was observed as in the FS20 group, the grooves were higher and more separated from each other, suggesting that resin cement retention would be lower. In this sense, femtosecond laser irradiation at step 40 produced fewer and more widely spaced grooves, and the irradiation time was reduced by half getting similar values in terms of adhesive effectiveness. Clinically,

time of application is a very important factor to be taken into consideration because it is necessary that the surface conditioning method can produce a pattern of engraving in order to ensure stable and durable bonding, but it must be carried out as fast as possible.

The tribochemical silica coating provided SBS values close to those obtained with femtosecond laser irradiation when cyclic loading was not applied. This high value (9.5 MPa) can be related directly to the roughness of the zirconia surface (Fig1C), created with this surface conditioning method, and although it did not follow any specific pattern, such as that elicited by femtosecond laser irradiation, it was as retentive as in the FS20 (Fig 1D) and FS40 (Fig 1E) subgroups. Thus, in our study it was observed that retention depends more on the engraving depths obtained than on the type, and this mainly affects the bond strength results. In addition, besides the influence of the surface roughness created, resin cement adhesion could be improved effectively by silica coating on zirconia surfaces which is what allows chemical retention to occur [Liu *et al.*, 2015]. In addition, the silica coating process allows chemical coupling through the silane [Gomes *et al.*, 2015]. After the silica particles have impacted the surface, the zirconia surface irregularities are infiltrated by ceramic primer Rely X<sup>TM</sup>. Silane coupling agents produce better contact and infiltration of the resin into the zirconia surface irregularities and protect against moisture through chemical bonding. The use of the MDP-primer after silica coating increased bond strength [May *et al.*, 2010].

Airborne-particle abrasion with 25- $\mu\text{m}$  Al<sub>2</sub>O<sub>3</sub> particles was less effective in improving bond strength than femtosecond laser irradiation and tribochemical silica coating. Although alumina particle sandblasting created a rough surface (Figure 16B) similar to that seen in the TSC group (Figure 16C) it does not improve bond strength

because the surface irregularities have insufficient micro depth, unlike the irregularities created in the FS20 group (Figure 16D). FS40 group (Figure 16E) and TSC group (Figure 16C), and therefore fails to generate sufficient micromechanical retention.

The control group showed lower SBS values than the other groups. This can be seen from the SEM images (Figure 16A), where it may be observed that in these zirconia samples, which were only subjected to wet-polishing with 600-grit silicon carbide paper, there were no surface irregularities such as shallow pits or microcracks to provide micromechanical retention. The Y-TZP zirconia surface roughness is influenced by the surface treatment applied and is directly related to the bonding properties [Kirmali *et al.*, 2015]. The strong and durable resin-zirconia bonding is vital for the longevity of dental restorations and this is only possible with a surface treatment that will allow the zirconia surface to be roughened [Abousheib 2011].

It is necessary to note that all dental restorations are clinically subject to occlusal masticatory forces that can reach values of up to 800 N [Zahran *et al.*, 2008]. Thus, although Y-TZP ceramics are hard and have high strength and fracture toughness [El-Korashy and El-Refai, 2014], their long-term success regarding the degree of adhesion achieved is especially dependent upon the surface roughness produced by the different surface conditioning methods [Usumez *et al.*, 2015] and the ability of these ceramics to withstand the cyclic forces, which can be simulated experimentally using cyclic loading [Koyama *et al.*, 2012].

The results regarding bond strength revealed that all the surface conditioning

methods, except abrasion with airborne alumina particles, afforded lower SBS values when the samples were subjected to cyclic loading. Under cyclic loading, zirconia fixed dental prostheses are subject to fracture during function, especially in the posterior area, and zirconia abutments exhibit a significantly lower fracture resistance [Foong *et al.*, 2013], with a significant reduction in preload [Butignon *et al.*, 2013]. It has been reported that when cyclic loading is applied, there is a distribution of stresses generated around the bonding interface, with a progressive cone cracking surface [Zhou *et al.*, 2007] associated with low fracture strength [Aboushelib, 2013]. Accordingly, on performing cyclic loading in our research the results can be considered to be more clinically relevant because they represent the mechanical degradation process that zirconia restorations undergo due to masticatory forces more faithfully. In another study, Ghazy *et al.* evaluated the influence of dynamic fatigue on the fracture loads and failure modes of different types of adhesive zirconia restorations subjected to different surface treatments and bonded with resin cement, and showed that dynamic fatigue reduced failure load to a significant extent and produced fatigue in the adhesion strength of zirconia restorations [Ghazy *et al.*, 2012], in agreement with the bond strength results obtained in our research.

The specific zirconia surface areas of each subgroup were examined to analyze the topography and morphology of the debonded interfaces; the results are shown in Table 11. They support the bond strength results and the differences among the experimental groups. Regardless of whether cyclic loading was applied or not, the control group showed a tendency towards adhesive failure at the resin-zirconia interface, where there was a very small amount of remains of the resin cement on the

zirconia surface of which more than 75% was appreciated without resin (Figures 17A, 18A), in accordance with the literature addressing resin cements [De Oyagüe *et al.*, 2009]. By contrast, in the APA25 (Figures 17C, 18C), TSC (Figures 17E, 18E), FS20 (Figures 17G, 18G) and FS40 (Figures 17I, 18I) groups mainly mixed failures were observed where there were adhesive and cohesive failures simultaneously and the zirconia surface was exposed between 25% and 75 %. There was a high prevalence of mixed failures in the TSC, FS20, and FS40 groups and adhesive failure in the control groups, regardless of whether cyclic loading was applied or not. These results show that the differences among the experimental groups were caused by the differences in surface roughness between the zirconia samples treated with the different conditioning methods (Figure 16) and not because cyclic loading was applied.





## *Vi. CONCLUSIONS*

The results of our research allow us to conclude the following:

1. Femtosecond laser irradiation and tribochemical silica coating create a consistent and profound surface roughness, improving the adhesive effectiveness of the zirconia-resin cement interface. This is due to that the adhesion of the interface is influenced by the micromechanical retention, and this last is based more on the engraving depth created by conditioning method than on the engraving pattern become a fundamental requirement for establishing a strong and durable bond with zirconia-based materials.
2. Femtosecond laser treatment, both step 20 as step 40, might be a reliable way to achieve suitable adhesion between resins and zirconia due to creates a pattern of deep grooves on the zirconia surface that are filled by resin cement. The difference between the different steps is that the time of irradiation at step 40 is half , and it is an important clinical factor to be taken into consideration. The surface conditioning method must produce a pattern of engraving in order to ensure stable and durable bonding, but it must also be carried out as fast as possible. In this sense, since femtosecond laser irradiation at step 40 produced fewer and more widely spaced grooves, the irradiation time was substantially reduced (indeed, by half). Accordingly, for practical purposes, and since efficiency is preferred over effectiveness, to achieve the best results in the shortest time possible it is best to use femtosecond laser in this step.
3. When cyclic loading is applied, the adhesive effectiveness of the zirconia-resin interface decreases when any of the zirconia surface treatments are applied

previously, except alumina particle abrasion, which is not affected by cyclic loading.





## *Vii. REFERENCES*

Abe Y, Braem MJ, Lambrechts P, Inoue S, Takeuchi M, Van Meerbeek B. Fatigue behavior of packable composites. *Biomaterials*. 2005;26(17):3405-9.

Abousheib MN. Evaluation of zirconia/resin bond strength and interface quality using a new technique. *J Adhes Dent*. 2011;13(3):255-60.

Aboushelib MN. Simulation of cumulative damage associated with long term cyclic loading using a multi-level strain accommodating loading protocol. *Dent Mater*. 2013;29(2):252-8.

Aboushelib MN, Feilzer AJ, Kleverlaan CJ. Bonding to zirconia using a new surface treatment. *J Prosthodont*. 2010;19(5):340-46.

Aboushelib MN, Kleverlaan CJ, Feilzer AJ. Selective infiltration-etching technique for a strong and durable bond of resin cements to zirconia-based materials. *J Prosthet Dent*. 2007;98(5):379-88.

Aboushelib MN, Matinlinna JP. Combined novel bonding method of resin to zirconia ceramic in dentistry: a pilot study. *J Adhesive Sci Technol*. 2011;25(1):1049-60.

Aboushelib MN, Matinlinna JP, Salameh Z, Ounsi H. Innovations in bonding to zirconia-based materials: Part I. *Dent Mater*. 2008;24(9):1268-72.

Aboushelib MN, Mirmohamadi H, Matinlinna JP, Kukk E, Ounsi HF, Salameh Z. Innovations in bonding to zirconia-based materials. Part II: Focusing on chemical interactions. Dent Mater. 2009;25(8):989-93.

Agustín-Panadero R, Román-Rodríguez JL, Ferreiroa A, Solá-Ruiz MF, Fons-Font A. Zirconia in fixed prosthesis: a literature review. J Clin Exp Dent. 2014;6(1):66-73.

Akin H, Ozkurt Z, Kimalı O, Kazazoglu E, Ozdemir A. Shear bond strength of resin cement to zirconia ceramic after aluminium oxide sandblasting and various laser treatments. Photomed Laser Surg. 2011;29(12):797-802.

Akpınar YZ, İrgin C, Yavuz T, Aslan MA, Kılıç HS, Usumez A. Effect of femtosecond laser treatment on the shear bond strength of a metal bracket to prepared porcelain surface. Photomed Laser Surg. 2015;33(4):206-12.

Akpınar YZ, Kepceoglu A, Yavuz T, Aslan MA, Demirtag Z, Kılıç HS, Usumez A. Effect of femtosecond laser beam angle on bond strength of zirconia-resin cement. Lasers Med Sci. 2015. [Epub ahead of print].

Álvarez-Fernandez MA, Peña-Lopez JM, González-González IR, Olay-Garcia MA. Características generales y propiedades de las cerámicas sin metal. RCOE. 2003;8(1):525-46.

Amaral R, Özcan M, Valandro LF, Bottino MA. Microtensile bond strength of a resin cement to glass infiltrated zirconia-reinforced ceramic: the effect of surface conditioning. *Dent Mater*. 2006;22(3):283-90.

Anic I, Vidovic D, Luic M, Tudja M. Laser induced molar tooth pulp chamber temperature changes. *Caries Res*. 1992;26(3):165-9.

Anthonsen SA, Anusavice KJ. Contrast ratio of veneering and core ceramics as a function of thickness. *Int J Prosthodont*. 2001;14(4):316-20.

Anusavice KJ. Phillips' science of dental materials. 11th ed. Missouri, USA: Saunders; 2003.

Armstrong S, Geraldeli S, Maia R, Raposo LH, Soares CJ, Yamagawa J. Adhesion to tooth structure: a critical review of "micro" bond strength test methods. *Dent Mater*. 2010;26(2):50-62.

Attia A, Kern M. Influence of cyclic loading and luting agents on the fracture load of two all-ceramic crown systems. *J Prosthet Dent*. 2004;92(6):551-6.

Atsu SS, Kilicarslan MA, Kucukesmen HC, Aka PS. Effect of zirconium oxide ceramic surface treatments on the bond strength to adhesive resin. *J Prosthet Dent.* 2006;95(6):430-6.

Ban S. Reliability and properties of core materials for all-ceramic dental restorations. *Jpn Dent Sci Rev.* 2008;44(1):3-21.

Beuer F, Stimmelmayr M, Gernet W, Edelhoff D, Güh JF, Naumann M. Prospective study of zirconia-based restorations: 3-year clinical results. *Quintessence Int.* 2010;41(8):631-7.

Blatz M, Phark J-H, Ozer F, Mante F, Saleh N, Bergler M, Sadan A. In vitro comparative bond strength of contemporary self-adhesive resin cements to zirconium oxide ceramic with and without air-particle abrasion. *Clin Oral Investig.* 2010;14(2):187-92.

Blatz M, Sadan A, Martin J, Lang B. In vitro evaluation of shear bond strengths of resin to densely-sintered high-purity zirconium-oxide ceramic after longterm storage and thermal cycling. *J Prosthet Dent.* 2004;91(4):356-62.

Blatz MB, Sadan A, Kern M. Resin-ceramic bonding: a review of the literature. *J Prosthet Dent.* 2003;89(3):268-74.

Blatz MB, Chiche G, Holst S, Sadan A. Influence of surface treatment and simulated aging on bond strengths of luting agents to zirconia. *Quintessence Int.* 2007;38(9):745-53.

Bloembergen N. Laser-induced electric breakdown in solids. *IEEE J Quant Electron.* 1974;10(3):375-86.

Boehm R, Rich J, Webster J, Janke S. Thermal stress effects and surface cracking associated with laser use on human teeth. *J Biomech Eng.* 1977;77(1):189-94.

Bourgeois F, Ben-Yakar A. Femtosecond laser nanoaxotomy properties and their effect on axonal recovery in *C. elegans*. *Opt Express.* 2008;16(8):5963.

Braem MJ, Davidson CL, Lambrechts P, Vanherle G. In vitro flexural fatigue limits of dental composites. *J Biomed Mater Res.* 1994;28(12):1397-402.

Braem M, Lambrechts P, Vanherle G. Clinical relevance of laboratory fatigue studies. *J Dent.* 1994;22(2):97-102.

Braun A, Krillke RF, Frentzen M, Bourauel C, Stark H, Schelle F. Heat generation caused by ablation of dental hard tissues with an ultrashort pulse laser (USPL) system. *Lasers Med Sci.* 2015;30(2):475-81.

Burke FJT. Trends in indirect dentistry: 3. Luting materials. Dent Update. 2005;32(5):251-4.

Butignon LE, Basilio M de A, Pereira R de P, Arioli Filho JN. Influence of three types of abutments on preload values before and after cyclic loading with structural analysis by scanning electron microscopy. Int J Oral Maxillofac Implants. 2013;28(3):161-70.

Calvalti AN, Foxton RM, Watson TF, Oliveira MT, Giannini M, Marchi GM. Y-TZP ceramics: key concepts for clinical application. Oper Dent. 2009;34(3):344-51.

Camposilvan E, Marro FG, Mestra A, Anglada M. Enhanced reliability of yttria-stabilized zirconia for dental applications. Acta Biomater. 2015;17(1):36-46.

Casucci A, Goracci C, Chieffi N, Monticelli F, Giovannetti A, Juloski J, Ferrari M. Microtensile bond strength evaluation of self-adhesive resin cement to zirconia ceramic after pre-treatments. Am J Dent. 2012;25(5):269-75.

Chen X, Liu X. Short pulsed laser machining: how short is short enough?. J Laser Appl. 1999;11(1):268-72.

Chevalier J. What future for zirconia as a biomaterial?. Biomaterials. 2006;27(4):535-43.

Chichkov BN, Momma C, Nolte S, von Alvensleben F, Tunnermann A. Femtosecond, picosecond and nanosecond laser ablation solids. *Appl Phys A*. 1996;63(1):109-15.

Choi H, Choi M, Choi K, Choi C. Blockade of vascular endothelial growth factor sensitizes tumor-associated vasculatures to angiolytic therapy with a high-frequency ultrashort pulsed laser. *Microvasc Res*. 2011;82(2):141-6.

Cox CJ, Pearson GJ, Palmer G. Preliminary in vitro investigation of the effects of pulsed Nd:YAG laser radiation on enamel and dentin. *Biomaterials*. 1994;15(14):1145-51.

Craig RG, Powers JM. Restorative dental materials. 11th ed. St. Louis: Mosby; 2002.

Cvikl B, Dragic M, Franz A, Raabe M, Gruber R, Moritz A. Long-term storage affects adhesion between titanium and zirconia using resin cements. *J Adhes Dent*. 2014;16(5):459-64.

De Hoff PH, Anusavice KJ, Wang Z. Three-dimensional finite analysis of the shear bond test. *Dent Mater*. 1995;11(2):123-31.

De Munck J, Braem M, Wevers M, Yoshida Y, Inoue S, Suzuki K, Lambrechts P, Van Meerbeek B. Microrotatory fatigue of tooth-biomaterial interfaces. *Biomaterials*. 2005;26(10):1145-53.

De Oyagüe RC, Moticelli F, Toledano M, Osorio E, Ferrari M, Osorio R. Influence of surface treatments and resin cement selection on bonding to densely-sintered zirconium-oxide ceramic. *Dent Mater*. 2009;25(2):172-9.

Della Bona A, Van Noort R. Shear vs tensile bond strength of the resin composite bonded to ceramic. *J Dent Res*. 1995;74(9):1591-6.

Denry I, Holloway JA. Ceramics for dental applications: a review. *Materials*. 2010;3(1):351-68.

Denry I, Kelly JR. State of the art of zirconia for dental applications. *Dent Mater*. 2008;24(3):299-307.

Dérand P, Dérand T. Bond strength of luting cements to zirconium oxide ceramics. *Int J of Prosthodont*. 2000;13(2):131-5.

Díaz-Romeral P, López E, Malumbres F, Gil LJ. Porcelanas dentales de alta resistencia para restauraciones de recubrimiento total: una revisión bibliográfica. Parte I. Rev Int Prot Estomatol. 2008;10(1):19-31.

Doronina LV, Fedotov IV, Voronin AA, Ivashkina OI, Zots MA, Anokhin KV, Rostova E, Fedotov AB, Zheltikov AM. Tailoring the soliton output of a photonic crystal fiber for enhanced two-photon excited luminescence response from fluorescent protein biomarkers and neuron activity reporters. Opt Lett. 2009;34(21):3373-5.

Drummond JL, Bapna MS. Static and cyclic loading of fiber-reinforced dental resin. Dent Mater. 2003;19(3):226-31.

El-Korashy DI, El-Refai DA. Mechanical properties and bonding potential of partially stabilized zirconia treated with different chemomechanical treatments. J Adhes Dent. 2014;16(4):365-76.

Elsaka SE. Effect of surface treatments on the bonding strength of self-adhesive resin cements to zirconia ceramics. Quintessence Int. 2013;44(6):407.

España-Tost AJ, Arnabat-Domínguez J, Berini-Aytés L, Gay-Escoda C. Aplicaciones del láser en Odontología. RCOE. 2004;9(5):497-511.

Ferracane JL. Hygroscopic and hydrolytic effects in dental polymer networks. Dent Mater. 2006;22(3):211-22.

Ferracane JL, Berge HX, Condon JR. In vitro aging of dental composites in water-effect of degree of conversion, filler volume, and filler/matrix coupling. J Biomed Mater Res. 1998;42(3):465-72.

Ferracane JL, Hopkin JK, Condon JR. Properties of heat-treated composites after aging in water. Dent Mater. 1995;11(6):354-8.

Ferracane JL, Stansbury JW, Burke FJT. Self-adhesive resin cements—chemistry, properties and clinical considerations. J Oral Rehabil. 2011;38(4):295-314.

Fons-Font A, Solá-Ruiz M, Martínez-González A. Clasificación actual de las cerámicas dentales. RCOE. 2001;6(1):645-56.

Foong JK, Judge RB, Palamara JE, Swain MV. Fracture resistance of titanium and zirconia abutments: an in vitro study. J Prosthet Dent. 2013;109(5):304-12.

Frankenberger R, Strobel WO, Krämer N, Lohbauer U, Winterscheidt J, Winterscheidt B, Petschelt A. Evaluation of the fatigue behavior of the resin-dentin bond with the use of different methods. J Biomed Mater Res B Appl Biomater. 2003;67(2):712-21.

Frederickson KS, White WE, Wheeland RG, Slaughter DR. Precise ablation of skin with reduced collateral damage using the femtosecond-pulsed, terawatt titanium-sapphire laser. Arch Dermatol. 1993;129(8):989-93.

Gale MS, Darvell BW. Thermal cycling procedures for laboratory testing of dental restorations. J Dent. 1999;27(2):89-99.

Gabel CV, Antonie F, Chuang CF, Samuel ADT, Chang C. Distinct cellular and molecular mechanisms mediate initial axon development and adult-stage axon regeneration in *C. elegans*. Development. 2008;135(6):1129-36.

Gamaly EG, Rode AV, Luther-Davies B, Tikhonchuk VT. Ablation of solids by fs lasers: Ablation mechanism and ablation thresholds for metals and dielectrics. Physics of Plasmas. 2002;9(1):949-57.

Garvie RC, Haninnk RH, Pascoe RT. Ceramic steel?. Nature. 1975;258(1):703-4.

Ghazy MH, Madina MM, Aboushelib MN. Influence of fabrication techniques and artificial aging on the fracture resistance of different cantilever zirconia fixed dental prostheses. J Adhes Dent. 2012;14(2):161-6.

Girard B, Cloutier M, Wilson DJ, Clokie CMI, Miller RJD, Wilson BC. Microtomographic analysis of healing of femtosecond laser bone calvaria wounds compared to mechanical instruments in mice with and without application of BMP-7. Lasers Surg Med. 2007;39(1):458-67.

Gomes AL, Castillo-Oyagüe R, Lynch CD, Montero J, Albaladejo A. Influence of sandblasting granulometry and resin cement composition on microtensile bond strength to zirconia ceramic for dental prosthetic frameworks. Am J Dent. 2013;41(1):31-41.

Gomes AL, Ramos JC, Santos del Riego S, Montero J, Albaladejo A. Thermocycling effect on microshear bond strength to zirconia ceramic using Er:YAG and tribochemical silica coating as surface conditioning. Lasers Med Sci. 2015;30(2):787-95.

Griggs JA. Recent advances in materials for all-ceramics restorations. Dent Clin North Am. 2007;51(3):713-27.

Guazzato M, Albakry M, Ringer SP, Swain MV. Strength, fracture toughness and microstructure of a selection of all-ceramic materials. Part II. Zirconia-based dental ceramics. Dent Mater. 2004;20(5):449-56.

Guo SX, Bourgeois F, Chokshi T, Durr NJ, Hilliard MA, Chronis N, Ben-Yakar A. Femtosecond laser nanoaxotomy lab-on-a chip for in vivo nerve regeneration studies. Nat Methods. 2008;5(6):531-3.

Hashimoto M, Ohno H, Sano H, Tay FR, Kaga M, Kodou Y, Oguchi H, Araki Y, Kubota M. Micromorphological changes in resin-dentin bonds after 1 year of water storage. J Biomed Mater Res. 2002;63(3):306-11.

Heisterkamp A, Mamom T, Kermani O, Drommer W, Welling H, Ertmer W, Lubatschowski H. Intrastromal refractive surgery with ultrashort laser pulses: in vivo study on the rabbit eye. Graefes Arch Clin Exp Ophthalmol. 2003;241(6):511-7.

Hoy CL, Durr NJ, Chen P, Piyawattanametha W, Ra H, Solgaard O, Ben-Yakar A. Miniaturized probe for femtosecond laser microsurgery and two-photon imaging. Optics Express. 2008;16(13):9996–10005.

Hummel SK, Pace LL, Marker VA. A comparision of two silicoating techniques. J Prosthodont. 1994;3(2):108-13.

Inokoshi M, De Munck J, Minakuchi S, Van Meerbeek B. Meta-analysis of bonding effectiveness to zirconia ceramics. J Dent Res. 2014;93(4):329-34.

Inokoshi M, Kameyama A, de Munck J, Minakuchi S, Van Meerbeek B. Durable bonding to mechanically and/or chemically pre-treated dental zirconia. *J Dent.* 2013;41(2):170-9.

International Standardization Organization. ISO TS 11405 dental materials guidance on testing of adhesion tooth structure. Geneva Switzerland: WHO; 1993.

Isgro G, Pallav P, Van der Zel JM, Feilzer AJ. The influence of the veneering porcelain and different surface treatments on the biaxial flexural strength of a heatpressed ceramic. *J Prosthet Dent.* 2003;90(5):465-73.

Janda R, Roulet JF, Wulf M, Tiller HJ. A new adhesive technology for all-ceramics. *Dent Mater.* 2003;19(6):567-73.

Juhasz T, Loesel HL, Kurtz RM, Horvath C, Bille JF, Mourou G. Corneal refractive surgery with femtosecond lasers. *IEEE J Sel Top Quant Electron.* 1999;5(1):902-10.

Kara O, Kara HB, Tobi ES, Ozturk AN, Kilic HS. Effect of various lasers on the bond strength of two zirconia ceramics. *Photomed Laser Surg.* 2015;33(2):69-76.

Kasraei S, Rezaei-Soufi L, Heidari B, Vafaee F. Bond strength of resin cement to CO<sub>2</sub> and Er:YAG laser-treated zirconia ceramic. *Restor Dent Endod.* 2014; 39(4):296-302.

Kautek W, Mitterer S, Krüger J, Husinsky W, Grabner G. Femtosecond pulse laser ablation of human corneas. *Appl Phys A*. 1994;58(5):513-8.

Kawai N, Lin J, Youmaru H, Shinya A, Shinya A. Effects of three luting agents and cyclic impact loading on shear bond strengths to zirconia with tribochemical treatment. *J Dent Sci*. 2012;7(1):118-24.

Keith O, Kusy RP, Whitley JQ. Zirconia brackets: an evaluation of morphology and coefficients of friction. *Am J Orthod Dentofacial Orthop*. 1994;106(6):605-14.

Kelly JR, Nishimura I, Campbell SD. Ceramics in dentistry: historical roots and current perspectives. *J Prosthet Dent*. 1996;75(1):18-32.

Kern M, Wegner SM. Bonding to zirconia ceramic: adhesion methods and their durability. *Dent Mater*. 1998;14(1):64-71.

Kirmali O, Kustarci A, Kapdan A, Er K. Efficacy of surface roughness and bond strength of Y-TZP zirconia after various pre-treatments. *Photomed Laser Surg* 2015;33(1):15-21.

Kitasako Y, Burrow MF, Nikaido T, Tagami J. The influence of storage solution on dentin bond durability of resin cement. *Dent Mater*. 2000;16(1):1-6.

Kohal RJ, Klaus G. A zirconia implant-crown system: a case report. Int J Periodontics Restorative Dent. 2004;24(2):147-53.

Kohal RJ, Wolkewitz M, Tsakona A. The effects of cyclic loading and preparation on the fracture strength of zirconium-dioxide implants: an in vitro investigation. Clinic Oral Implants Res. 2011;22(8):808-14.

Kohns P, Zhou P, Stromann R. Effective laser ablation of enamel and dentin without thermal side effects. J Laser Appl. 1997;9(3):171-4.

Kolodney H, Puckett AD, Brown K. Shear strength of laboratory-processed composite resins bonded to a silica-coated nickel-chromium-beryllium. J Prosthet Dent. 1992;67(3):419-22.

Kosmac T, Oblak C, Jevnikar P, Funduk N, Marion L. The effect of surface grinding and sandblasting on flexural strength and reliability of Y-TZP zirconia ceramic. Dent Mater. 1999;15(6):426-33.

Kosmac T, Oblak C, Jevnikar P, Funduk N, Marion L. Strength and reliability of surface treated Y-TZP dental ceramics. J Biomed Mater Res. 2000;53(4):304-13.

Koutayas S, Vagkopoulou T, Pelekanos S, Koidis P, Strub JR. Zirconia in dentistry.

Part 2. Evidence-based clinical breakthrough. Eur J Esthet Dent. 2009;4(4):348-80.

Koyama T, Sato T, Yoshinari M. Cyclic fatigue resistance of yttria-stabilized tetragonal zirconia polycrystals with hot isostatic press processing. Dent Mater J. 2012;31(6):1103-10.

Lange FF. Transformation toughening, Part 3. Experimental observations in the  $ZrO_2$ - $Y_2O_3$  system. J Mater Sci. 1982;17(1):240-6.

Lizarelli RFZ, Kurachi C, Misoguti L, Bagnato VS. Characterization of enamel and dentin response to Nd:YAG picosecond laser ablation. J Clin Laser Med Surg. 1999;17(3):127-31.

Lizarelli RF, Kurachi C, Misoguti L, Bagnato VS. A comparative study of nanosecond and picosecond laser ablation in enamel: morphological aspects. J Clin Laser Med Surg. 2000;18(3):151-7.

Liu D, Tsou JK, Matlinna JP, Wong HM. Effects of some chemical surface modifications on resin zirconia adhesion. J Mech Behav Biomed Mater. 2015;46(1):23-30.

Loesel FH, Fischer JP, Gotz MH, Horvath C, Juhasz T, Noack F, Suhm N, Bille JF. Non-thermal ablation of neural tissue with femtosecond laser pulses. *Applied Physics B.* 1998;66(1):121-8.

Lorenzo MC, Portillo M, Moreno P, Montero J, Castillo-Oyagüe R, García A, Albaladejo A. In vitro analysis of femtosecond laser as an alternative to acid etching for achieving suitable bond strength of brackets to human enamel. *Lasers Med Sci.* 2014;29(3):897-905.

Lorenzo MC, Portillo M, Moreno P, Montero J, García A, Santos del Riego SE, Albaladejo A. Ultrashort pulsed laser conditioning of human enamel: in vitro study of the influence of geometrical processing parameters on shear bond strength of orthodontic brackets. *Lasers Med Sci.* 2015;30(2):891-900.

Luengo MC, Portillo M, Sánchez JM, Peix M, Moreno P, García A, Albaladejo A.. Evaluation of micromorphological changes in tooth enamel after mechanical and ultrafast laser preparation of surface cavities. *Lasers Med Sci.* 2013;28(1):267-73.

Lubatschowski H, Maatz G, Heisterkamp A, Hetzel U, Drommer W, Welling H, Ertmer W. Application of ultrashort laser pulses for intrastromal refractive surgery. *Graefes Arch Clin Exp Ophthalmol.* 2000;238(1):33-9.

Lung CYK, Matinlinna JP. Aspects of silane coupling agents and surface conditioning in dentistry: an overview. Dent Mater. 2012;28(5):467-77.

Luthardt RG, Sandkuhl O, Reitz B. Zirconia-TZP and alumina-advanced technologies for the manufacturing of single crowns. Eur J Prosthodont Restor Dent. 1999;7(4):113-9.

Luthardt RG, Holzhüter M, Sandkuhl O, Herold V, Schnapp JD, Kuhlisch E, Walter M. Reliability and properties of ground Y-TZP- zirconia ceramics. J Dent Res. 2002;81(7):487-91.

Luthardt RG, Holzhüter MS, Rudolph H, Herold V, Walter MH. CAD/CAM machining effects on Y-TZP zirconia. Dent Mater. 2004;20(7):655-62.

Lüthy H, Loeffel O, Hammerle CHF. Effect of thermocycling on bond strength of luting cements to zirconia ceramic. Dent Mater. 2006;22(2):195-200.

Maatz G, Heisterkamp A, Lubatschowski H, Barcikowski S, Fallnich C, Welling H, Ertmer W. Chemical and physical side effects at application of ultrashort laser pulses for intrastromal refractive surgery. J Opt A. 2000;2(1):59-64.

Maeda FA, Bello-Silva MS, de Paula Eduardo C, Miranda Junior WG, Cesar PF. Association of different primers and resin cements for adhesive bonding to zirconia ceramics. *J Adhes Dent.* 2014;16(3):261-5.

Manicone PF, Iommetti PR, Raffaelli L. An overview of zirconia ceramics: basic properties and clinical applications. *J Dent* 2007;35(11):819-26.

Marion JE, Kin BM. Medical applications of ultra-short pulse lasers. *Proc SPIE.* 1999;3910(1):42-50.

Martinéz-Rus F, Pradiés-Ramiro G, Suárez García MJ, Rivera Gómez B. Cerámicas dentales: clasificación y criterios de selección. *RCOE.* 2007;12(1):253-63.

Matinlinna JP, Vallitu PK. Bonding of resin composites to etchable ceramic surfaces-an insight overview of the chemical aspects on surface conditioning. *J Oral Rehabil.* 2007;34(8):622-30.

May LG, Passos SP, Capelli DB, Ozcan M, Bottino MA, Valandro LF. Effect of silica coating combined to a MDP-based primer on the resin bond to Y-TZP ceramic. *J Biomed Mater Res B Appl Biomater.* 2010;95(1):69-74.

McLean JW, Hughes TH. The reinforcement of dental porcelain with ceramic oxides. Br Dent J. 1965;119(6):251-67.

Meric G, Ruyter IE. Influence of thermal cycling on flexural properties of composites reinforced with unidirectional silica-glass fibers. Dent Mater. 2008;24(8):1050-7.

Mirmohammadi H, Aboushelib MN, Kleverlaan CJ, de Jager N, Feilzer AJ. The influence of rotating fatigue on the bond strength of zirconia-composite interfaces. Dent Mater. 2010;26(7):627-33.

Mirmohammadi H, Aboushelib MN, Salameh Z, Kleverlaan CJ, Feilzer AJ. Influence of enzymatic and chemical degradation on zirconia resin bond strength after different surface treatments. Am J Dent. 2010;23(6):327-30.

Momma C, Chichkov B, Nolte S, von Alvensleben F, Tünnermann A, Welling H. Short-pulse laser ablation of solid targets. Opt Commun. 1996;129(1):134-42.

Monaco C, Caldari M, Scotti R. Clinical evaluation of tooth-supported zirconia-based fixed dental prostheses: a retrospective cohort study from the AIOP clinical research group. Int J Prosthodont. 2015;28(3):236-8.

Moradabadi A, Roudsari SE, Yekta BE, Rahbar N. Effects of surface treatment on bond strength between dental resin agent and zirconia ceramic. *Mater Sci Eng C Mater Biol Appl.* 2014;34(1):311-7.

Nakonieczny D, Walke W, Majewska J, Paszenda Z. Characterization of magnesia-doped yttria-stabilized zirconia powders for dental technology applications. *Acta Bioeng Biomech.* 2014;16(4):99-106.

Neev J, Carrasco WA, Armstrong WB, Da Silva LB, Feit MD, Matthews DL, Perry MD, Rubenchik AM, Stuart BC. Applications of ultrashort pulse lasers for hard tissue surgery. *Proc SPIE.* 1996;2671(1):149-57.

Neev J, Da Silva LB, Feit MD, Perry MD, Rubenchik AM, Stuart BC. Ultrashort pulse lasers for hard tissue ablation. *IEEE J Sel Top Quant Electron.* 1996;2(4):790-800.

Nicolodelli G, Kurachi C, Bagnato VS. Femtosecond laser ablation profile near an interface: Analysis based on the correlation with superficial properties of individual materials. *Appl Surf Sci.* 2011;257(1):419-22.

Niemz MH, Eisenmann L, Pioch T. A comparison of 3 laser systems for dental enamel ablation. *Schweiz Monatsschr Zahnmed.* 1993;103(10):1252-6.

Niemz MH. Thres hold dependence of laser-induced optical breakdown on pulse duration. *Appl Phys Lett.* 1995;66(10):1181-3.

Niemz MH. Cavity preparation with Nd:YLF picosecond laser. *J Dent Res.* 1995;74(5):1194-9.

Niemz MH, Kasenbacher A, Strassl M, Bäcker A, Beyerti A, Nickel D, Giesen A. Tooth ablation using a CPA-free thin disk femtosecond laser system. *Appl Phys.* 2004;79(1):269-71.

Nikaido T, Kunzelman KH, Chen H, Ogata M, Harada N, Yamaguchi S, Cox CF, Hickel R, Tagami J. Evaluation of thermal cycling and mechanical loading on bond strength of a self-etching primer system to dentin. *Dent Mater.* 2002;18(3):269-75.

Nishimura N, Schaffer CB, Friedman B, Tsai PS, Lyden PD, Kleinfeld D. Targeted insult to individual subsurface cortical blood vessels using ultrashort laser pulses: Three models of stroke. *Nat Methods.* 2006;3(2):99-108.

Nolte S, Momma C, Jacobs H, Tunnermann A, Chichkov BN, Wellegehausen B, Welling H. Ablation of metals by ultrashort laser pulses. *J Optical Soc Am B-Optical Phys.* 1997;14(10):2716-22.

Odhner J, Levis R. Optical spectroscopy using gas-phase femtosecond laser filamentation. *Annu Rev Phys Chem.* 2014;65(1):605-28.

Oltra-Arimon D, España-Tost AJ, Berini-Aytés L, Gay-Escoda C. Aplicaciones del láser de baja potencia en odontología. *RCOE.* 2004;9(5):517-24.

Oraevsky A, Da Silva L, Rubenchik A, Feit M, Glinsky M, Perry M, Mammini B, Small W, Stuart B. Plasma mediated ablation of biological tissues with nanosecond-to-femtosecond laser pulses: relative role of linear and non-linear absorption. *IEEE J Sel Top Quant Electron.* 1996;2(1):801-9.

Oyagüe RC, Monticelli F, Toledano M, Osorio E, Ferrari M, Osorio R. Effect of water aging on microtensile bond strength of dual-cured resin cements to pre-treated sintered zirconium-oxide ceramics. *Dent Mater.* 2009;25(3):392-9.

Ozcan M, Bernasconi M. Adhesion to zirconia used for dental restorations: a systematic review and meta-analysis. *J Adhes Dent.* 2015;17(1):7-26.

Paranhos MP, Burnett LH Jr, Magne P. Effect of Nd:YAG laser and CO<sub>2</sub> laser treatment on the resin bond strength to zirconia ceramic. *Quintessence Int.* 2011;42(1):79-89.

Passos SP, May LG, Barca DC, Ozcan M, Bottino MA, Valandro LF. Adhesive quality of self-adhesive and conventional adhesive resin cement to Y-TZP ceramic before and after aging conditions. *Oper Dent.* 2010;35(6):689-96.

Perry MD, Stuart BC, Banks PS, Feit MD, Yanovsky V, Rubenchik AM. Ultrashort-pulsed laser machinig of dielectric materials. *J Appl Phys.* 1999;85(9):6803-10.

Pétercsák A, Radics T, Hegedus C. Advantages and disadvantages of applying yttrium stabilized zirconium-dioxide post and core restorations. *Fogorv Sz.* 2014;107(1):9-13.

Peutzfeldt A, Asmussen E. Silicoating. Evaluation of a new method of bonding composite resin to metal. *Scand J Dent Res.* 1988;96(2):171-6.

Piconi C, Maccauro G. Zirconia as a ceramic biomaterial. *Biomaterials.* 1999;20(1):1-25.

Piwowarczyk A, Lauer H, Sorensen J. The shear bond strength between luting cements and zirconia ceramics after two pre-treatments. *Oper Dent.* 2005;30(3):382-8

Pike P, Parigger C, Splinter R, Lockhart P. Temperature distribution in dental tissue after interaction with femtosecond laser pulses. *Appl Opt.* 2007;46(34):8374-8.

Plötz C, Schelle F, Bouraue C, Frentzen M, Meister J. Ablation of porcine bone tissue with an ultrashort pulsed laser (USPL) system. *Lasers Med Sci*. 2015;30(3):977-83

Portillo M, Lorenzo MC, Sánchez JM, Peix M, Albaladejo A, García A, Moreno P. Morphological alterations in dentine after mechanical treatment and ultrashort pulse laser irradiation. *Lasers Med Sci*. 2012;27(1):53-8.

Probster L, Diel J. Slip casting alumina ceramics for crown and bridge restorations. *Quintessence Int*. 1992;23(1):25-31.

Pronko PP, Dutta SK, Squier SJ, Rudd JV, Du D, Mourou G. Machining of sub-micron holes using a femtosecond laser at 800 nm. *Opt Commun*. 1995;114(1):106-10.

Qeblawi DM, Muñoz CA, Brewer JD, Monaco EA. The effect of zirconia surface treatment on flexural strength and shear bond strength to a resin cement. *J Prosthet Dent*. 2010;103(4):210-20.

Queiroz JR, Massi M, Nogueira L Jr, Sobrinho AS, Bottino MA, Ozcan M. Silica-based nano-coating on zirconia surfaces using reactive magnetron sputtering: effect on chemical adhesion of resin cements. *J Adhes Dent*. 2013;15(2):151-9.

Rraigrodski AJ. Contemporary materials and technologies for all-ceramic fixed partial dentures: a review of the literature. *J Prosthet Dent.* 2004;92(6):557-62.

Ratkay-Traub I, Ferincz IE, Juhasz T, Kurtz RM, Krueger RR. First clinical results with the femtosecond neodymium-glass laser in refractive surgery. *J Refract Surg.* 2003;19(2):94-103.

Rego Filho F de A, Dutra-Corrêa M, Nicolodelli G, Bagnato VS, de Araujo MT. Influence of the hydration state on the ultrashort laser ablation of dental hard tissues. *Lasers Med Sci.* 2013;28(1):215-22.

Rinke S, Lattke A, Eichholz P, Kramer K, Ziebolz D. Practice-based clinical evaluation of zirconia abutments for anterior single-booth restorations. *Quintessence Int.* 2015;46(1):19-29.

Ruff O, Ebert F, Stephen E. Contributions to the ceramics of highly refractory materials: II. System zirconia-lime. *Z Anorg Allg Chem.* 1929;180(1):215-24.

Rüttermann S, Fries L, Raab WH, Janda R. The effect of different bonding techniques on ceramic/resin shear bond strength. *J Adhes Dent.* 2008;10(3):197-203.

Sandford MA, Walsh LJ. Differential thermal effects of pulsed vs continuous CO<sub>2</sub> laser radiation on human molar teeth. *J Clinical Las Med Sur.* 1994;12(1):139-42.

Santerre JP, Shajii L, Leung BW. Relation of dental composite formulations to their degradation and the release of hydrolyzed polymeric-resin-derived products. *Crit Rev Oral Biol Med.* 2001;12(1):136-51.

Sarmento HR, Campos F, Sousa RS, Machado JP, Souza RO, Bottino MA, Ozcan M. Influence of air-particle deposition protocols on the surface topography and adhesion of resin cement to zirconia. *Acta Odontol Scand.* 2014;72(5):346-53.

Serbin J, Bauer T, Fallnich C, Kasenbacher A, Arnold WH. Femtosecond lasers as novel tool in dental surgery. *Appl Surf Sci.* 2002;197(1):737-40.

Shahin R, Kern M. Effect of air abrasion on the retention of zirconia ceramic crowns luted with different cements before and after artificial aging. *Dent Mater.* 2010;26(9):922-8.

Shenoy A, Shenoy N. Dental ceramics: an update. *J Conserv Dent.* 2010;13(4):195-203.

Solá-Ruiz MF, Agustin-Panadero R, Fons-Font A, Labaig-Rueda C. A prospective evaluation of zirconia anterior partial fixed dental prostheses: clinical results after seven years. *J Prosthet Dent.* 2015;113(6):578-84.

Söderholm KJ, Shang SW. Molecular orientation of silane at the surface of colloidal silica. *J Dent Res.* 1993;72(6):1050-4.

Sorensen JA, Engleman MJ, Torres TJ, Avera SP. Shear bond strength of composite resin to porcelain. *Int J Prosthodont.* 1991;4(1):17-23.

Spohr AM, Borges GA, Júnior LH, Mota EG, Oshima HM. Surface modification of in-ceram zirconia ceramic by Nd:YAG laser, rocatec system, or aluminum oxide sandblasting and its bond strength to a resin cement. *Photomed Laser Surg.* 2008;26(3):203-8.

Stern D, Schoenlein RW, Puliafito CA, Dobi ET, Birngruber R, Fujimoto JG. Corneal ablation by nanosecond, picosecond, and femtosecond lasers at 532 and 625 nm. *Arch Ophthalmol.* 1989;107(4):587-92.

Strickland D, Mourou, G. Compression of amplified chirped optical pulses. *Opt Commun.* 1985;55(1):447-9.

Stuart BC, Feit MD, Rubenchik AM, Shore BW, Perry MD. Laser-induced damage in dielectrics with nanosecond to subpicosecond pulses. *Phys Rev Lett.* 1995;74(12):2248-51.

Stuart BC, Feit MD, Herman S, Rubenchik AM, Shore BW, Perry M. Optical ablation by high-power short-pulse lasers. *J Opt Soc Am B.* 1996;13(2):459-68.

Sudsangiam S, Van Noort R. Do dentin bond strength tests serve a useful purpose?. *J Adhes Dent.* 1999;1(1):57-67.

Sukumaran VG, Bharadwaj N. Ceramics in dental applications. *Trends Biomater Artif Organs.* 2006;20(1):7-11.

Sulewski JG. Revisión histórica de la odontología de láseres. En: Convissar RA. Clínicas odontológicas de Norteamérica. Láseres y amplificación de la luz en odontología. México DF: McGraw-Hill Interamericana; 2000:781-817.

Sun YC, Vorobyev A, Li H, Guo CL, Lü PJ. Femtosecond pulsed laser ablation of dental hard tissues with numerical control: a roughness and morphology study. *Zhonghua Kou Qiang Yi Xue Za Zhi.* 2012;47(8):486-9.

Sundh A, Molin M, Sjögren G. Fracture resistance of yttrium oxide partially stabilized zirconia all-ceramic bridges after veneering and mechanical fatigue testing. Dent Mater. 2005;21(5):476-82.

Tagami J, Nikaido T, Nakajima M, Shimada Y. Relationship between bond strength tests and other in vitro phenomena. Dent Mater. 2010;26(2):94-9.

Tezvergil A, Lassila LVJ, Vallittu PK. The effect of fiber orientation on the thermal expansion coefficients of fiber-reinforced composites. Dent Mater. 2003;19(6):471-7.

Thompson JY, Stoner BR, Piascik JR, Smith R. Adhesion/cementation to zirconia and other non-silicate ceramics: Where are we now?. Dent Mater. 2011;27(1):71-82.

Tinschert J, Zwez D, Marx R, Anusavice KJ. Structural reliability of alumina-, feldspar-, leucite-, mica- and zirconia-based ceramics. J Dent. 2000;28(7):529-35.

Tsai PS, Friedman B, Ifarraguerri AI, Thompson BD, Lev-Ram V, Schaffer CB, Xiong Q, Tsien RY, Squier JA, Kleinfeld D. All-optical histology using ultrashort laser pulses. Neuron. 2003;39(1):27-41.

Tsai PS, Friedman B, Squier JA, Kleinfeld D. Ultrashort pulsed laser light: a cool tool for ultraprecise cutting of tissue and cells. Opt Photonic News. 2004;14(1):24-9.

Usumez A, Hamdemicri N, Koroglu BY, Simsek I, Parlar O, Sari T. Bond strength of resin cement to zirconia ceramic with different surface treatments. *Lasers Med Sci.* 2013;28(1):259-66.

Vagkopoulou T, Koutayas S, Koidis P, Strub JR. Zirconia in dentistry. Part 1. Discovering the nature of an upcoming bioceramic. *Eur J Esthet Dent.* 2009;4(2):130-51.

Valandro LF, Özcan M, Amaral R, Vanderlei A, Bottino MA. Effect of testing methods on the bond strength of resin to zirconia-alumina ceramic: microtensile versus shear test. *Dent Mater J.* 2008;27(6):849-55.

Van Noort R. Introduction to dental materials. London: Elsevier Health Sciences; 2002.

Van Noort R, Noroozi S, Howard IC, Cardew G. A critique of bond strength measurements. *J Dent.* 1989;17(2):61-7.

Velez N, Earnest DE, Staren ED. Diagnostic and interventional ultrasound for breast disease. *Am J Surg.* 2000;180(4):284-7.

Watanabe W, Arakawa N, Matsunaga S, Higashi T, Fukui K, Isobe K, Itoh K. Femtosecond laser disruption of subcellular organelles in a living cell. Opt Express. 2004;12(18):4203-13.

Wegner SM, Kern M. Long-term resin bond strength to zirconia ceramic. J Adhes Dent. 2000;2(2):139-47.

Weinstein M, Katz S, Weinstein AB. (US Patent. No. 3,052,983) Porcelain-covered metal-reinforced teeth; 1962.

Weinstein M, Weinstein AB. (US Patent. No. 3,052,982) Fused porcelain to metal teeth; 1962.

Willershausen B, Callaway A, Ernst CP, Stender E. The influence of oral bacteria on the surfaces of resin-based dental restorative materials-an in vitro study. Int Dent J. 1999;49(4):231-9.

Wolfart M, Lehmann F, Wolfart S, Kern M. Durability of the resin bond strength to zirconia ceramic after using different surface conditioning methods. Dent Mater. 2007;23(1):45-50.

Yang B, Barloi A and Kern M. Influence of air-abrasion on zirconia ceramic bonding using an adhesive composite resin. Dent Mater. 2010;26(1):44-50.

Yang B, Lange-Jansen HC, Scharnberg M, Wolfart S, Ludwig K, Adelung R, Kern M. Influence of saliva contamination on zirconia ceramic bonding. Dent Mater. 2008;24(4):508-13.

Yanik MF, Cinar H, Cinar HN, Chisholm AD, Jin Y, Ben-Yakar A. Neurosurgery: functional regeneration after laser axotomy. Nature. 2004;432(7019):822.

Yoshida K, Tsuo Y, Astuta M. Bonding of dual-cured resin cement to zirconia ceramic using phosphate acid ester monomer and zirconate coupler. J Biomed Mater Res B Appl Biomater. 2006;77(1):28-33.

Zach L, Cohen G. Pulp response to externally applied heat. Oral Surg Oral Med Oral Pathol. 1965;19(1):515-30.

Zahran M, El-Mowafy O, Tam L, Watson PA, Finer Y. Fracture strength and fatigue resistance of all-ceramic molar crowns manufactured with CAD/CAM technology. J Prosthodont. 2008;17(5):370-7.

Zhou J, Mah J, Shrotriya P, Mercer C, Soboyejo WO. Contact damage in an yttria stabilized zirconia: implications. *J Mater Sci Mater Med*. 2007;18(1):71-8.





## *Viii. APPENDIX*

*Viii.1 APPENDIX 1.*

*ORiGiNAL*

*PUBLICATIONS.*

M. Vicente· AL. Gomes, J. Montero, E. Rosel, V. Seoane, A. Albaladejo.

**Influence of cyclic loading on the adhesive effectiveness of resin-zirconia interface  
after femtosecond laser irradiation and conventional surface treatments.**

Article send to the *Journal of Lasers in Surgery and Medicine*.

Impact Index: 2.61- JCR Science Edition: 2014.

Category: Surgery.

Category position: 49/198 (T1/Q1).

*Article pending of publication.*

## Decision Letter (LSM-15-0206.R2)

**From:** lsm@manuscriptmgt.com  
**To:** maria\_vp89@hotmail.com  
**CC:** maria\_vp89@hotmail.com, acaseiro@gmail.com, javimont@usal.es, evarosel@hotmail.com, dr.seoane@sonrident.es, albertoalbaladejo@hotmail.com  
**Subject:** Lasers in Surgery & Medicine - Manuscript LSM-15-0206.R2  
**Body:** Date:03-Nov-2015

Ref.: LSM-15-0206.R2

Dear Miss Vicente Prieto:

I am pleased to inform you that your manuscript, Influence of cyclic loading on the adhesive effectiveness of resin-zirconia interface after femtosecond laser irradiation and conventional surface treatments., is now acceptable for publication in Lasers in Surgery & Medicine.

Thank you for your support of Lasers in Surgery & Medicine. I look forward to seeing more of your work in the future.

Your article cannot be published until you have signed the appropriate license agreement. Within the next few days you will receive an email from Wiley's Author Services system which will ask you to log in and will present you with the appropriate license for completion.

Sincerely,

Brian J. Wong, M.D., Ph.D  
Editor-in-Chief, Lasers in Surgery & Medicine

**Date Sent:** 03-Nov-2015

**Lasers in Surgery and  
Medicine**



Lasers in Surgery and Medicine

**Influence of cyclic loading on the adhesive  
effectiveness of resin-zirconia interface after femtosecond  
laser irradiation and conventional surface treatments.**

Journal:	<i>Lasers in Surgery &amp; Medicine</i>
Manuscript ID	LSM-15-0206.R2
Wiley - Manuscript type:	Preclinical Reports
Date Submitted by the Author:	22-Oct-2015
Complete List of Authors:	Vicente Prieto, María; Clínica Odontológica. Facultad de Medicina. Universidad de Salamanca.  Gomes, Ana; Clínica Odontológica. Facultad de Medicina. Universidad de Salamanca.  MONTERO, JAVIER; UNIVERSIDAD DE SALAMANCA, CIRUGÍA; ClínicaOdontológica. Facultad de Medicina. Universidad de Salamanca  Rosel, Eva; Clínica Odontológica. Facultad de Odontología. Universidad de Granada  Seoane Mato, Vicente; Clínica Odontológica. Facultad de Medicina. Universidad de Salamanca  ALBALADEJO MARTÍNEZ, ALBERTO; Clínica Odontológica. Facultad de Medicina. Universidad de Salamanca; UNIVERSIDAD DE SALAMANCA, CIRUGÍA.
Key Words:	shear bond strength, surface treatments, femtosecond laser, zirconia.

SCHOLARONE™  
Manuscripts

	Journal	MSP No.	Dispatch: November 7, 2015	CE: Sujan
LSM	22442	No. of Pages: 9		PE: Michele Heal

# Influence of Cyclic Loading on the Adhesive Effectiveness of Resin-Zirconia Interface After Femtosecond Laser Irradiation and Conventional Surface Treatments

Mara<sup>Q2</sup> Vicente,<sup>1</sup> Ana L. Gomes,<sup>1</sup> Javier Montero,<sup>2</sup> Eva Rosel,<sup>3</sup> Vicente Seoane,<sup>1</sup> and Alberto Albaladejo<sup>2\*</sup>

<sup>1</sup>Dental Clinic<sup>Q3</sup> (Faculty of Medicine), University of Salamanca. Paseo Universidad de Coimbra, s/n, 37007, Salamanca, Spain

<sup>2</sup>Dental Clinic (Faculty of Medicine), University of Salamanca. Paseo Universidad de Coimbra, s/n, 37007, Salamanca, Spain

<sup>3</sup>Dental Clinic (Faculty of Odontology), University<sup>Q4</sup> of Granada. Colegio Máximo, Campus Universitario de Cartuja, 18011, Granada, Spain

**Background and Objective:** The aim of this study was to evaluate the influence of cyclic loading on the shear bond strength (SBS) of a self-adhesive resin cement to zirconia surfaces after femtosecond laser irradiation at different steps and several conventional surface treatments.

**Materials and Methods:** One hundred fifty square-shaped zirconia samples were divided into five groups according their surface treatment: NT Group—no surface treatment; APA25 Group—airborne abrasion with 25 µm alumina particles; TSC Group—tribochemical silica coating; FS20 Group—femtosecond laser irradiation (800 nm, 4 mJ, 40 fs/pulse, 1 kHz, step 20); and FS40 Group—femtosecond laser irradiation (same parameters except step 40). Self-adhesive resin cement cylinders were bonded at the centre of the zirconia surface. For each experimental group, half of the specimens were subject to cyclic loading under 90 N (50.000 cycles, 3 cycles/sec) and the rest of the specimens were stored in distilled water at 37°C. All subgroups were tested for SBS with a universal testing machine at a crosshead speed of 0.5 mm/min, until fracture. The results were analyzed statistically.

**Results:** When cyclic loading was applied, all surface treatments had lower SBS values, except APA25. The four surface treatments had the same SBS values when cyclic loading was employed.

**Conclusions:** Use of femtosecond laser irradiation could be an alternative to conventional surface treatments to achieve suitable adhesion zirconia and resin cements. Femtosecond laser irradiation at step 40 is preferable because it is more efficient and faster. Lasers Surg. Med. 9999:1–9, 2015. © 2015 Wiley Periodicals, Inc.

**Key words:** adhesion; ceramics; shear bond strength; surface treatment

## INTRODUCTION

Zirconia ceramics have been used for oral rehabilitation for decades as crowns and fixed dental prostheses [1,2], post and/or core [3], orthodontic brackets [4], oral

implants [5], and implant abutments [6], and they have been developed with sufficient strength and toughness with respect to these demands for use [7]. In particular, yttria tetragonal zirconia polycrystal (Y-TZP) is a zirconia ceramic which, after sintering, forms stable tetragonal structure with the most favorable properties for dental applications [8].

The problem with zirconia ceramics is that traditional adhesive chemistry is not effective and surface conditioning methods are needed to improve the adhesive bonding between the zirconia and the resin cements [9]. Among recent methods of zirconia surface treatment, femtosecond laser irradiation has been proposed; this involves the use of a laser based on titanium/sapphire crystals (Ti/S), which produces extremely short pulses below the picosecond scale, in the femtosecond domain ( $1\text{ fs} = 10^{-15}\text{ s}$ ). It is used in biological, industrial, and medical fields, among which are dental applications. Thus, research is now beginning to focus on the use of femtosecond lasers in dentistry as surface treatments to perform the conditioning of biological surfaces [10–12], encouraging results having been obtained in the sense of improvements in adhesive effectiveness.

Regarding the adhesion of non-biological surfaces such as zirconia, an investigation assessing zirconia–resin interface adhesion has been published recently, with promising results [13]. However, in this study, the authors did not perform any degrading of the interface and in this sense it should be recalled that in clinical settings, all

---

Conflict of Interest Disclosures: All authors have completed and submitted the ICMJE Form for Disclosure of Potential Conflicts of Interest and none were reported.

\*Correspondence to: Alberto Albaladejo Martínez, Clínica Odontológica, Facultad de Medicina, Universidad de Salamanca (USAL), Paseo Universidad de Coimbra s/n. C.P.: 37007. Salamanca, Spain. E-mail: albertoalbaladejo@hotmail.com

Accepted 3 November 2015

Published online in Wiley Online Library  
(wileyonlinelibrary.com).

DOI 10.1002/lsm.22442

zirconia restorations are subjected to cyclic forces ranging from 60 to 250 N during masticatory function, and may even reach values of 500–800 N in the posterior zone [14]. Accordingly, it is crucial to investigate bond strength values obtained under dynamic conditions in order to obtain more clinical results and hence make progress in attempts to validate femtosecond laser irradiation as an ideal surface-conditioning method to improve adhesion in enamel, dentine, and zirconia. Another important aim is to improve the parameters that can facilitate its use, such as reducing the space between each irradiation, and therefore the overall irradiation time, but still obtaining a high adhesive effectiveness.

To simulate occlusal masticatory forces *in vitro*, cyclic loading is used [15]. Cyclic loading is the repeated or fluctuating application of stresses, strains, or intensities to locations on structural components, and attempts to replicate the clinical conditions that zirconia restorations are subjected to due to masticatory forces [16]. The technique is based on a computer-controlled masticatory simulator [17] that produces a mechanical degradation of the zirconia–resin [18] interface through the continuous application of impact on it.

The aim of this study was to evaluate the influence of cyclic loading on the shear bond strength (SBS) of a self-adhesive resin cement on zirconia surfaces after femtosecond laser irradiation at different steps and several conventional surface treatments.

## MATERIALS AND METHODS

### Preparation of Zirconia Samples

The study used 150 samples of densely sintered Y-TZP (Cercon®, DeguDent, Hanau, Germany). The specimens, which were square-shaped and measured 6 × 6 × 1 mm, were obtained using a precision cutting machine (Isomet 5000; Buehler, Lake Bluff, Illinois). Each sample surface was wet-polished with 600-grit silicon carbide paper on a polishing machine (Phoenix Beta; Buehler, Lake Bluff, IL).

### Experimental Groups

Once the zirconia samples had been polished, they were randomly assigned to four experimental groups according to the surface treatment to be applied ( $n = 30$ ).

**Group 1: Control-no treatment (NT).** No surface treatment was applied.

**Group 2: Airborne particle abrasion with 25 µm alumina particles (APA 25).** The zirconia surface was blasted with alumina particles ( $\text{Al}_2\text{O}_3$ ) with an average particle size of 25 µm under a pressure of 0.25 MPa for 20 seconds at a perpendicular distance of 10 mm from the holder.

**Group 3: Tribocochemical silica coating (TSC).** In this case, the zirconia surface was treated with a tribocochemical silica coating (30 µm alumina and silica particles) with the Rocatec system (Rocatec™ Soft, 3M Espe, Seefeld, Germany). Rocatec particles were applied under a pressure of 0.25 MPa for 20 seconds at a perpendicular distance

of 10 mm. Silica coating was followed by silanization, which was performed following manufacturer's instructions with a Rely X™ ceramic primer (3M Espe, Seefeld, Germany).

**Group 4: Femtosecond laser irradiation at step 20 (FS20).** The zirconia surface was irradiated with a femtosecond laser. The laser pulses were generated by a commercial Ti:Sapphire oscillator-regenerative amplifier system (Mantis-Legend, Coherent Inc. Santa Clara, CA), providing 1 kHz trains of pulses centered at 800 nm, with an energy of 4.0 mJ and a duration of 40 fs. Only a fraction of the pulse energy of the amplifier output is used in the experiments, using a variable neutral-density filter and measured with a thermal detector (S302C, Thorlabs Inc. Newton, New Jersey). The laser pulses were focused by means of a fused silica singlet lens ( $f = 100$  mm), yielding a spot diameter of approximately 20 µm.

The specimens were fixed on a computer-controlled XYZ-motorized stage (PT3-Z8, Thorlabs Inc. Newton, NJ) at atmospheric pressure. The experimental conditions were chosen to obtain a more uniform pattern across the surface, thus minimizing the depth of the grooves generated by laser ablation. Thus, the pulse energy was 0.015 mJ, the scanning velocity 0.25 mm/s, and the scanning step 20 µm.

**Group 5: Femtosecond laser irradiation at step 40 (FS40).** In this group, the zirconia surface was irradiated with a femtosecond laser with the same parameters as the previous group except that the scanning step was 40 µm.

### Bonding Procedure

After performing the different surface treatments on the zirconia samples, all specimens were washed with ethanol and dried, before that, a self-adhesive resin cement was bonded to their surface according to manufacturer's recommendations: Clearfil™ SA Cement (CLE) (Clearfil™ SA Cement, Kuraray, Osaka, Japan).

For application of the cement, a cylindrical silicone mould with a 3 mm internal diameter, 1 mm thickness, and 1 mm in height was used. It was positioned at the centre of the samples, and the cement was placed on them against the zirconia surface and polymerized for 40 seconds (XL 3000, 3M/ESPE; light intensity 500 mW/cm<sup>2</sup>, distance 0) from above and towards the contact area from a lateral position.

The mould was removed and the cylinder cement was light-cured for a further 40 seconds. Thus, a resin cement cylinder of 3 mm diameter and 1 mm in height bonded to the zirconia surface was obtained.

### Cyclic Loading

All experimental groups were divided into two subgroups according to whether cyclic loading was applied or not. Thus, half of the specimens of each group ( $n = 15$ ) were mounted in acrylic resin moulds for cyclic loading under 90 N (50,000 cycles, 3 cycles/sec) with the force applied perpendicularly to the zirconia surface opposite where the resin was cemented. This compressive load was applied using a spherical stainless steel plunger, 5 mm in

diameter, attached to a cyclic loading machine (S-MMT-250NB; Shimadzu, Tokyo, Japan). The rest of the specimens from each group ( $n = 15$ ), the other subgroup, were not subjected to cyclic loading and were stored in water until cyclic loading for the other zirconia samples had been completed.

### Shear Bond Strength (SBS) Test

With the cement cylinder on their surface, all subgroups were tested for SBS with a universal testing machine (AGS-X Autograph, Shimadzu Corporation, Kyoto, Japan), applying a shear load with a crosshead speed of 0.5 mm/min, until fracture.

To calculate the bond strength values in MPa, the maximum load recorded upon failure (in Newtons N) was divided by the bonding area (in square millimeters).

### Failure Mode Analysis

After the SBS-test, each fractured specimen was examined under an Axio M1 (Carl Zeiss, Germany) light microscope at 40 $\times$  magnification to determine the failure modes. These were classified according to the amount of cement deposited on the surface, or what it is the same, based on the percentage of zirconia surface appreciated: adhesive (more of 75% of zirconia surface exposed, failure in adhesion), cohesive (less than 25%), or mixed-adhesive and cohesive failures simultaneously (between 25% and 75%, zirconia samples showing residual cement on their surfaces with both adhesive and cohesive failures).

### Scanning Electron Microscopy (SEM) Examination

Five zirconia surfaces from each experimental subgroup ( $n = 5$ ) were prepared for surface morphology analysis with a variable pressure SEM (Zeiss EVO MA25; Carl Zeiss, Jena, Germany). Specific regions across the zirconia surface were explored with the scanning electron microscope, focusing with different magnifications ( $\times 70$  and  $\times 1000$ ) in order to obtain a panoramic view of the effect of laser processing and the effect of the other conditioning methods.

In addition, representative fractured samples were dehydrated for 48 hours in a desiccator (Sample Dry Keeper Simulate Corp., Tokyo, Japan) and were sputter-coated with a 10 nm platinum layer in a Polaron E5100 SEM coating unit (Polaron Equipment Ltd., Hertfordshire, England, UK).

Specific zirconia surface areas were examined with the scanning electron microscope, focusing with different magnifications (from  $\times 30$  to  $\times 1000$ ) in order to analyze the morphology of the debonded interfaces and identify possible differences among the experimental groups with respect to the surface topography and morphology of the debonded interfaces.

### Statistical Analyses

The bond-strength values were measured in MPa. The data were analyzed with SPSS v21 (Statistical Package for the Social Sciences, Chicago, IL), using a  $P$ -value below

0.05 as the threshold for statistical significance. ANOVA tests were applied to compare the SBS among the subgroups regarding the use of different zirconia surface treatments.

When the ANOVA test detected significant differences, Bonferroni post-hoc comparisons were performed to quantify the differences between two subgroups. The Chi-square test was used to detect differences in the types of failures among subgroups.

## RESULTS

### Shear Bond Strength (SBS) Test

The mean values and standard deviations (SD) of SBS for all the different surface treatment subgroups are shown in Table 1. The results obtained using one way ANOVA indicated that the SBS values varied according to the surface treatment method ( $P < 0.001$ ) in both loaded and unloaded specimens.

The paired  $T$  tests comparisons indicated that all surface method conditionings had significantly lower SBS values after the cyclic loading, except APA25, for which similar values were observed in both subgroups.

The Bonferroni post-hoc inter-group comparisons found that among unloaded specimens, the APA25 subgroup obtained higher SBS values than the control subgroup, but they were significantly lower than the FS20 and FS40 SBS values ( $P < 0.05$ ), which were similar to each other. However, comparable values were observed within the unloaded specimens of the APA25 and TSC subgroups ( $P = 0.94$ ) after bonferroni post-hoc comparisons. By contrast, after cyclic loading as applied, the four surface treatments afforded the same SBS values, which were significantly higher than those of the control subgroup values ( $P < 0.001$ ).

The bond failure-mode analyses are shown in Table 2. In the control group, most of the failures were adhesive, while in the treatment groups, they were mostly mixed-adhesive and cohesive failures simultaneously, and none of the samples of either group had cohesive failure, this comparison being statistically significant ( $P < 0.05$ ) except for the APA25 subgroup ( $P = 0.14$ ) among the unloaded samples. Among the loaded samples, there were not significant differences between subgroups ( $\chi^2 = 8.2$ , df:4;  $P = 0.08$ ), although mixed failures were clearly more common among the treated samples than in controls. In addition, the distribution of the adhesive failure rates was not significantly different after loading in any subgroups.

### SEM Observations

The SEM micrographs in Figure 1 show the zirconia surface morphology after the different surface treatment methods had been applied (magnification power,  $\times 700$ ). In image A, which represents the NT group, marked scratches running in the same direction on its surface as result of the polishing procedure can be seen. Image B corresponds to the APA25 group and reveals granule-shaped micro-retentions on the surface, due to the impact of the high-speed 25  $\mu\text{m}$  alumina particles. Image C

**TABLE 1. Comparison of the SBS Among the Zirconia Surface Treatment Subgroups**

		Airbone particle abrasion with 25 µm alumina particles (APA25)	n = 15	n = 15	Femtosecond laser irradiation at step 20 (FS20)	n = 15	Femtosecond laser irradiation at step 40 (FS40)	n = 15
	Mean standard deviation (SD)	Mean standard deviation (SD)	Mean standard deviation (SD)	Mean standard deviation (SD)	Mean standard deviation (SD)	Mean standard deviation (SD)	Mean standard deviation (SD)	
Unloaded subgroups	4.4 (1.3) a*	8.1 (3.6) b	9.5 (2.3) bc*	10.8 (1.9) c*	10.7 (1.4) c*	10.7 (1.4) c*	F = 20.4; P < 0.001	
Loaded subgroups	3.1 (0.5) a*	7.2 (3.4) b	7.0 (1.7) b*	8.5 (1.0) b*	7.7 (0.4) b*	7.7 (0.4) b*	F = 19.0; P < 0.001	

Significant differences ( $P < 0.01$ ) between unloaded and loaded specimens within the same subgroup. The different letters refer to significant inter-group comparisons after Bonferroni corrections ( $P < 0.05$ ). The results obtained using indicated that the SBS values varied according to the surface treatment method ( $P < 0.001$ ) in both loaded and unloaded specimens; and all surface treatments groups had significantly lower SBS values when cyclic loading was applied except APA25, for which similar values were obtained in both subgroups. When cyclic loading was not applied, the APA25 subgroup obtained higher SBS values than the control subgroup, but they were lower than the FS20 and FS40 SBS values, which were similar to each other. By contrast, when cyclic loading was applied, the four surface method conditionings afforded the same SBS values, which were higher than those of the control subgroup values. ANOVA with Bonferroni corrections.

**TABLE 2. Failure Modes Within the Subgroups**

		Airbone particle abrasion with 25 µm alumina particles (APA25)	n = 15 N (%)b	n = 15 N (%)b	Femtosecond laser irradiation at step 20 (FS20)	n = 15 N (%)b	Femtosecond laser irradiation at step 40 (FS40)	n = 15 N (%)b
	No treatment (Control)	n = 15 N (%)a	n = 15 N (%)b	n = 15 N (%)b	n = 15 N (%)b	n = 15 N (%)b	n = 15 N (%)b	
Failure mode of unloaded subgroups	Adhesive	10 (66.7)	5 (33.3)	3 (20.0)	4 (26.7)	1 (6.7)	Chi:14.2 (df = 4); P = 0.007	
	Cohesive	0	0	0	0	0		
	Mixed (adhesive and cohesive)	5 (33.3)	10 (66.7)	12 (80.0)	11 (73.3)	14 (93.3)		
Failure mode of loaded subgroups	Adhesive	9 (60.0)	3 (20.0)	3 (20.0)	3 (20.0)	4 (26.7)	Chi:8.2 (df = 4); P = 0.08	
	Cohesive	0	0	0	0	0		
	Mixed (adhesive and cohesive)	6 (40.0)	12 (80.0)	12 (80.0)	12 (80.0)	11 (73.3)		
	Chi:0.1; P = 1.0	Chi:0.7; P = 0.7	Chi:0.0; P = 1.0	Chi:0.1; P = 1.0	Chi:0.2; P = 0.3			

The different letters refer to significant inter-group comparisons after two-by-two Chi Square Tests taking the control as reference. In the control group, most of the failures were adhesive, while in the treatment groups they were mostly mixed-adhesive and cohesive failures simultaneously, and none of the samples of either group had cohesive failure, this comparison being statistically significant ( $P < 0.05$ ) except for the APA25 subgroup ( $P = 0.14$ ) among the unloaded samples. Among the loaded samples there were not significant differences between subgroups ( $\chi^2 = 8.2$ ; df = 4;  $P = 0.08$ ), although mixed failures were clearly more common among the treated samples than in controls. In addition, the distribution of the adhesive failure rates was not significantly different after loading in any subgroups.

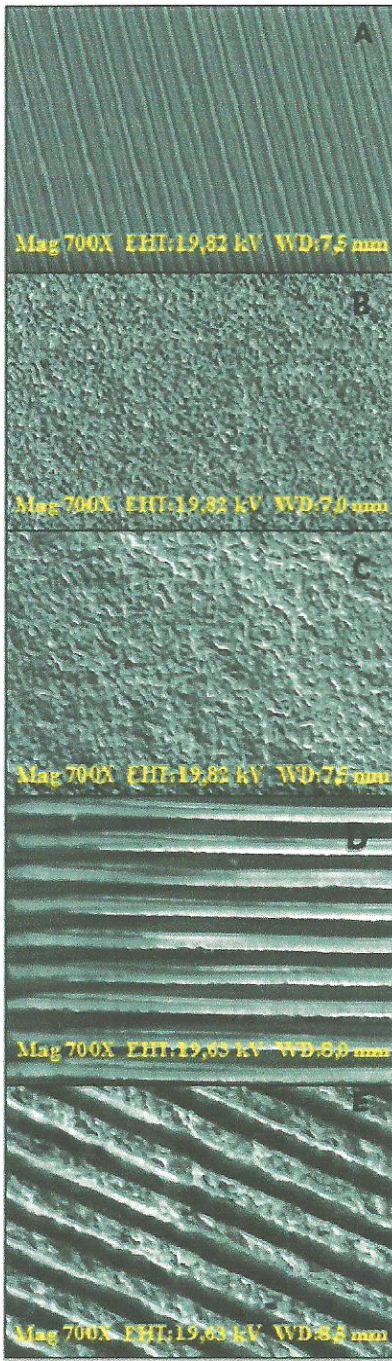


Fig. 1. SEM micrographs of zirconia ceramic surfaces after conditioning treatments at  $\times 700$  magnification: (A) No treatment (NT) with marked scratches on the surface; (B) airborne-particle abrasion with  $25\text{ }\mu\text{m}$  alumina particles (APA 25) with granule-shaped micro-retentions on the surface; (C) tribochemical silica coating (TSC) that creates a rough appearance; (D) Femtosecond laser irradiation at step 20 (FS20) with welldefined pattern of deep grooves; (E) Femtosecond laser irradiation at step 40 (FS40) with the same pattern of furrows that FS20 but they are higher and wider apart.

represents the TSC group and reveals a rough appearance as a result of the coating and solidification of the tribochemical silica particles. Image D, which corresponds to the FS20 group, and image E, which represents the FS40 group, show a well-defined pattern of deep grooves, which are higher and wider apart in the FS40 group.

Figures 2 and 3 show representative SEM images of the debonded zirconia surfaces of all the subgroups after SBS, at magnification powers of  $\times 30$  and  $\times 700$ .

Figure 2 shows the debonded zirconia surfaces of the subgroups to which cyclic loading were applied. Images A and B represent the control subgroup and show adhesive failure, with a very small amount of remains of the resin cement on the zirconia surface of which more than 75% was appreciated without resin. Images C and D (APA25 subgroup), images E and F (TSC subgroup), images G and H (FS20 subgroup), and images I and J (FS40 subgroup) exhibit mixed failures, that is adhesive and cohesive failures simultaneously, with residual cement on the zirconia surface exposed between 25% and 75% of it.

Figure 3 shows the debonded zirconia surfaces of the other subgroups, to which cyclic loading was not applied. As in Figure 2, images A and B (Control subgroup) show adhesive failure, where there is a very small part of resin cement residual on the zirconia surface of which more than 75% was appreciated without resin. Images C and D (APA25 subgroup), images E and F (TSC subgroup), images G and H (FS20 subgroup), and images I and J (FS40 subgroup) exhibit mixed failures, adhesive and cohesive failures simultaneously, with a large cohesive phase and visible pores in the remaining residual cement.

In either group, both cyclic loading and non-cyclic loading, cohesive failure, in which the zirconia surface is exposed at least 25%, is not observed.

## DISCUSSION

All dental restorations are clinically subject to occlusal masticatory forces that can reach values of up to 800 N [19]. Thus, although Y-TZP ceramics are hard and have high strength and fracture toughness [20], their long-term success regarding the degree of adhesion achieved is especially dependent upon the surface roughness produced by the different surface conditioning methods [9] and the ability of these ceramics to withstand the cyclic forces, which can be simulated experimentally using cyclic loading [15].

The results regarding bond strength revealed that all the surface conditioning methods, except abrasion with airborne alumina particles, afforded lower SBS values when the samples were subjected to cyclic loading. Under cyclic loading, zirconia fixed dental prostheses are subject to fracture during function, especially in the posterior area, and zirconia abutments exhibit a significantly lower fracture resistance [21], with a significant reduction in preload [22]. It has been reported that when cyclic loading is applied, there is a distribution of stresses generated around the bonding interface, with a progressive cone cracking surface [23] associated with low fracture strength [24]. Accordingly, on performing cyclic loading

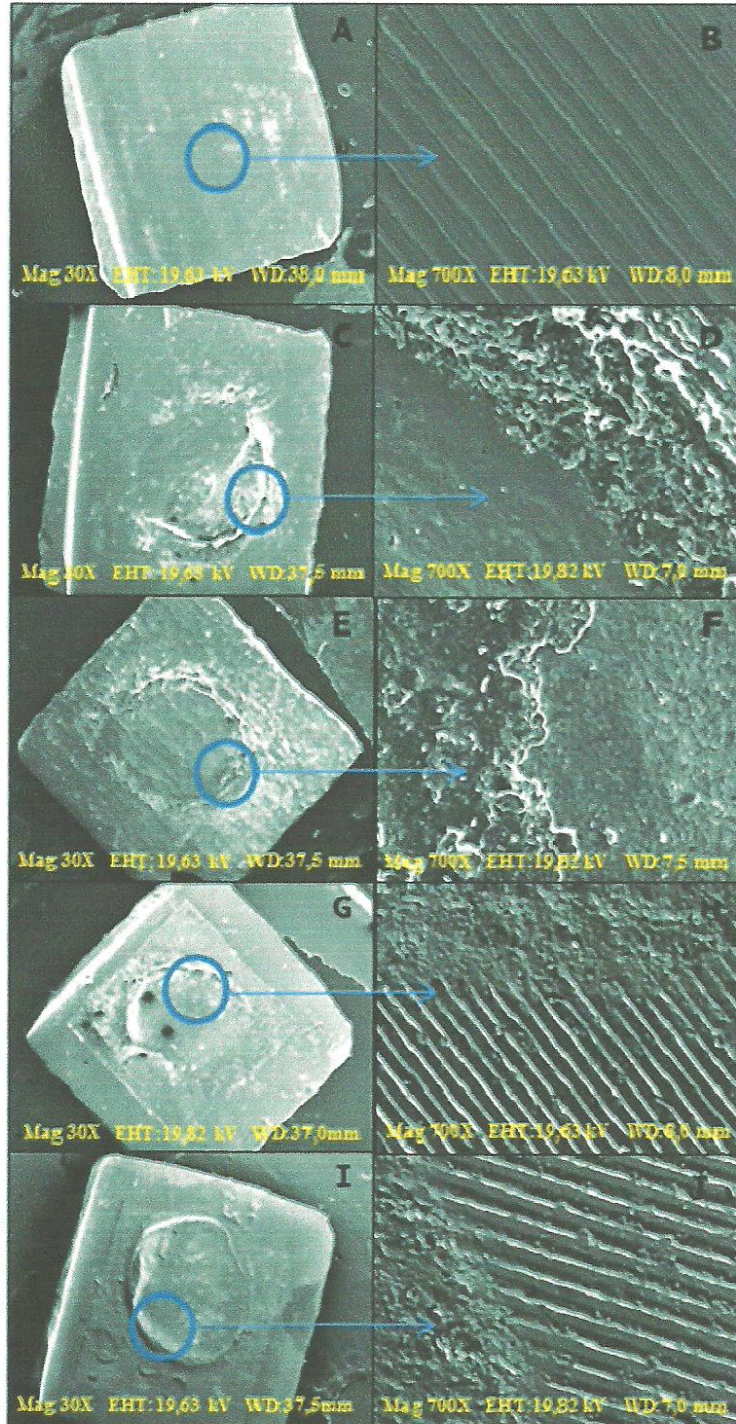


Fig. 2. Representative zirconia surface SEM images ( $\times 30$  and  $\times 700$  magnification) of the most common failure type for the subgroups in which the cyclic loading was applied. Images A and B (NT subgroup) show adhesive failure with a very small amount of remains of the resin cement on the zirconia surface of which more than 75% was appreciated without resin. Images C and D (APA 25 subgroup), E and F (TSC subgroup), G and H (FS20 subgroup), and I and J (FS40 subgroup) show mixed-mixed failures, that is adhesive and cohesive failures simultaneously, with residual cement on the zirconia surface exposed between 25% and 75% of it.

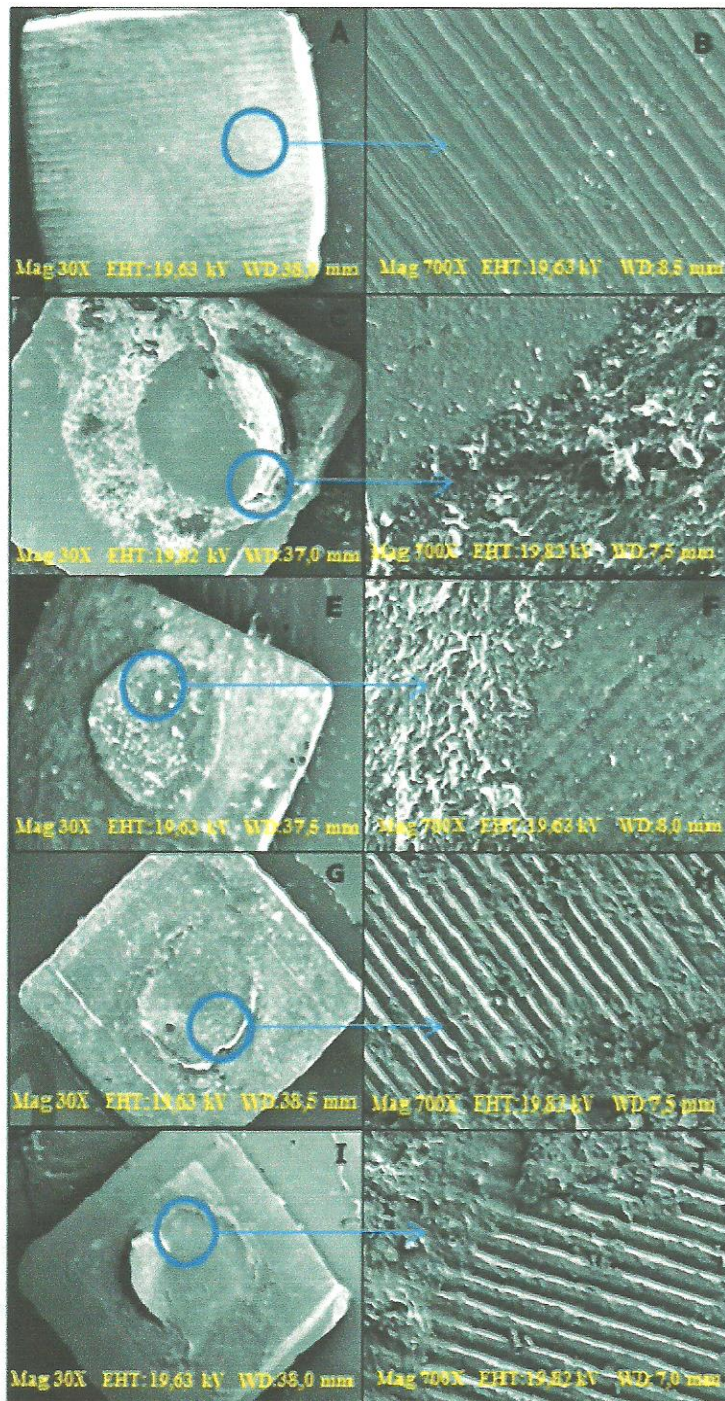


Fig. 3. Representative SEM images ( $\times 30$  and  $\times 700$  magnification) of the zirconia surface of the most common failure type for subgroups to which cyclic loading was not applied. Images A and B (NT subgroup) where there is a very small part of resin cement residual on the zirconia surface of which more than 75% was appreciated without resin. Images C and D (APA 25 subgroup), E and F (TSC subgroup), G and H (FS20 subgroup), and I and J (FS40 subgroup) exhibit mixed failures, adhesive and cohesive failures simultaneously, with a large cohesive phase and visible pores in the remaining residual cement.

in our research, the results can be considered to be more clinically relevant because they represent the mechanical degradation process that zirconia restorations undergo due to masticatory forces more faithfully. In another study, Ghazy et al. [25] evaluated the influence of dynamic fatigue on the fracture loads and failure modes of different types of adhesive zirconia restorations subjected to different surface treatments and bonded with resin cement, and showed that dynamic fatigue reduced failure load to a significant extent and produced fatigue in the adhesion strength of zirconia restorations, in agreement with the bond strength results obtained in our research.

Airborne-particle abrasion with 25 µm Al<sub>2</sub>O<sub>3</sub> particles afforded the same bond strength results with and without cyclic loading. Currently, the literature does not seem to have any references to studies that have evaluated the cyclic loading on zirconia surfaces sandblasted with 25 µm Al<sub>2</sub>O<sub>3</sub> particles. Only Nishigori et al. [26] investigated the influence of yttria-stabilized tetragonal zirconia polycrystal surface treatment and cyclic loading on shear bond strength after airborne-particle abrasion with 50 µm alumina at 0.4 MPa pressure for 10 seconds. They reported that cyclic loading significantly reduced shear bond strength in comparison with specimens not subjected to cyclic loading after airborne-particle abrasion. This contrasts with our own findings, although the results cannot be compared because those authors used a different particle size at higher pressure and for a shorter (50%) time than in our study.

The FS20 and FS40 groups displayed higher bond strengths, regardless of whether cyclic loading was applied (the same SBS values as TSC) or not (the same SBS values as TSC and APA25). Femtosecond laser irradiation creates a pattern of deep grooves on the zirconia surface (Fig. 1D and E) that are filled by resin cements. In a recent study [13], applied femtosecond laser irradiation to zirconia surfaces and obtained an abrasion similar to that obtained in our study, with a gentle, precise, and clear zirconia surface and an increase in the adhesive efficiency of the zirconia-resin interface. Thus, the use of a femtosecond laser may be valid for the conditioning of non-biological surfaces with minimum thermal and mechanical damage to the surfaces [27]. In addition, it should be noted that it has been demonstrated that femtosecond laser irradiation can be used as an alternative to drills in conservation dentistry [11] and for the ablation of enamel [12] or dentine [28] in a similar way to surface conditioning methods. These clinical findings, together with those obtained here, support the use of femtosecond laser irradiation as a future alternative for the treatment of dental cavities and the conditioning of different surfaces on which elements are to be cemented in dentistry, replacing the traditional methods employed currently. Despite this, further research into this issue is required.

Regardless of whether cyclic loading was applied or not, the FS20 and FS40 subgroups had similar bond strength values, which were higher than those obtained with the other conditioning methods (Table 1). The SEM observations suggest considerable quality differences in the

zirconia ceramic architecture after femtosecond laser irradiation as compared with the other conditioning methods, but also differences between the FS20 (Fig. 1D) and FS40 (Fig. 1E) subgroups. In the FS40 subgroups, although the same pattern of grooves was observed as in the FS20 subgroups, the grooves were higher and more separated from each other, suggesting that resin cement retention would be lower. However, the FS40 subgroups obtained similar values in terms of adhesive efficiency. An important clinical factor to be taken into consideration is the time of application of surface treatment. The surface conditioning method must produce a pattern of engraving in order to ensure stable and durable bonding, but it must also be carried out as fast as possible. In this sense, since femtosecond laser irradiation at step 40 produced fewer and more widely spaced grooves, the irradiation time was substantially reduced (indeed, by half). Accordingly, for practical purposes, and since efficiency is preferred over effectiveness, to achieve the best results in the shortest time possible it is best to use femtosecond laser in this step.

The specific zirconia surface areas of each subgroup were examined to analyze the topography and morphology of the debonded interfaces; the results are shown in Table 2. Regardless of whether cyclic loading was applied or not, the control group showed a tendency towards adhesive failure at the resin-zirconia interface, where there was a very small amount of remains of the resin cement on the zirconia surface of which more than 75% was appreciated without resin (Figs. 2A and 3A). By contrast, in the APA25 (Figs. 2C and 3C), TSC (Figs. 2E and 3E), FS20 (Figs. 2G and 3G), and FS40 (Figs. 2I and 3I) groups mainly mixed failures were observed where there were adhesive and cohesive failures simultaneously and the zirconia surface was exposed between 25% and 75%. There was a high prevalence of mixed failures in the TSC, FS20, and FS40 groups and adhesive failure in the control groups, regardless of whether cyclic loading was applied or not. These results show that the differences among the experimental groups were caused by the differences in surface roughness between the zirconia samples treated with the different conditioning methods (Fig. 1) and not because cyclic loading was applied (Figs. 2 and 3).

## CONCLUSIONS

The results of the present study show that when cyclic loading is applied, the adhesive effectiveness of the zirconia-resin interface decreases when any of the zirconia surface treatments are applied previously, except alumina particle abrasion, which is not affected by cyclic loading. Zirconia treatment with femtosecond laser irradiation and tribochemical silica coating improve the bond strength of the zirconia-resin interface. Femtosecond laser irradiations at step 20 and at step 40 have similar SBS values, but the time of irradiation at step 40 is half. Therefore, femtosecond laser irradiation at step 40 is preferable because it is more efficient and faster, and it could be a reliable way to achieve suitable adhesion zirconia and resin cements.

## ACKNOWLEDGMENTS

The authors are grateful to the Pulsed Laser Center (CLPU, Spain), for allowing SEM observation of the samples; Dr Marta Ortiz, from the Department of Human Anatomy and Histology, School of Medicine and Dentistry, University of Salamanca, for providing good quality SEM images; and SGiker Laser Facility (UPV/EHU, MICINN, GV/EJ, ESF) for technical support. The authors received no financial support and declare no potential conflicts of interest with respect to the authorship and publication of this article.

## REFERENCES

- Monaco C, Caldari M, Scotti R. Clinical evaluation of tooth-supported zirconia-based fixed dental prostheses: A retrospective cohort study from the AIOP clinical research group. *Int J Prosthodont* 2015;28(3):236–238.
- Solá-Ruiz MF, Agustín-Panadero R, Fons-Font A, Labaig-Rueda C. A prospective evaluation of zirconia anterior partial fixed dental prostheses: Clinical results after seven years. *J Prosthet Dent* 2015;113(6):578–584.
- Pétercsák A, Radics T, Hegedus C. Advantages and disadvantages of applying yttrium stabilized zirconium-dioxide post and core restorations. *Fogorv Sz* 2014;107(1):9–13.
- Keith O, Kusy RP, Whitley JQ. Zirconia brackets: An evaluation of morphology and coefficients of friction. *Am J Orthod Dentofacial Orthop* 1994;106(6):605–614.
- Kohal RJ, Wolkeitz M, Tsakona A. The effects of cyclic loading and preparation on the fracture strength of zirconium-dioxide implants: An *in vitro* investigation. *Clinic Oral Implants Res* 2011;22(8):808–814.
- Rinke S, Lattke A, Eichholz P, Kramer K, Ziebolz D. Practice-based clinical evaluation of zirconia abutments for anterior single-tooth restorations. *Quintessence Int* 2015;46(1):19–29.
- Guazzato M, Albakry M, Ringer SP, Swain MV. Strength, fracture toughness, and microstructure of a selection of all-ceramic materials. Part II. Zirconia-based dental ceramics. *Dent Mater* 2004;20:449–456.
- Calvalti AN, Foxton RM, Watson TF, Oliveira MT, Giannini M, Marchi GM. Y-TZP ceramics: Key concepts for clinical application. *Oper Dent* 2009;34(3):344–351.
- Usumez A, Hamdemirci N, Koroglu BY, Simsek I, Parlar O, Sari T. Bond strength of resin cement to zirconia ceramic with different surface treatments. *Lasers Med Sci* 2013;28(1):259–266.
- Luengo MC, Portillo M, Sánchez JM, Peix M, Moreno P, García A, Montero J, Albaladejo A. Evaluation of micromorphological changes in tooth enamel after mechanical and ultrafast laser preparation of surface cavities. *Lasers Med Sci* 2013;28(1):267–273.
- Lorenzo MC, Portillo M, Moreno P, Montero J, Castillo-Oyagüe R, García A, Albaladejo A. In vitro analysis of femtosecond laser as an alternative to acid etching for achieving suitable bond strength of brackets to human enamel. *Lasers Med Sci* 2014;29(3):897–905.
- Lorenzo MC, Portillo M, Moreno P, Montero J, García A, Santos del Riego SE, Albaladejo A. Ultrashort pulsed laser conditioning of human enamel: *In vitro* study of the influence of geometrical processing parameters on shear bond strength of orthodontic brackets. *Lasers Med Sci* 2015;30(2):891–900.
- Akpınar YZ, Kepceoglu A, Yavuz T, Aslan MA, Demirtag Z, Kılıç HS, Usumez A. Effect of femtosecond laser beam angle on bond strength of zirconia-resin cement. *Lasers Med Sci* 2015 [Epub ahead of print].
- Agustín-Panadero R, Román-Rodríguez JL, Ferreiroa A, Solá-Ruiz MF, Fons-Font A. Zirconia in fixed prostheses. A literature review. *J Clin Exp Dent* 2014;6(1):66–73.
- Koyama T, Sato T, Yoshinari M. Cyclic fatigue resistance of yttria-stabilized tetragonal zirconia polycrystals with hot isostatic press processing. *Dent Mater J* 2012;31(6):1103–1110.
- Attia A, Kern M. Influence of cyclic loading and luting agents on the fracture load of two all-ceramic crown systems. *J Prosthet Dent* 2004;92:551–556.
- Kawai N, Lin J, Youmaru H, Shinya A, Shinya A. Effects of three luting agents and cyclic impact loading on shear bond strengths to zirconia with tribochemical treatment. *J Dent Sci* 2012;7:118–124.
- Mirmohammadi H, Aboushelib MN, Kleverlaan CJ, de Jager N, Feilzer AJ. The influence of rotating fatigue on the bond strength of zirconia-composite interfaces. *Dent Mater* 2010;26:627–633.
- Zahran M, El-Mowafy O, Tam L, Watson PA, Finer Y. Fracture strength and fatigue resistance of all-ceramic molar crowns manufactured with CAD/CAM technology. *J Prosthodont* 2008;17:370–377.
- El-Korashy DI, El-Refai DA. Mechanical properties and bonding potential of partially stabilized zirconia treated with different chemomechanical treatments. *J Adhes Dent* 2014;16(4):365–376.
- Foong JK, Judge RB, Palamara JE, Swain MV. Fracture resistance of titanium and zirconia abutments: An *in vitro* study. *J Prosthet Dent* 2013;109(5):304–312.
- Butignon LE, Basilio Mde A, Pereira Rde P, Arioli Filho JN. Influence of three types of abutments on preload values before and after cyclic loading with structural analysis by scanning electron microscopy. *Int J Oral Maxillofac Implants* 2013;28(3):161–170.
- Zhou J, Mah J, Shrotriya P, Mercer C, Soboyejo WO. Contact damage in an yttria stabilized zirconia: Implications. *J Mater Sci Mater Med* 2007;18(1):71–78.
- Aboushelib MN. Simulation of cumulative damage associated with long term cyclic loading using a multi-level strain accommodating loading protocol. *Dent Mater* 2013;29(2):252–258.
- Ghazy MH, Madina MM, Aboushelib MN. Influence of fabrication techniques and artificial aging on the fracture resistance of different cantilever zirconia fixed dental prostheses. *J Adhes Dent* 2012;14(2):161–166.
- Nishigori A, Yoshida T, Bottino MC, Platt JA. Influence of zirconia surface treatment on veneering porcelain shear bond strength after cyclic loading. *J Prosthet Dent* 2014;112(6):1392–1398.
- Kara O, Kara HB, Tobi ES, Ozturk AN, Kilic HS. Effect of various lasers on the bond strength of two zirconia ceramics. *Photomed Laser Surg* 2015;33(2):69–76.
- Portillo M, Lorenzo MC, Sánchez JM, Peix M, Albaladejo A, García A, Moreno P. Morphological alterations in dentine after treatment and ultrashort pulse laser irradiation. *Lasers Med Sci* 2012;27(1):53–58.



M. Vicente, AL. Caseiro, J Montero, A Alvarado, V Seoane, A. Albaladejo.

**Effect of femtosecond laser treatment on effectiveness of resin-zirconia adhesive: an *in vitro* study.**

Article send to the *Journal of Lasers in Medical Sciences*.

Impact Index: - JCR Science Edition:.

Category: Surgery.

Category position: 45/195 (T1/Q1).

*Article pending of acceptation.*

•

**Title:**

**Effect of femtosecond laser treatment on effectiveness of resin-zirconia adhesive: an *in vitro* study.**

**Authors:**

**M. Vicente<sup>1</sup>, AL. Caseiro<sup>1</sup>, J Montero<sup>2</sup>, A Alvarado<sup>2</sup>, V Seoane<sup>1</sup>, A. Albaladejo<sup>2</sup>.**

1 Dental Clinic (Faculty of Medicine), University of Salamanca. Paseo Universidad de Coimbra, s/n, 37007, Salamanca, Spain.

2 Contracted Professor, Dental Clinic (Faculty of Medicine), University of Salamanca. Paseo Universidad de Coimbra, s/n, 37007, Salamanca, Spain.

**Corresponding author:**

Alberto Albaladejo Martínez

Clínica Odontológica. Facultad de Medicina.

Universidad de Salamanca (USAL).

Paseo Universidad de Coimbra s/n.

C.P.: 37007. Salamanca, Spain.

Phone:+34-923294400.

E-mail: albertoalbaladejo@hotmail.com.

## **Abstract**

**Objective:** The aim of this study was to evaluate the effect of femtosecond laser treatment on the shear bond strength (SBS) of self-adhesive resin cement on zirconia surfaces and to contrast it with other different surface-conditioning methods.

**Background Data:** When aesthetics is compromised, dental ceramics are excellent materials for dental restorations; owing to their optical properties and biocompatibility zirconia ceramics are particularly interesting. Self-adhesive resin cements are the most suitable for bonding to zirconia ceramics, but traditional adhesive chemistry is ineffective and surface treatments are required to improve the adhesive bonding between resin and zirconia. **Methods:** Sixty square-shaped zirconia samples were polished and divided randomly into four groups ( $n=15$ ) according their surface treatment: the NT Group - no surface treatment; the APA25 Group - airborne abrasion with 25  $\mu\text{m}$  alumina particles; the TSC Group - tribochemical silica coating, and the FS Group - femtosecond laser irradiation (800 nm, 4 mJ, 40 fs/pulse, 1 kHz). Self-adhesive resin cement cylinders (3 mm diameter and 2 mm height) were bonded at the centre of the zirconia surface. The samples were stored in distilled water at 37 ° C for 72 h and were then tested for SBS with a universal testing machine at a crosshead speed of 0.5 mm / min, until fracture. Five zirconia surfaces for each experimental treatment were prepared for surface morphology analysis by scanning electron microscopy (SEM). Failure modes were recorded and a third of the samples were subjected to morphological analysis of the debonded SEM surface. **Results:** The NT group showed lower SBS values than the other groups. Femtosecond laser treatment was afforded higher values than the control and APA 25 groups and similar values to those of the TSC group. In the APA25 group, the surface conditioning method had values close

to those of the TSC group, but lower than those obtained with femtosecond laser treatment. ***Conclusions:*** The treatment of zirconia with femtosecond laser irradiation creates a consistent and profound surface roughness, improving the adhesive effectiveness of the zirconia-resin cement interface. Femtosecond laser treatment is a reliable way to achieve adequate adhesion between resin and zirconia.

**Keywords:** Femtosecond laser; zirconia; shear bond strength; adhesion; surface treatment.

## **1. Introduction**

Currently, aesthetic dentistry has become one of the main areas of interest in dentistry. When aesthetics is compromised, dental ceramics are excellent materials for dental restorations; specifically, zirconia ceramics [1, 2] offer an excellent option. They have several important characteristics, such as good optical properties and biocompatibility, and achieve good adhesion values that, clinically, minimize debonded surfaces [3]. Zirconia ceramics are currently the focus of clinical and industrial activity and extensive research [4, 5].

Zirconia ceramics display the fundamental characteristics and properties of biomedical appliances, especially when the zirconia is partially stabilized with yttrium oxide ( $\text{Y}_2\text{O}_3$ ) [6, 7]. Yttria tetragonal zirconia polycrystal (Y-TZP) ceramics exhibit hardness, high strength, fracture toughness, wear resistance, low thermal conductivity, good frictional and non-magnetic behavior, and corrosion resistance to acids and alkalis, among others properties [8-9]. Regarding bonding to Y-TZP, among the resin cement luting systems that we be used for its bonding, self-adhesive resin cements are the most adequate due to their properties and the simplicity of the cementation technique [10-12].

Traditional adhesive chemistry is ineffective on zirconia surfaces [13]. Accordingly, surface treatments are needed to improve the adhesive bonding between the resin cement and the Y-TZP [14-16] ceramic. The most popular clinical surface conditioning techniques to improve the resin-zirconia interface are sandblasting [17-19], silica coating [20-22] and  $\text{CO}_2$ laser irradiation, and Er:YAG [23,24]. Nevertheless, there is still no ideal zirconia surface conditioning method able to that provide sufficient effectiveness of adhesion on zirconia surfaces. It is therefore necessary to find an adhesion protocol with a view to obtaining a resin-zirconia bond with high efficiency

and durability [25, 26].

One of the new surface treatments currently being explored is irradiation with femtosecond laser, which emits optical pulses with a duration well below 1 picosecond, in the domain of femtoseconds ( $1 \text{ fs} = 10^{-15} \text{ s}$ ). Within the group of femtosecond lasers, is the Titanium: Sapphire laser, which is based on a femtosecond Ti: Sapphire centenary oscillator producing wavelengths near the infrared (795nm) and energies in the range 10 nanoJ, with a repeat rate of 80 MHz. This system has an output amplifier, creating a pulse duration of 120 fs.

It would be of great clinical use if femtosecond lasers could be employed to perform the conditioning of biological and non-biological surfaces on which elements are cemented in Dentistry. Some studies have already addressed studies the enamel-bracket interface, [27,28], obtaining encouraging results in the sense of improvements in adhesive effectiveness and the possibility of replacing traditional conditioning agents that cause biological damage to tooth enamel. Regarding adhesion to porcelain, in a recent study the authors analyzed zirconia surface conditioning with a femtolaser to improve the porcelain-bracket interface [29]. It was reported that femtosecond lasers could represent a new alternative to conventional surface treatments, and they have therefore become a new study object in the search for improvements in the interface adhesion of this non-biological surface; in this sense they could become a valid option for improving resin-zirconia interface adhesion, as proposed here.

The aim of this study was to evaluate the effect of femtosecond laser treatment on the shear bond strength (SBS) of self-adhesive resin cements to zirconia surfaces and

to compare such treatment with more conventional surface conditioning methods.

## **2. Material and methods**

### *2.1 Preparation of zirconia samples*

The study used sixty samples of densely sintered Y-TZP (Cercon®, DeguDent, Hanau, Germany). The specimens, which were square-shaped and measured 6x6x1 mm, were obtained using a precision cutting machine (Isomet 5000; Buehler, Lake Bluff, Illinois, USA). Each sample surface was wet-polished with 600-grit silicon carbide paper on a polishing machine (Phoenix Beta; Buehler, Lake Bluff, Illinois, USA). The manufacturer's composition and application mode of the materials used in the experiment are detailed in Table 1.

### *2.2 Experimental groups*

Once the zirconia samples had been polished, they were assigned randomly into four experimental groups according to the surface treatment to be applied ( $n=15$ ).

#### *2.2.1 Group 1: Control- No treatment (NT).*

No surface treatment was applied.

#### *2.2.2 Group 2: Airborne particle abrasion with 25 $\mu\text{m}$ alumina particles (APA 25).*

The zirconia surface was blasted with alumina particles ( $\text{Al}_2\text{O}_3$ ) with an average particle size of 25  $\mu\text{m}$  under a pressure of 0.25 MPa for 20 seconds at a perpendicular distance of 10 mm from the holder.

#### *2.2.3 Group 3: Tribocochemical silica coating (TSC).*

In this case, the zirconia surface was treated with a tribocochemical silica coating

(30 µm alumina with silica particles) with the Rocatec system (Rocatec™ Soft, 3M Espe, Seefeld, Germany). Rocatec particles were applied under a pressure of 0.25 MPa for 20 seconds at a perpendicular distance of 10 mm. Silica coating was followed by silanization, which was performed following manufacturer's instructions with a Rely X™ ceramic primer (3M Espe, Seefeld, Germany).

#### *2.2.4 Group 4: Femtosecond laser (FS).*

The zirconia surface was irradiated with a femtosecond laser. The laser pulses were generated by a commercial Ti:Sapphire oscillator-regenerative amplifier system (Mantis-Legend, Coherent), providing 1 kHz trains of pulses centered at 800 nm, with an energy of 4.0 mJ and a duration of 40 fs. The pulse energy used in the experiments was finely controlled with a variable neutral-density filter and measured with a thermal detector (S302C, Thorlabs). The laser pulses were focused by means of a fused silica singlet lens ( $f=100$  mm), yielding a spot diameter of approximately 20 µm.

The specimens were fixed on a computer-controlled XYZ-motorized stage (PT3-Z8, Thorlabs) at atmospheric pressure. The experimental conditions were chosen to obtain a more uniform pattern across the surface, thus minimizing the depth of the grooves generated by laser -. Thus, the pulse energy was 0.015 mJ, the scanning velocity 0.25 mm/s and the scanning step was 0.02 mm.

### *2.3 Bonding procedure*

After performing the different surface treatments on the zirconia samples, a self-adhesive resin cement was used according to manufacturer's recommendations:

Clearfil™ SA Cement (*CLE*) (Clearfil™ SA Cement, Kuraray, Osaka, Japan).

For application of the cement, a cylindrical silicone mould with a 3-mm internal diameter, 1 mm thickness and 1 mm in height was used. It was positioned at the centre of the samples, and the cement was placed on them against the zirconia surface and polymerized for 40 s (XL 3000, 3M/ESPE; light intensity 500 mW/cm<sup>2</sup>, distance 0) from above and towards the contact area from a lateral position.

The mould was removed and the cylinder cement was light cured for a further 40 seconds. Thus a resin cement cylinder of 3 mm diameter and 1 mm in height bonded to the zirconia surface was obtained.

#### *2.4 Shear bond strength (SBS) test*

The samples were stored in distilled water at 37 ° C. After 72 h, all zirconia samples, with the cement cylinder on their surface, were tested for SBS with a universal testing machine (AGS-X Autograph, Shimadzu Corporation, Kyoto, Japan), applying a shear load with a crosshead speed of 0.5 mm / min, until fracture.

To calculate the bond strength values in MPa, the maximum load recorded upon failure (in Newtons N) was divided by the bonding area (in square millimetres).

#### *2.5 Failure mode analysis*

After the SBS-test, each fractured specimen was examined under an Axio M1 (Carl Zeiss, Germany) light microscope at 40X magnification to determine the failure modes. These were classified as adhesive (no remnants of resin cement on the zirconia surface, failure in adhesion) or mixed (zirconia samples showing residual cement on their surface, with both adhesive and cohesive failures).

## *2.6 Scanning electron microscope (SEM) examination*

Five zirconia surfaces from each experimental group ( $n=5$ ) were prepared for surface morphology analysis with a variable pressure SEM (Zeiss EVO MA25; Carl Zeiss, Jena, Germany). Specific regions across the zirconia surface were explored with the scanning electron microscope, focusing with different magnifications ( $\times 70$  and  $\times 1000$ ) to obtain a panoramic view of the effect of laser processing and the effect of the other conditioning methods.

In addition, representative fractured samples were dehydrated for 48h in a desiccator (Sample Dry Keeper Simulate Corp., Tokyo, Japan) and were sputter-coated with a 10-nm platinum layer in a Polaron E5100 SEM coating unit (Polaron Equipment Ltd., Hertfordshire, England, UK).

Specific zirconia surface areas were examined with the scanning electron microscope, focusing with different magnifications (from  $\times 30$  to  $\times 1000$ ), in order to analyze the morphology of the debonded interfaces and identify possible differences among the experimental groups with respect to the surface topography and morphology of the debonded interfaces.

## *2.7. Statistical analysis*

The bond strength values were measured in MPa. The data were analyzed with SPSS v21 (Statistical Package for the Social sciences, Chicago, IL), using a p-value below 0.05 as the threshold for statistical significance. ANOVA tests were applied to compare the SBS among the subgroups regarding the use of different zirconia surface treatments.

When the ANOVA test detected significant differences, Bonferroni post-hoc

comparisons were performed to quantify the differences between two subgroups. The Chi-square test was used to detect differences in the types of failures among groups. The table was decomposed into 2x2 and the risk of adhesive failure was calculated by reference to the control group (Odds Ratio and Relative Risk).

### **3. Results**

#### *3.1 Shear bond strength (SBS) test:*

The mean values and standard deviations (SD) of SBS for all the different surface treatment groups are shown in Table 2.

The results obtained using ANOVA revealed that the variance of SBS within the groups was significantly different ( $F = 19,4$ ;  $p < 0.001$ ). The Bonferroni post-hoc inter-group comparisons indicated that the control group (NT) had lower SBS values than the other groups. Femtosecond laser treatment afforded higher values than the control and APA 25 groups and similar values to those seen for TSC. The surface conditioning method in the APA25 group had values close to those of the TSC group, but lower than those obtained with femtolaser treatment.

Bond failure-modesanalyses are shown in Table 3. In the control group, the majority of failures were adhesive, while in other treatment groups they were mostly mixed. The 2x2 failure rate comparison using the reference control group revealed significant differences in the TSC and FS groups (Chi: 4;  $p= 0.06$ ); but not in the APA25 group (Chi: 3.3;  $p= 0.143$ ). The risk of adhesive failure was significantly higher in the control group than in the TSC and FS (OR =5.5) groups.

#### *3.2 SEM Observations*

The SEM micrographs in fig.1 show the zirconia surface morphology after the different surface treatment methods had been applied. Images A and B represent the NT

group at a magnification power of 70 and 1000 respectively. They show marked scratches running in the same direction as result of the polishing procedure. Images C and D, which correspond to the APA25 group, display granule-shaped micro-retentions over the surface, due to the impact of the high-speed 25 µm alumina particles. Images E and F, which represent the TSC group, show a rough appearance as a result of the coating and solidification of the tribochemical silica particles. The FS group (images G and H) show a well-defined pattern of deep horizontal furrows.

Fig. 2 shows representative SEM images of debonded zirconia surfaces, after SBS, at two different powers of magnification. In the figure, image A shows adhesive failure with no visible remains of the resin cement. Images C, E and G display mixed failures with residual cement on the zirconia surface with a large visible cohesive phase. Details of the debonded areas can be observed in images B, D, F, H at a magnification power of 700.

#### 4. Discussion

Y-TZP ceramics are now very popular dental restoration materials owing to their exceptional properties, such as fracture toughness and biocompatibility [30]. However, their long-term success depends not only these properties, but also on others, such as the type of cement [31], the cementing procedure [32] and, especially, the surface roughness, because the surface conditioning procedure seems to be a more relevant factor in bonding to zirconia surfaces [15, 25].

The results regarding bond strength demonstrated that femtosecond laser irradiation was more effective in improving bond strength than airborne-particle abrasion with 25-µm alumina particles and no surface treatment (Table 2). The SEM

observations suggested considerable quality differences in the zirconia ceramic architecture after femtosecond laser irradiation (Fig 1G) as compared with the other conditioning methods, and this could be related to these higher values (10.8 MPa). Kara *et al.* [24] have reported that femtosecond laser irradiation is an effective surface treatment for roughening the surfaces of zirconia ceramics. It produces a pattern of deep horizontal furrows on the zirconia surface (Fig 1H), allowing greater retention of resin cements, which become intertwined within these grooves to form a single bonded structure, thereby increasing bond strength. By contrast, in the control group (Fig 1B) there is no abrasion or irregularities on the surface that provide micromechanical retention, only the effect of wet-polished with 600-grit silicon carbide paper. Also, in the APA25 group, alumina particle sandblasting created a rough surface (Fig 1D), but the surface irregularities have insufficient micro depth and therefore both groups exert less mechanical retention than the FS group (Fig 1H) and TSC group (Fig 1F).

In recent studies [27, 28] an abrasion pattern similar to that obtained in our study when applying femtosecond laser on the enamel surface, also showing increased adhesive efficiency, has been reported. Thus, the use of a femtosecond laser may be valid for conditioning on enamel and zirconia, as we show here. Thus, the use of femtosecond lasers is increasingly supported as an alternative in the field of adhesion in dentistry, replacing drills in conservation dentistry [33] and also serving as both a conditioning agent and for the ablation of different types of surfaces -whether they are biological, such as the enamel [27, 28] or dentine [34], or non-biological, such as porcelain [29] or zirconia, as in the present case- with a minimum amount of thermal and mechanical damage to the surfaces [35, 36].

The TSC group had SBS values close to those of the FS group. This high value (9.5 MPa) can be related directly to the architecture of the zirconia surface after application of the tribochemical silica coating (Fig 1E), which mainly affects the bond strength results because the surface roughness seems to be a more relevant factor in bonding to zirconia surfaces [33].

In view of the SBS values obtained, although the pattern of engraving is different than that achieved with the shown by femtosecond laser, because the FS group (Fig 1H) has a horizontal stripe pattern and the TSC group (1F) creates irregularities that do not obey any specific pattern, both are equally retentive. It may therefore be concluded that the retention depends more on the engraving depths obtained than on the type. Accordingly, besides the influence of the roughness of the surface created, resin cement adhesion could be effectively improved by silica coating on zirconia surfaces [37]. In addition, the silica coating process allows chemical coupling through the silane [22]. After the silica particles have impacted the surface, the zirconia surface irregularities are infiltrated by ceramic primer Rely X<sup>TM</sup>. Silane coupling agents produce better contact and infiltration of the resin into the zirconia surface irregularities and protect against moisture through chemical bonding. In their study May *et al.* [20] determined that use of the MDP-primer after silica coating increased bond strength.

Airborne-particle abrasion with 25-μm Al<sub>2</sub>O<sub>3</sub> particles was less effective in improving bond strength than femtosecond laser irradiation. Although alumina particle sandblasting created a rough surface (Fig 1C) similar to that seen in the TSC group (Fig 1E) it does not improve bond strength because the surface irregularities have insufficient micro depth (Fig 1D), unlike the irregularities created in the FS (Fig 1H) and TSC (Fig 1F) groups, and therefore fails to generate sufficient micromechanical retention. In a recent study, Akpinar *et al.* tested the zirconia-bracket interface with the

use of a cementing agent. Although our study focused directly on the zirconia-resin interface, disregarding differences the data can be said to be comparable [29]

The Control group showed lower SBS values than the other groups. This can be seen from the SEM images (Fig 1A), where it may be observed that in these zirconia samples, which were only subjected to wet-polishing with 600-grit silicon carbide paper, there were no surface irregularities (Fig 1B) such as shallow pits or microcracks to provide micromechanical retention. The Y-TZP zirconia surface roughness is influenced by the surface treatment applied and is directly related to the bonding properties [38]. Aboushei *et al.* [25] reported that a strong and durable resin-zirconia bonding is vital for the longevity of dental restorations and this is only possible with a surface treatment that will allow the zirconia surface to be roughened.

The specific zirconia surface areas of each group were examined to analyze the topography and morphology of the debonded interfaces. The bond failure modes assessed are shown in Table 3. They support the bond strength results and the differences among the experimental groups. The Control group showed a tendency towards adhesive failure at the resin-zirconia interface, with no resin cement remains on the zirconia surface (Fig 2A), in accordance with the literature addressing resin cements [39]. In the APA25, TSC and FS groups mainly mixed failures were observed (Fig 2B, 2C, 2D) with significant differences in the TSC (Chi: 4; p= 0.06) and FS groups, but not in the APA25 group (Chi: 3.3; p= 0.143).

The high prevalence of mixed failures and the fact that the risk of adhesive failure was significantly higher in the Control group than in the TSC and FS groups

show that the different results among the experimental groups were caused by the differences in surface roughness between the zirconia samples treated with the different conditioning methods (Fig 1).

## **5. Conclusions**

The results of the present study show that zirconia treatment with femtosecond laser irradiation and tribochemical silica coating create consistent roughness on its surface, improving the adhesive effectiveness of the zirconia-resin cement interface, with higher bond strength values in the FS group. Accordingly, micromechanical retention based more on the engraving depth created by conditioning method than on the engraving pattern is a fundamental requirement for establishing a strong and durable bond with zirconia-based materials, and femtosecond laser treatment might be a reliable way to achieve suitable adhesion between resins and zirconia.

## **6. Acknowledgments**

The authors are grateful to the Pulsed Laser Center (CLPU, Spain) for allowing SEM observation of the samples; Dr Marta Ortiz, from the Department of Human Anatomy and Histology, School of Medicine and Dentistry, University of Salamanca, for providing good quality SEM images; Dr Raul Montero, from the School of Science and Technology, University of the País Vasco for FS laser use and facilities. The authors received no financial support and declare no potential conflicts of interest with respect to the authorship and publication of this article.

## **References**

1. Denry I, Kelly JR. State of the art of zirconia for dental applications. *Dent Mater.* 2008;24:299-307.
2. Vagkopoulou T, Koutayas S, Koidis P, Strub JR. Zirconia in Dentistry: Part 1. Discovering the nature of an upcoming bioceramic. *Eur J Esthet Dent.* 2009;4:130-51.
3. Manicone PF, Iommetti PR, Raffaelli L. An overview of zirconia ceramics: basic properties and clinical applications. *J Dent.* 2007;35(11):819-26.
4. Gomes AL, Montero J. Zirconia implant abutments: a review. *Med Oral Patol Oral Cir Bucal.* 2011;16(1):50-5.
5. Ozcan M, Bernasconi M. Adhesion to zirconia used for dental restorations: a systematic review and meta-analysis. *J Adhes Dent.* 2015;17(1):7-26.
6. Calvalti AN, Foxton RM, Watson TF, Oliveira MT, Giannini M; Marchi GM. Y-TZP ceramics: key concepts for clinical application. *Oper Dent.* 2009;34(3):344-51.
7. Nakanieczny D, Walke W, Majewska J, Paszenda Z. Characterization of magnesia-doped yttria-stabilized zirconia powders for dental technology applications. *Acta Bioeng Biomech.* 2014;16(4):99-106.
8. Kosmac T, Oblak C, Jevnikar P, Funduk N, Marion L. Strength and reliability of surface treated Y-TZP dental ceramics. *J Biomed Mater Res.* 2000;53(4):304-13.
9. El-Korashy DI, El-Refai DA. Mechanical properties and bonding potential of

- partially stabilized zirconia treated with different chemomechanical treatments. *J Adhes Dent.* 2014;16(4):365-76.
10. Ferracane JL, Stansbury JW, Burke FJT. Self-adhesive resin cements—chemistry, properties and clinical considerations. *J Oral Rehabil.* 2011;38(4):295-314.
11. Casucci A, Goracci C, Chieffi N, Monticelli F, Giovannetti A, Juloski J, Ferrari M. Microtensile bond strength evaluation of self-adhesive resin cement to zirconia ceramic after different pre-treatments. *Am J Dent.* 2012;25(5):269-75.
12. Maeda FA, Bello-Silva MS, de Paula Eduardo C, Miranda Junior WG, Cesar PF. Association of different primers and resin cements for adhesive bonding to zirconia ceramics. *J Adhes Dent.* 2014;16(3):261-5.
13. Kern M, Wegner SM. Bonding to zirconia ceramic: adhesion methods and their durability. *Dent Mater.* 1998;14(1):64-71.
14. Elsaka SE. Effect of surface treatments on the bonding strength of self-adhesive resin cements to zirconia ceramics. *Quintessence Int.* 2013;44(6):407.
15. Usumez A, Hamdemirci N, Koroglu BY, Simsek I, Parlar O, Sari T. Bond strength of resin cement to zirconia ceramic with different surface treatments. *Lasers Med Sci.* 2013;28(1):259-66.
16. Moradabadi A, Roudsari SE, Yekta BE, Rahbar N. Effects of surface treatment on bond strength between dental resin agent and zirconia ceramic. *Mater Sci Eng C Mater Biol Appl.* 2014;34:311-7.
17. Akin H, Ozkurt Z, Kimali O, Kazazoglu E, Ozdemir A. Shear bond strength of

- resin cement to zirconia ceramic after aluminium oxide sandblasting and various laser treatments. Photomed Laser Surg. 2011;29:797-802.
18. Gomes AL, Castillo-Oyagüe R, Lynch CD, Montero J, Albaladejo A. Influence of sandblasting granulometry and resin cement composition on microtensile bond strength to zirconia ceramic for dental prosthetic frameworks. Am J Dent. 2013;41(1):31-41.
19. Sarmento HR, Campos F, Sousa RS, Machado JP, Souza RO, Bottino MA, Ozcan M. Influence of air-particle deposition protocols on the surface topography and adhesion of resin cement to zirconia. Acta Odontol Scand. 2014;72(5):346-53.
20. May LG, Passos SP, Capelli DB, Ozcan M, Bottino MA, Valandro LF. Effect of silica coating combined to a MDP-based primer on the resin bond to Y-TZP ceramic. J Biomed Mater Res B Appl Biomater. 2010;95(1):69-74.
21. Queiroz JR, Massi M, Nogueira L Jr, Sobrinho AS, Bottino MA, Ozcan M. Silica-based nano-coating on zirconia surfaces using reactive magnetron sputtering: effect on chemical adhesion of resin cements. J Adhes Dent. 2013;15(2):151-9.
22. Gomes AL, Ramos JC, Santos del Riego S, Montero J, Albaladejo A. Thermocycling effect on microshear bond strength to zirconia ceramic using Er.YAG and tribochemical silica coating as surface conditioning. Laser Med Sci. 2015;30(2):787-95.
23. Kasraei S, Rezaei-Soufi L, Heidari B, Vafaei F. Bond strength of resin cement

- to CO<sub>2</sub> and Er:YAG laser-treated zirconia ceramic. *Restor Dent Endod.* 2014;39(4):296-302.
24. Kara O, Kara HB, Tobi ES, Ozturk AN, Kilic HS. Effect of various lasers on the bond strength of two zirconia ceramics. *Photomed Laser Surg.* 2015;33(2): 69-76.
25. Abousheib MN. Evaluation of zirconia/resin bond strength and interface quality using a new technique. *J Adhes Dent.* 2011;13(3):255-60.
26. Cvikel B, Dragic M, Franz A, Raabe M, Gruber R, Moritz A. Long-term storage affects adhesion between titanium and zirconia using resin cements. *J Adhes Dent.* 2014;16(5):459-64.
27. Lorenzo MC, Portillo M, Moreno P, Montero J, Castillo-Oyagüe R, García A, Albaladejo A. In vitro analysis of femtosecond laser as an alternative to acid etching for achieving suitable bond strength of brackets to human enamel. *Lasers Med Sci.* 2014;29(3):897-905.
28. Lorenzo MC, Portillo M, Moreno P, Montero J, García A, Santos del Riego SE, Albaladejo A. Ultrashort pulsed laser conditioning of human enamel: in vitro study of the influence of geometrical processing parameters on shear bond strength of orthodontic brackets. *Laser Med Sci.* 2015;30(2):891-900.
29. Akpinar YZ, Irgin C, Yavuz T, Aslan MA, Kilic HS, Usumez A. Effect of femtosecond laser treatment on the shear bond strength of a metal bracket to prepared porcelain surface. *Photomed Laser Surg.* 2015;33(4):206-12:206-12.
30. Camposilvan E, Marro FG, Mestra A, Anglada M. Enhanced reliability of yttria-stabilized zirconia for dental applications. *Acta Biomater.* 2015;17:36-46.

31. Passos SP, May LG, Barca DC, Ozcan M, Bottino MA, Valandro LF. Adhesive quality of self-adhesive and conventional adhesive resin cement to Y-TZP ceramic before and after aging conditions. *Oper Dent.* 2010;35(6):689-96.
32. Inokoshi M, De Munck J, Minakuchi S, Van Meerbeek B. Meta-analysis of bonding effectiveness to zirconia ceramics. *J Dent Res.* 2014;93(4):329-34.
33. Luengo MC, Portillo M, Sánchez JM, Peix M, Moreno P, García A, Montero J, Albaladejo A. Evaluation of micromorphological changes in tooth enamel after mechanical and ultrafast laser preparation of surface cavities. *Lasers Med Sci.* 2013;28(1):267-73.
34. Portillo Muñoz M, Lorenzo Luengo MC, Sánchez Llorente JM, Peix Sánchez M, Albaladejo A, García A, Moreno Pedraz P. Morphological alterations in dentine after mechanical treatment and ultrashort pulse laser irradiation. *Lasers Med Sci.* 2012;27(1):53-8.
35. Pike P, Parigger C, Splinter R, Lockhart P. Temperature distribution in dental tissue after interaction with femtosecond laser pulses. *Appl Opt.* 2007;46:8374-8.
36. Girard B, Cloutier M, Wilson DJ, Clokie CMI, Miller RJD, Wilson BC. Microtomographic analysis of healing of femtosecond laser bone calvaria wounds compared to mechanical instruments in mice with and without application of BMP-7. *Lasers Surg Med.* 2007;39:458-67.
37. Liu D, Tsou JK, Matinlinna JP, Wong HM. Effects of some chemical surface modifications on resin zirconia adhesión. *J Mech Behav Biomed Mater.*

2015;46:23-30.

38. Kirmali O, Kustarci A, Kapdan A, Er K. Efficacy of surface roughness and bond strength of Y-TZP zirconia after various pre-treatments. Photomed Laser Surg. 2015;33(1): 15-21.
39. De Oyagüe RC, Moticelli F, Toledano M, Osorio E, Ferrari M; Osorio R. Influence of surface treatments and resin cement selection on bonding to densely-sintered zirconium-oxide ceramic. Dent Mater. 2009;25(2):172-9.

**Table 1.** Materials brands, manufacturer, composition and manipulation sequence used in the study.

<i>Material</i>	<i>Manufacturer</i>	<i>Composition and/or conditions</i>	<i>Manipulation Sequence</i>
Y-TZP ceramic.	Cercon®, DeguDent, Hanau, Germany.	Sixty squares, measuring 6 mm x 6 mm x 1 mm, of yttria-stabilized polycrystalline tetragonal zirconia. Zirconium oxide and yttrium oxide: 5%. Hafnium oxide: <2%. Aluminum oxide + silicon oxide: <1%.	The zirconia samples received different surface treatments, after which, the resin was placed on over their surface.
Polishing machine.	Phoenix Beta; Buehler, Lake Bluff, Illinois, USA.	600-grit silicon carbide paper was used for the polishing.	Each zirconia sample surface was wet-polished before receiving the respective surface treatment.
APA 25.	Renfert GmbH, Hilzingen, Germany.	Alumina particles ( $\text{Al}_2\text{O}_3$ ) with an average size of 25 $\mu\text{m}$ .	Zirconia samples were sandblasted for 20 s at 0.25 MPa at a perpendicular distance of 10 mm.
Rocatec™ Soft.	3M Espe, Seefeld, Germany.	30 $\mu\text{m}$ silica with modified aluminium oxide.	Zirconia samples were sandblasted for 20 s at 0.25 MPa at a perpendicular distance of 10 mm.

Rely X™ ceramic primer.	3M Espe, Seefeld, Germany.	Ethyl alcohol, water, methacryloxypropyltrimethoxysilane.	Silica coating was followed by silanization. Rely X™ ceramic primer was applied on the zirconia bonding surface for 40 s with gentle air drying.
Ti:Sapphire oscillator - regenerative amplifier system.	Mantis-Legend, Coherent, USA.	$\lambda=800\text{nm}$ Duration/pulse= 40 fs Energies= 4mJ Repetition rate= 1KHz	The laser pulses were focused by means of a fused silica singlet lens ( $f=100\text{ mm}$ ), yielding a spot diameter of 20 $\mu\text{m}$ .
Clearfil™ SA Cement	Kuraray, Osaka, Japan	MDP, hydrophobic aromatic dimethacrylate, hydrophobic aliphatic dimethacrylate, colloidal silica, barium glass.	The cement was dispensed from a dual-barreled automix syringe with a spiral mixing tip. For the application of cement, a silicone cylindrical mould (3 mm internal diameter, 1 mm thickness and 1 mm height) was positioned at the centre of the specimens, and the cement was placed on them (the mould) against the zirconia surface. The specimens were self-cured for 5 min and each axial surface was light-cured for 40 s.

Curing light	XL 3000, 3M/ESPE.	Light intensity was 500 mW/cm <sup>2</sup> .	The surface of the zirconia samples was polymerized for 40 s from above and towards the contact area from a lateral position.
Universal SBS testing machine.	AGS-X Autograph, Shimadzu Corporation, Kyoto, Japan	A shear load was applied with a crosshead speed of 0.5 mm / min, until fracture.	All zirconia samples, with a cement cylinder on their surface, were tested for shear bond strength.  To calculate the bond strength values in MPa, the maximum load recorded upon failure (in Newtons N) was divided by the bonding area (in square millimetres).
Axio M1 light microscope.	Carl Zeiss, Germany.	At ×40 magnification.	After the SBS-test, each fracture specimen was examined under a light microscope to determine the failure mode. Failure modes were classified as adhesive (no remnants of resin cement) or mixed (both adhesive and cohesive failures).

**Table 2.** Means and standard deviations (SD) of the shear bond strength (SBS) values (MPa) obtained in the experimental groups. ANOVA with Bonferroni corrections.

	<b>NT(Control)</b> (n=15) MEAN(SD)	<b>APA25</b> (n=15) MEAN(SD)	<b>TSC</b> (n=15) MEAN(SD)	<b>FS</b> (n=15) MEAN(SD)	
SBS	4.4(1.3)A	8.1(3.6)B	9.5(2.3)BC	10.8(1.9)C	F=19.4; p<0.001
Different letters refer to significant inter-group comparisons after Bonferroni corrections.					

The control group (NT) had lower SBS values than the other groups. Femtosecond laser treatment afforded higher values in than the control and APA 25 groups and similar values to those seen for TSC. The surface conditioning method in the APA25 group had values close to those of the TSC group, but lower than those obtained with to femtolaser treatment.

**Table 3.** Modes of bond failure and risk of adhesive failures taking the control group as reference.

	<b>Control-NT</b> (N=15) N(%)	<b>APA25</b> (N=15) N(%)	<b>TSC</b> (N=15) N(%)	<b>FS</b> (N=15) N(%)
Adhesive	10(66.7)	5(33.3)	4(26.7)	4(26.7)
Mixed	5(33.3)	10(66.7)	11(73.3)	11(73.3)
Relative Risk (CI-95%)	2.3(1.0-5.1)	0.5(0.2-1.1)	0.4(0.2-1.0)	0.4(0.2-1.0)
OR (CI-95%)		4.0(0.9-18.3)	5.5(1.2-26.4)	5.5(1.2-26.4)

. In the control group, the majority of failures were adhesive, while in other treatment groups they were mostly mixed. The 2x2 failure rate comparison using the reference control group revealed significant differences in the TSC and FS but not in the APA25 group.

**Figure 1**

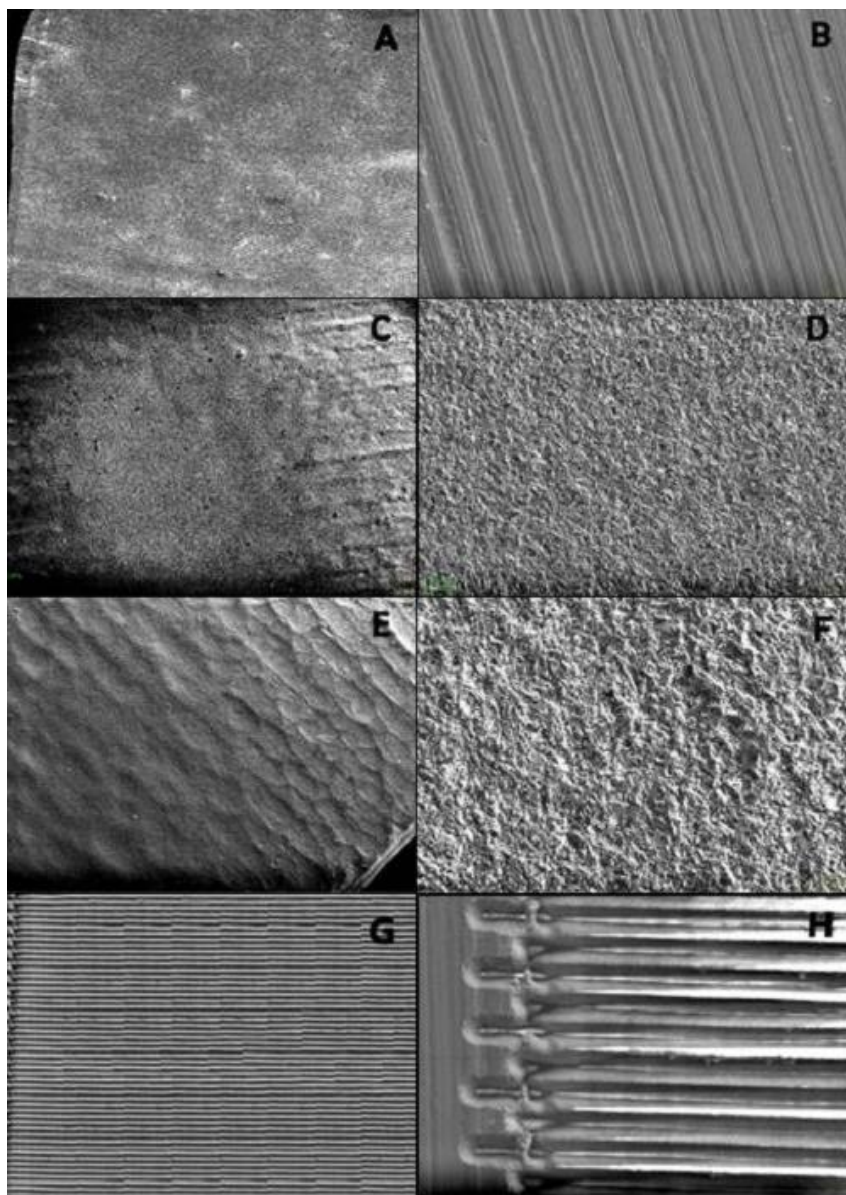


Fig. 1 SEM micrographs of zirconia ceramic surfaces after conditioning treatments (X70 and X1000 magnification). : A, B- No treatment (NT); C, D- Airborne-particle abrasion with 25- $\mu\text{m}$  alumina particles (APA 25); E, F- Tribochemical silica coating (TSC); G, H- Femtosecond laser (FS).

**Figure 2**

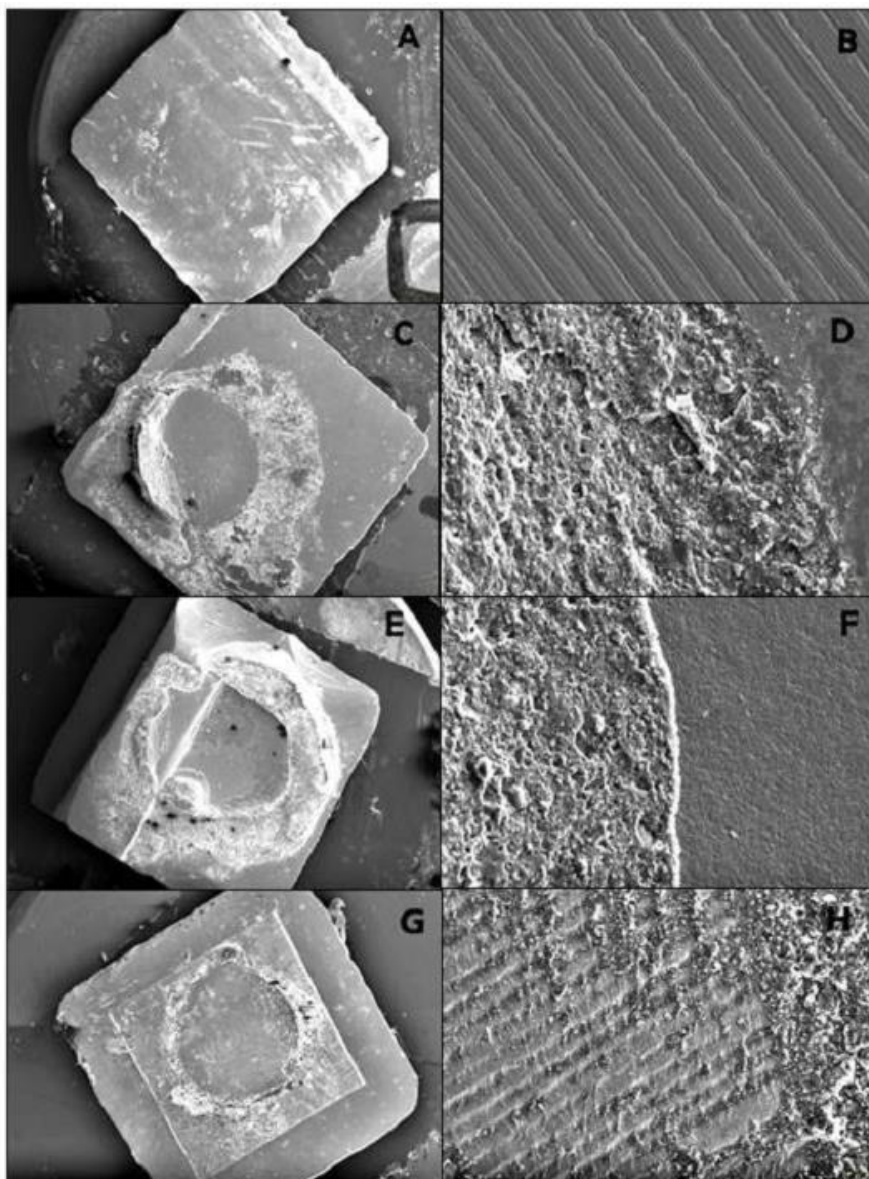


Fig 2. Representative zirconia surface SEM images (X30 and X700 magnification) of the most common failure type for each group. A and B (NT group) shows an adhesive failure where there are no visible resin cement remains on the ceramic surface due to complete detachment; C and D (APA 25 group); E and F (TSC group); G and H (FS group) show mixed failure, with a cohesive phase and visible pores in the remaining residual cement.



*Viii.2 APPENDIX 2.*  
*TESIS RESUMIDA*  
*EN ESPAÑOL.*

# Introducción

## **LAS CERÁMICAS DENTALES: EL CIRCONIO.**

La Sociedad Americana de Cerámica define las cerámicas como materiales inorgánicos, no metálicos, que son típicamente de naturaleza cristalina, y que se forman por la unión de elementos metálicos y no metálicos, tales como: aluminio y oxígeno ( $\text{Al}_2\text{O}_3$ ), de calcio y oxígeno ( $\text{CaO}$ ) o silicio y nitrógeno ( $\text{Si}_3\text{N}_4$ ) (Sukumaran *et al.*, 2006). Además tienen estructura cristalina, por lo general, con arreglo regular y periódico de los átomos que lo componen, y pueden presentar un enlace iónico o covalente.

La primera vez que se utilizaron las cerámicas en el ámbito odontológico fue en 1774, por parte de Alexis Duchateau, un farmacéutico parisino, con la ayuda de Nicholas Dubois de Chemant, que hizo la primera prótesis de porcelana, que es un tipo de cerámica de alta calidad, en la fábrica de porcelana Guerhard(Kelly *et al.*, 1996). En 1791, Dubois de Chemant patentado su idea y en 1792 se comenzaron a vender.

No fue hasta 1950 cuando se impulsó la producción de cerámica dental, por parte de Weinstein que presenta las coronas de metal-cerámica. Se patentó la formulación de porcelana feldespática que permitió el control de la temperatura de sinterización y la expansión térmica, así como los componentes que se podrían utilizar para producir aleaciones que unidos químicamente eran compatibles con las porcelanas feldespáticas (Luthardt *et al.*, 1999).

Actualmente, las cerámicas dentales, así como las resinas acrílicas, los metales y los composites, son materiales esenciales en la restauración dental y son el mejor material a utilizar cuando la estética se ve comprometida puesto que todas las restauraciones cerámicas ayudan a conservar el color natural de los tejidos blandos, y no hay ningún cambio en la pigmentación de color una vez que el gingival del material es similar a los dientes, y todo ello con unas propiedades mecánicas ideales.

Las cerámicas dentales presentan unos propiedades, tanto mecánicas como estéticas, ideales que las convierten en un material esencial para las restauraciones dentales (Álvarez-Fernandez *et al.*, 2003). Entre sus principales propiedades se encuentran las siguientes:

1. La biocompatibilidad;
2. Excelentes características ópticas tales como transparencia, color, brillo, alta reflexión y textura, lo que implica una variedad de opciones para mimetizar la estabilidad natural de los dientes.
3. Compatibilidad con otros materiales como los metales y resinas.
4. Baja conductividad térmica y un módulo de elasticidad similar a los tejidos dentales duros.
5. Radiopacidad, que permite la evaluación de la precisión marginal y diagnóstico de caries secundaria.
6. La dureza y la resistencia a la abrasión.
7. La resistencia mecánica.

8. Proceso de producción fácil y de coste razonable.

A la hora de clasificar las cerámicas dentales podemos atender a varios criterios de clasificación como puede ser su composición química, por su contenido cristalina o bien por el proceso de laboratorio empleado para su obtención.

En cuanto a su composición química, las cerámicas se pueden clasificar en:

*1. Cerámica feldespática:*

- **clásica o tradicional:** se utiliza en el recubrimiento núcleos de cerámica o metal.
- **reforzada o de alta resistencia:** cristales de leucita o disilicato de litio que se utilizan para fortalecer cerámica feldespática.

*2. Cerámica de alúmina:* se compone de una fase de matriz de vidrio y al menos de un 35% en volumen de alúmina. Un núcleo aluminoso es más fuerte que la porcelana feldespática, y las partículas de alúmina son más fuertes que el vidrio y más eficaces para prevenir la propagación de grietas (Van Noort *et al.*, 1989).

Pueden ser:

- **clásica.**
- **reforzada o de alta resistencia.**

*3. Cerámica de circonio.*

El óxido de circonio ( $ZrO_2$ ) es un óxido cristalino de color blanco que pertenece a los metales. El circonio puro no se encuentra como tal en la naturaleza, sino que se encuentra en varios minerales que contienen un

porcentaje de óxido de circonio alto (80-90%), con trazas de  $TiO_2$  y  $Fe_2O_3$ .

El circonio es un cristal polimórfico, lo que significa que presenta una estructura cristalina diferente a diferentes temperaturas sin cambios en la química y estas son:

1. *Cúbica* (C): forma prismática con sección cuadrada, estable a temperaturas superiores a 2370 °C hasta la temperatura de fusión (2680 °C) con moderadas propiedades mecánicas.
2. *Tetragonal* (T): forma prismática con sección rectangular, estable entre 1170-1370 °C y con mejorar las propiedades cuando se compara con la forma cúbica.
3. *Monocíclico* (M): forma irregular prismática con sección tetagonal, estable en 1170 °C con bajas propiedades mecánicas.

La adición de óxidos de estabilización como  $CaO$ ,  $MgO$ , y  $Y_2O_3$  al circonio permite la creación de materiales multifásicos conocidos como circonio parcialmente estabilizada (PSZ) que, a temperatura ambiente, consiste en una fase de óxido de circonio cúbico principalmente, una menor concentración de tetragonal y monoclinica (Piconi *et al.*, 1999).

Además, en 1975, Garvie encontró tres similitudes entre PSZ y acero que les permitieron hacer el paralelismo entre ambos materiales y llamo al PSZ "acero cerámico" (Garvie *et al.*, 1975). Ambos materiales tienen propiedades similares en relación con el módulo de elasticidad y el coeficiente de expansión térmica (Kelly *et al.*, 2008).

El PSZ se puede conseguir en el sistema ZrO<sub>2</sub>- Y<sub>2</sub>O<sub>3</sub> conseguir, así mismo, producir porcelana, que a temperatura ambiente, sólo se presenta en fase tetragonal llamada TZP (policristal de circonio tetragonal). El TZP contiene aproximadamente 2-3% de Y<sub>2</sub>O<sub>3</sub> y están completamente constituida por granos de circonio tetragonal nanométricos. La fracción presente tetragonal, a temperatura ambiente, depende del tamaño del grano, del contenido de ytrio, entre otros, y de estos factores dependerán sus propiedades mecánicas (Lange, 1982).

Por otro lado se encuentra el óxido de circonio parcialmente estabilizado con itrio o Y-PSZ que presenta excepcionales propiedades fundamentales de gran interés para aparatos biomédicos, tales como alta resistencia, dureza, tenacidad a la fractura, resistencia al desgaste, baja conductividad térmica, buen comportamiento de fricción y no magnético, módulo de elasticidad similar al acero, resistencia a la corrosión a los ácidos y álcalis y coeficiente de expansión térmica similar hierro lo (Vagkopoulou *et al.*, 2009).

En Odontología, el circonio tiene numerosas aplicaciones clínicas entre las que se incluye la fabricación de carillas, coronas parciales y dentaduras completas (PC) y parciales fijas (PPF), implantes y pilares de implantes.

Además, encontramos circonio como componente auxiliar en fresas de corte y brocas quirúrgicas, aditamientos extracoronales, y los *brackets* de ortodoncia (Koutayas *et al.*, 2009).

## **LA ADHESIÓN DE LAS CERÁMICAS DENTALES.**

La adhesión se define como el fenómeno en el que dos superficies se mantienen unidas por fuerzas físicas o químicas, o ambas, a menudo con la ayuda de un adhesivo (International *et al.*, 1993.). La adhesión implica un contacto entre adhesivo y adherente por interacciones físicas y químicas.

En cuanto a la adhesión de aditamientos prostodónticos se refiere, una fuerte adhesión proporciona una alta retención, mejora la adaptación marginal y previene la infiltración (Blatz *et al.*, 2003). Este tipo de unión se basa en interconexiones micromecánicas y en una adhesión química del adhesivo a la superficie de la cerámica, que requiere la creación de rugosidades.

Con respecto a la adhesión de las cerámicas, hay que hacer una diferenciación en relación al tipo de cerámica que se quiere adherir:

1. La adhesión de las cerámicas de vidrios que contienen sílice es un proceso predecible con resultados duraderos cuando se procede a utilizar el grabado con ácido fluorhídrico (HF) consiguiendo una superficie favorable para la unión de la cerámica de vidrio (Sorensen *et al.*, 1991; Blatz *et al.*, 2003). Este tratamiento ácido también aumenta la densidad de grupos hidroxilo (-OH) en la superficie, que las potencia las conexiones entre las superficies con sílice y los silanos (Matinlinna *et al.*, 2007).
2. En relación a las cerámicas de alúmina y de circonio, su composición y propiedades mecánicas que difieren sustancialmente de las de la cerámica clásica, hacen que el grabado ácido con HF sea inútil, por lo que requiere la

aplicación de nuevas técnicas para conseguir una adhesión fuerte y duradera (Kern *et al.*, 1998). La adhesión química tradicional no es eficaz en la superficie de óxido de circonio, una vez que es no polar e inerte.

## **LA ADHESIÓN DEL CIRCONIO: TRATAMIENTOS DE SUPERFICIE.**

La adhesión química tradicional no es eficaz en la superficie de óxido de circonio (Kern *et al.*, 1998; Blatz *et al.*, 2004). Por ello, para conseguir una buena adhesión de las cerámicas dentales, y en concreto del circonio, a los cementos de resina, es imprescindible que la superficie esté limpia, seca y acondicionada a través de una serie de tratamientos de superficie (Monaco *et al.*, 2011; Casucci *et al.*, 2012) destinados a incrementar la energía de superficie del sustrato para mejorar su afinidad para el agente adhesivo. Con ello se pretende que la energía de superficie del sustrato a ser mayor que las fuerzas de cohesión de las moléculas del agente adhesivo, de manera que la humectabilidad es tan alto como sea posible.

Entre las técnicas que se emplean para el acondicionamiento de superficie se encuentran las siguientes:

### **1. Arenado:**

Este procedimiento se utiliza para convertir en rugosa la superficie de óxido de circonio (Mosharraf *et al.*, 2001; Gomes *et al.*, 2012). En los laboratorios dentales, el procedimiento habitual es la utilización de partículas de alúmina ( $\text{Al}_2\text{O}_3$ ) contenidas en el aire con un tamaño medio de 50 micrómetros a una presión de 380 kPa durante aproximadamente 10-15 segundos a una

distancia perpendicular de 10 mm desde el soporte (Blatz *et al.*, 2003). Algunas partículas de alúmina pueden quedar incrustadas en la superficie durante el arenado formándose así un revestimiento.

## **2. Revestimiento con sílice triboquímico:**

El principio básico de este procedimiento son los cambios químicos y fisicoquímicos de la materia durante la aplicación de energía mecánica (Fischer, 1988).

El resultado del impacto de las partículas es la transferencia de energía cinética. La energía absorbida por la superficie del sustrato provocar su fusión microscópica, y momentáneamente la temperatura de la superficie se incrementa a 1200 ° C. Las partículas de sílice revestidas por alúmina penetran en la superficie y se incrustan dejando la superficie parcialmente recubierto de sílice (Spohr *et al.*, 2008). Esta superficie puede ser posteriormente impregnada por un silano. El revestimiento de sílice triboquímico se consigue utilizando tanto el Rocatec™ Soft con  $\text{Al}_2\text{O}_3$ - $\text{SiO}_2$  partículas de 30 micras; como el Rocatec™ Plus con  $\text{Al}_2\text{O}_3$ - $\text{SiO}_2$  partículas de 110 micras, con una presión de 280 kPa para 13 s/cm<sup>2</sup> en un perpendicular distancia de 10 mm (Lung *et al.*, 2010).

## **3. Grabado ácido con ácido fluorhídrico:**

Otro de los métodos de acondicionamiento de la superficie es el grabado ácido de la misma con ácido fluorhídrico. Existen distintas concentraciones del ácido, que pueden ser al 5%, al 9,5% y al 9,6%. Generalmente, la concentración que se emplean es la de grabado ácido con fluorhídrico al 9,6% durante dos minutos ya que se ha comprobado que es la más eficaz (Ural *et al.*, 2010).

Tras ello, se aplica agua y aire a presión sobre la superficie durante 30 segundos y se deja secar (Usumez *et al.*, 2013). Tras el grabado ácido, se puede aplicar o no silano, dejándolo actuar 30 minutos hasta que se seca la superficie.

#### **4. Irradiación con láser:**

Otro de los métodos de tratamiento de la superficie de circonio es la irradiación con el láser Nd: YAG o el láser Er: YAG o el láser de CO<sub>2</sub> (Cavalcanti *et al.*, 2009; Akin y cols., 2011, Paranhos *et al.*, 2011), y la posterior aplicación de silano. Se ha demostrado que la fuerza adhesiva del circonio tratado con láser es superior cuando se compara con la que se obtiene con el chorro de arena (Spohr *et al.*, 2008). Sin embargo las fuerzas medidas varían considerablemente dependiendo del tipo de láser utilizado (Akyl *et al.*, 2010).

Actualmente, la investigación está empezando a centrarse en el uso de la irradiación con un láser de femtosegundo como tratamiento de superficie para llevar a cabo el acondicionamiento de la superficie del circonio (Akpinar *et al.*, 2015) habiéndose obtenido resultados alentadores en la mejora de la eficacia adhesiva.

## **EL LASER DE FEMTOSEGUNDOS COMO MÉTODO DE ACONDICIONAMIENTO DE LA SUPERFICIE.**

En Odontología, la utilización del láser ha tenido una constante evolución y desarrollo; cada vez son más las especialidades odontológicas en las que se aplican las diferentes variedades de láser ya sea en procesos diagnósticos o terapéuticos (Oltragrimon *et al.*, 2004).

La aplicación del láser en Odontología debe basarse en el conocimiento de una serie de procesos físicos y biológicos que dependen de diversos factores, y en concreto, los fenómenos de absorción dependen básicamente de dos factores: la longitud de onda del láser y las características ópticas del tejido que debe ser irradiado (España-Tost *et al.*, 2004).

La cavidad bucal contiene tejidos muy distintos entre sí; por tanto las características ópticas de los tejidos que la conforman no van a tener el mismo comportamiento cuando sean irradiadas con la misma longitud de onda. Es decir, podríamos necesitar una longitud de onda diferente para cada uno de los tejidos que hay en la cavidad bucal. Cuando con el mismo láser irradiamos dos tejidos diferentes, los efectos que se producen también serán diferentes. Cada láser solo va a emitir en una única longitud de onda y que por lo tanto podremos obtener diferentes efectos sobre los tejidos tratados (España-Tost *et al.*, 2004).

En cuanto a la utilización del láser en la práctica dental, algunas de sus principales indicaciones, tanto en la terapeútica dental como en la odontología estética, prostodoncia, cirugía, y ortodoncia son, entre otras:

1. Preparación de cavidades.
2. Eliminación de obturaciones antiguas.
3. Sellado de fosas y fisuras.
4. Hiperestesia dentinaria.
5. Endodoncia.
6. Carillas y obturaciones del sector anterior.
7. Blanqueamiento dental.
8. Tallado dental.
9. Lesiones en tejidos blandos.
10. Lesiones premalignas.
11. Acondicionamiento de las superficies dentales y cerámicas para aumentar la eficacia adhesiva.

El femtoláser o láser de femtosegundos es un láser perteneciente al grupo de los láseres de pulso ultracorto, los cuales son un pulso de luz láser con una duración extremadamente corta, en concreto, de menos de cientos de picosegundos.

El espectacular avance de los conocimientos sobre los procesos no lineales en materiales, junto al de la optoelectrónica, ha permitido disponer muy recientemente de fuentes de radiación láser que son capaces de emitir pulsos de muy corta duración y suficiente energía que, convenientemente focalizados, dan lugar a densidades de energía capaces de producir la ablación directa de materiales sólidos tanto metálicos como dieléctricos. El mecanismo consiste básicamente en la ionización por procesos no lineales de los átomos o moléculas de la superficie del material irradiado, formándose un plasma denso que se expande al término del pulso, típicamente de duración en torno

a los 100 fs, sin tiempo para que se produzca difusión del calor en la estructura sólida, que requiere tiempos del orden de las decenas de ps, dando lugar a la eliminación del material sin apenas calentamiento. Esto convierte a los láseres ultracortos e intensos en una herramienta muy prometedora a la hora de producir mecanizado de gran precisión y calidad con dimensiones típicas de micras.

Las ventajas se pueden resumir en: primero, el mínimo daño térmico y mecánico que se produce en el material adyacente a la zona de procesado, no observándose restos de material fundido y resolidificado, ni grietas o fisuras; segundo, la aplicabilidad universal del proceso, ya que se puede emplear para cualquier tipo de material y no se necesitan entornos de trabajo con condiciones específicas; y tercero, la posibilidad de depositar sobre el material las cantidades deseadas de energía con gran rapidez y precisión, lo que se traduce en una enorme precisión dimensional y calidad geométrica del mecanizado, una elevada reproducibilidad y la ausencia de postprocesado.

El mayor inconveniente de esta tecnología radica en la baja velocidad de proceso, requisito primordial en cualquier aplicación industrial, lo que, de momento, impide la competencia con otros procesos de menor precisión y calidad, como el mecanizado con láseres de pulsos algunos órdenes de magnitud más largos. Asimismo, al no ser una tecnología madura, el coste de inversión en equipos es todavía exageradamente alto en relación a procedimientos ya existentes. Hoy en día asistimos al debate del futuro industrial de esta tecnología, aunque parece claro que ya se empiezan a encontrar aplicaciones concretas en entornos industriales relacionados con las microtecnologías y nanotecnologías.

Dentro de los láseres de femtosegundos o femtoláser, nos encontramos con el láser de Titanio-Zafiro. El primer láser de Ti-Zafiro fue construido en 1982 por Peter Moulton (Moulton, 1982); y a lo largo de los años se han ido perfeccionando, desarrollando láser de pulsos ultracortos de alta intensidad que producen pulsos extremadamente cortos, por debajo del picosegundo.

El láser de Titanio-Zafiro, perteneciente al grupo de los femtoláser, es un material láser muy eficiente. Su longitud de onda se encuentra en el rango de 670 a 1070 nm, con el pico centrado en los 800nm. Su medio activo es el zafiro. La cantidad de iones del Titánio dentro del material huésped que es el Zafiro, es de alrededor del 0,1% y estos están reemplazando a átomos de Aluminio en el cristal, ya que posee una estructura cristalina hexagonal. Su punto de fusión es de 2050 °C y tiene una densidad de 3,98g/cm<sup>3</sup>, y una dureza de 9 en la escala de Mohs. El rango de absorción se encuentra entre 400 y 600nm con el pico máximo en los 488-490 nm. Por otro lado, el rango de emisión se encuentra entre 600 y 1050 nm con un pico máximo situado en los 795 nm. El espectro de fluorescencia va desde los 600 a 1050 nm. La potencia de bombeo del láser de titanio-zafiro es de 3 a 10W y está disponible en modo continuo y pulsado. La potencia típica de salida a 800 nm es de 150 a 1000 mW. Longitud de pulso en picosegundos ( $10^{-12}$ seg) y femtosegundos ( $10^{-15}$ seg).

Los pulsos de láser ultracortos se han popularizado principalmente para aplicaciones médicas, fundamentalmente, con su introducción en el campo de la Oftalmología (femto-LASIK) en 2003 (Heisterkamp *et al*, 2003; Ratkay-Traub *et al.*, 2003). Sin embargo, la ablación ultrarrápida se ha utilizado ampliamente en biología (Tsai *et al.*, 2004), que comprende el corte de orgánulos subcelulares en las células

cultivadas (Konig y Tirlapur, 2002, Watanabe *et al.*, 2004; Hoy *et al.*, 2008) y procesos axonales de regeneración en los organismos multicelulares (Yanik *et al.*, 2004; Bourgeois y Ben-Yakar, 2008; Gabel *et al.*, 2008; Guo *et al.*, 2008), la ablación de hueso, dentina y el esmalte (Neev *et al.*, 1996 ; Perry *et al.*, 1999; Niemz, 2004; Nicolodelli *et al.*, 2011; Braun *et al.*, 2013 ;. Luengo *et al.*, 2013, Rego Filho *et al.*, 2013; Portillo *et al.*, 2015; Luengo *et al.*, 2015), la córnea (Stern *et al.*, 1989; Kautek *et al.*, 1994; Juhasz *et al.*, 1999; Lubatschowski *et al.*, 2000; Maatz *et al.*, 2000; Odhner y Levis , 2014; Plötz *et al.*, 2014) epitelios (Frederickson *et al.*, 1993), y los tejidos neurales (Oraevsky *et al.*, 1996; Suhm *et al.*, 1996; Loesel et al., 1998; Tsai *et al.* , 2003; Doronina *et al.*, 2009) Vascular (Nishimura *et al.*, 2006; Choi *et al.*, 2011).

En los últimos años, láser de femtosegundo ha comenzado a ser utilizados en odontología para la ablación de diferentes tejidos dentales y cerámicas como el circonio para aumentar la eficacia adhesiva, entre otros objetivos,dando prometedores resultados.

## **SIMULACIÓN DE LAS CONDICIONES ORALES: EL CICLADO MECÁNICO.**

El ambiente oral es muy complicado tanto química como mecánicamente y causa alteraciones físico-químicas en los materiales de restauración dental como la cerámicas de circonio. La evaluación de la tenacidad a la fractura y la predicción de la duración bajo situaciones clínicas han asumido posiciones importantes en Odontología (Drummond *et al.*, 2003).

En cuanto a la complejidad mecánica del medio oral, en la mayoría de los casos el estrés aplicado al circonio es generalmente bajo y repetido (fatiga) en lugar de ser un impacto único. La carga oclusal normal se estima entre 5 y 20 MPa (Braem *et al.*, 1994), aunque ocasionalmente se puede apreciar un pico de estrés más alto que se produce durante el movimiento parafuncional y el estrés puede aumentar a 100 Mpa en esa zona e incluso hasta más alto (Abe *et al.*, 2005).

Los fallos por fatiga pueden provenir de defectos inherentes existentes en un material que se aglutan y permiten la fractura a través de una reducción de la capacidad de soporte de la carga. Por otra parte, las fallos por fatiga pueden provenir de un defecto bien definido (o crack) que sufre de extensión hasta alcanzar una longitud crítica. La sobrecarga también puede promover defectos y/o grietas existentes bajo extensión a través de un proceso considerado como el crecimiento de grietas por fatiga, y puede producirse bajo las fuerzas de la masticación, y así de ese modo facilitar la fractura (Aroa *et al.*, 1999).

Para imitar el estrés mecánico en vivo en las restauraciones de circonio, es posible utilizar en un simulador de masticación y medir la eficacia de unión en la interfase entre

la superficie de circonio y los cementos de resina después (Nikaido *et al.*, 2002; Frankenberger *et al.*, 2003). De este modo, para simular las fuerzas masticatorias oclusales *in vitro*, se utiliza el ciclado mecánico (Koyama *et al.*, 2012) que es la aplicación repetida o fluctuante de tensiones o intensidades en los componentes estructurales y así replicar las condiciones clínicas a las que las restauraciones de circonio son sometidos a debido a las fuerzas de la masticación (Attia y Kern, 2004). La técnica se basa en un simulador masticatorio controlado por ordenador que produce una degradación mecánica de la interfase circonio-resina (Mirmohammadi *et al.*, 2010) a través de la aplicación continua de impacto en dicha interfase.

Bajo el ciclado mecánico, las prótesis dentales de circonio están sujetas a la fractura durante su función, especialmente en el área posterior, y los pilares de implantes de circonio presentan una resistencia a la fractura significativamente menor (Foong *et al.*, 2013), con una reducción significativa de la precarga (Butignon *et al.*, 2013), entre otros efectos.

## Objetivos y justificación

En la actualidad, el número de adultos que demandan tratamientos de ortodoncia ha aumentado y algunos de estos pacientes suele llevar algún tipo de restauración de cerámica en la boca. Esto ha provocado que los ortodoncistas estén expuestos a problemas como el tener que adherir aditamentos de ortodoncia en dientes restaurados con cerámicas dentales como el circonio. Por esta razón, es necesario establecer un protocolo de adhesión, por un lado, en ortodoncia para lograr la efectividad adhesiva adecuada para evitar la desunión de los *brackets* en la superficie de circonio para obtener un mayor nivel de adhesión para minimizar el riesgo de fracaso durante el tratamiento; y, por el otro lado, en la odontología restauradora, para llegar a cementar restauraciones de circonio en diferentes sustratos biológicos, tales como el esmalte o la dentina.

Las cerámicas de circonio son materiales esenciales en la restauración dental, y se han utilizado para la rehabilitación oral durante décadas. El problema que presentan estas cerámicas es que la adhesión química tradicional es ineficaz y se necesitan tratamientos de superficie para mejorar la unión adhesiva entre el cemento de resina y el circonio. Sin embargo, todavía no existe ningún método de acondicionamiento de la superficie de circonio ideal capaz de proporcionar una eficacia suficiente de adherencia en las superficies de circonio en la odontología restauradora, así como en ortodoncia para cementar *brackets* y tubos, siendo necesario buscar nuevas alternativas que nos garantizan una unión fuerte y duradera. Por todo ello, la investigación se está empezando a centrar en el uso del láser de femtosegundo en odontología como

tratamientos de superficie para llevar a cabo el acondicionamiento de superficies biológicas y no biológicas habiéndose obtenido resultados alentadores en el sentido de mejorar la eficacia adhesiva.

También es necesario tener en cuenta que todas las restauraciones de circonio son sometidas a fuerzas cíclicas que van desde 60 N a 250 N durante la función masticatoria, e incluso pueden alcanzar valores de 800 N. Por consiguiente, es crucial investigar los valores de resistencia adhesiva bajo condiciones dinámicas utilizando la carga cíclica con el fin de obtener resultados más clínicos y por lo tanto hacer progresos en los intentos para validar la irradiación con láser de femtosegundo como un método ideal como acondicionamiento de la superficie.

Los objetivos específicos de este estudio fueron:

- 1) investigar el efecto de diferentes métodos de acondicionamiento de la superficie del circonio (la abrasión con partículas de alúmina de 25- $\mu\text{m}$ , el revestimiento con sílice triboquímico, y la irradiación con el láser de femtosegundos) a fin de evaluar la eficacia adhesiva de la interfase circonio-resina.
- 2) evaluar si la irradiación con láser de femtosegundos influye en la resistencia a la fuerza de la cizalla de la interfase de circonio con el cemento de resina y determinar cuáles son los mejores parámetros de irradiación para proporcionar una adhesión adecuada.
- 3) evaluar cómo afecta el ciclado mecánico en la eficacia adhesiva de la interfase circonio-resina.

## Material y métodos

Ciento cincuenta muestras, de forma cuadrada, de circonio (que medían 6x6x1mm) se dividieron en cinco grupos de acuerdo a su tratamiento de superficie: Grupo 1- no tratamiento (NT): ningún método de acondicionamiento de superficies; Grupo 2- abrasión con partículas de alúmina de 25 micras (APA 25): arenado con partículas de  $\text{Al}_2\text{O}_3$ ; Grupo 3- recubrimiento de sílice triboquímico (TSC): recubrimiento de sílice seguido por silanización; Grupo 4- láser de femtosegundo a *step 20* (FS20): irradiación láser de femtosegundo (800 nm, 4 mJ, 40 fs / pulso, 1 kHz, *step 20*), y el Grupo 5- láser de femtosegundo a *step 40* (FS40): irradiación láser de femtosegundo (misma los parámetros excepto *step 40*).

Después de realizar los diferentes tratamientos de superficie sobre las muestras de óxido de circonio, se adhirió un cemento de resina autoadhesivo (Clearfil <sup>TM</sup> SA Cemento, Kuraray, Osaka, Japón) a la de la superficie de circonio utilizando un molde de silicona cilíndrico con un diámetro interno de 3 mm, 1 mm de espesor y de 1 mm de altura situado en el centro de las muestras. Se colocó el cemento en estos moldes contra la superficie de circonio y se polimerizó durante 40 segundos (XL 3000, 3M / ESPE; intensidad de la luz 500 mW / cm<sup>2</sup>, la distancia 0) desde arriba y hacia el área de contacto desde una posición lateral.

Todos los grupos experimentales se dividieron en dos subgrupos en función de si se aplicó o no el ciclado mecánico. Por lo tanto, la mitad de los especímenes de cada grupo ( $n=15$ ) fueron montadas en moldes de resina acrílica para realizar el ciclado mecánico bajo 90 N (50.000 ciclos, 3 ciclos/segundo) con la fuerza aplicada

perpendicularmente a la superficie opuesta donde se unió la resina. El resto de las muestras ( $n=15$ ) se almacenaron en agua destilada a 37 ° C.

Todos los subgrupos se ensayaron para el test de SBS con una máquina de ensayo universal (AGS-X autógrafo, Shimadzu Corporation, Kyoto, Japón). Se aplicó una carga de cizallamiento con una velocidad de cruceta de 0,5 mm / min, hasta la fractura de la interfase del circonio con el cemento de resina.

Después de la prueba de SBS, cada muestra fracturada se examinó bajo un microscopio de luz M1 Axio (Carl Zeiss, Alemania) a 40 aumentos para determinar los modos de fractura y varias muestras fracturadas representativas fueron examinadas con el microscopio electrónico de barrido (Zeiss EVO MA25; Carl Zeiss, Jena, Alemania) con el fin de analizar la morfología de las interfaces desligada. Cinco superficies de circonio de cada subgrupo experimental ( $n =5$ ) se prepararon para el análisis de morfología de la superficie con el microscopio electrónico.

Los datos fueron analizados con SPSS v21. ANOVA, t de Student, pruebas de chi cuadrado y regresiones lineales se realizaron ( $p <0,05$ ) para comparar los valores del SBS entre los subgrupos para analizar las diferencias existentes de los diversos tratamientos de superficie del circonio.

## Resultados

Los resultados obtenidos indicaron que los valores de SBS varían de acuerdo con el método de tratamiento de superficie aplicado en todos los grupos tanto en las muestras sometidas a carga cíclica, como en las que no.

Cuando no se aplicó el ciclado mecánico, el subgrupo APA25 obtuvo valores SBS más altos que el subgrupo control, pero significativamente más bajos que los valores obtenidos en los subgrupos FS20, FS40 y TSC que fueron similares entre sí.

Si se aplica el ciclado mecánico, los cuatro tratamientos de superficie muestran los mismos valores de SBS que son más altos que los del subgrupo control.

Si no se aplica el ciclado mecánico, el subgrupo APA25 obtiene valores SBS más altos que el subgrupo control, pero significativamente más bajos que los valores obtenidos en los subgrupos FS20, FS40 y TSC que fueron similares entre ellos.

En cuanto al tipo de fallo más común, observamos que en el grupo control la mayoría eran adhesivos, mientras que en los grupos de tratamiento eran en su mayoría mixtos, es decir adhesivos y cohesivos simultáneamente. En ningún caso, encontramos fallos cohesivos únicamente.

## Conclusiones

Los resultados de nuestra investigación nos permiten concluir lo siguiente:

- 1) La irradiación con el láser de femtosegundo y el revestimiento con sílice triboquímico crean una rugosidad en la superficie consistente y profunda, mejorando la eficacia adhesiva de la interfase del circonio con el cemento de resina. Esto es debido a que la adhesión de la interfase se ve influenciada por la retención micromecánica, y esta última se basa más en la profundidad de grabado creado por el método de acondicionamiento que en el patrón de grabado convirtiéndose en un requisito fundamental para el establecimiento de una unión fuerte y duradera.
- 2) El tratamiento con láser de femtosegundo, tanto a *step* 20 como a 40, puede ser un método de acondicionamiento de superficie eficaz para lograr la adhesión adecuada entre el circonio y los cementos de resina debido a que crea un patrón de surcos profundos en la superficie de circonio que son llenados por el cemento de resina. La diferencia entre los diferentes *step* es que el tiempo de irradiación en el *step* 40 es la mitad, y el tiempo es un factor clínico muy importante para ser tomado en consideración. El método de acondicionamiento de superficies debe producir un patrón de grabado con el fin de asegurar una unión estable y duradera, pero también debe ser llevado a cabo lo más rápido posible. En este sentido, ya que la irradiación con láser de femtosegundo en el *step* 40 produce menos ranuras y que están más ampliamente espaciadas, el tiempo de irradiación se reduce sustancialmente (de hecho, a la mitad). En consecuencia, lo mejor es utilizar láser de femtosegundo a *step* 40 ya que se prefiere la eficiencia, a fines prácticos, más que la eficacia, para así lograr los mejores resultados

en el menor tiempo posible.

3) Cuando se aplica el ciclado mecánico, la eficacia adhesiva de la interfase circonio-resina disminuye en cualquiera de los tratamientos de superficie realizados excepto en la abrasión con partículas de alúmina, que no se ve afectada por el ciclado.



# *Viii.3 APPENDIX 3. THEMATIC INDEX.*

## A

**Ablation** 79,80,81,83,84,87,90,91,93,94,95,119,138.

**Adhesion** 23,24,27,60,61,62,63,64,66,67,69,70,72,100,111,125,136,138,139,140,141,145.

**Adhesion protocol** 23,24,111,136.

**Adhesive effectiveness** 23,24,27,68,77,91,111,112,139,145.

**Adhesive failure** 107,128,129,130,142.

**Airborne particle abrasion** 24,25,67,70,73,112,118.

**Alumina particles** 24,25,44,60,64,66,69,112,116,118,129,137,141.

## B

**Bond strength** 24,25,66,68,69,70,71,72,73,91,92,93,98,99,104,105,106,107,108,111,112,137,138,139,140,141,142.

**Bonding** 23,24,27,38,60,61,62,63,64,65,66,69,70,74,92,93,98,99,100,101,106,111,112,119,123,136,137,139,140,141,145.

**Brackets** 23,24,30,31,59,92,111,136.

## C

**Ceramics** 23,38,39,40,41,42,43,44,45,46,47,48,49,50,52,53,55,60,61,62,66,68,70,73,91,96,97,104,105,111,136,137,140.

**Chemical adhesion** 23,60,70.

**Cohesive failure** 107,123,128,129,130,142.

**Conditioning methods** 23,25,117,124,137,138,140,141,142.

**Cyclic loading** 24,25,26,27,97,100,101,102,103,104,112,117,120,121,128,129,130,132,133,139,141,142,145.

## D

**Dentin** 23,24,62,76,91,92,93,94,95,111,136,138.

## E

*Enamel* 23,24,62,91,92,93,94,95,111,136,137,138.

*Energy* 55,61,64,66,69,77,78,79,80,81,82,83,84,87,88,89,90,95,116,119.

*Er:YAG laser* 68,69,72,74,92.

## F

*Failure modes* 26,123,128,141.

*Femtosecond laser* 24,25,27,68,75,80,85,88,90,91,92,93,94,95,111,112,118,119,137,138,139,145.

*Fracture resistance* 40,46,101,102,104,141.

## G

*Groups* 25,26,51,61,68,69,70,71,72,73,74,77,92,93,94,102,103,104,117,118,120,122,124,127,128,129,132,133,136,137,138,139,140,142.

## I

*Intensity* 25,81,82,83,89,107,116,120.

*Interface* 23,24,25,26,27,69,72,74,92,98,99,100,101,105,106,112,124,136,138,141,142,145.

*Irradiation* 24,25,27,68,69,71,74,75,91,92,94,112,118,119,137,138,139,145.

*Irregularities* 60,62,137,139,140.

## L

*Laser irradiation* 24,25,27,68,69,71,74,75,91,92,112,118,119,137,138,139,145.

## M

*Masticatory forces* 100,101,105,140,141.

*Materials* 27,38,41,42,45,47,50,51,52,53,55,56,62,80,81,82,87,91,96,97,98,100,104,106,111,116,117,145.

**Mechanical adhesion** 60,70.

**Micro-retentions** 129.

**Microscope** 26,67,117,123,124.

**Mixed failure** 128,129,130,142.

**Morphology analysis** 26,123

## N

**Nd:YAG laser** 68,71,72,73,74

## O

**Orthodontic attachments** 23,24,111,136.

**Orthodontics** 23,24,76,111,136.

## P

**Porcelain** 38,39,40,41,44,45,46,47,50,51,52,56,102.

**Pulses** 78,79,80,81,82,83,87,88,89,90,92,93,94,95,118,119.

## R

**Resin cement** 23,24,25,27,62,63,64,65,66,67,69,70,71,72,73,74,91,104,105,111,112,119,120,129,130,134,137,138,139,141,142,145.

**Roughness** 27,60,67,68,69,70,71,73,94,95,103,137,139,140,142,145.

## S

**Samples** 25,26,71,90,92,93,94,104,115,117,119,120,121,123,124,128,140,141,142.

**Scanning electron microscope** 26,117,123,124.

**Self-adhesive resin cement** 23,25,70,71,72,73,119,136.

**Shear bond strength** 25,70,72,73,92,93,104,122,127.

**Specimens** 25,68,70,71,72,74,89,93,100,102,104,105,106,115,116,119,120,121,127,128.

**Subgroups** 25,26,71,72,73,92,103,120,122,124,127,128,129,139.

**Substrates** 23,24,111,112,136.

**Surface** 23,24,25,26,27,57,60,61,62,63,64,64,66,67,68,69,70,71,72,73,74,75,77,78,81,82,83,84,85,89,90,91,92,93,94,95,96,101,103,104,107,111,112,115,117,118,119,120,122,123,124,127,128,129,130,131,132,133,136,137,138,139,140,141,142,145.

## T

**Ti:Sapphire laser** 85,86,92,93

**Tribochemical silica coating** 25,27,67,118,139,145.

## U

**Ultrashort laser** 81,90,92,93.

## V

**Velocity** 90,116,119

## W

**Wavelength** 75,76,77,78,79,81,82,86,89,93,97.

## Y

**Y-TZP** 58,59,63,69,70,71,73,74,91,98,103,115,116,140.

## Z

**Zirconia** 23,24,25,26,27,41,44,47,52,53,54,55,56,59,62,63,64,65,66,67,68,69,70,71,72,73,74,91,95,96,97,98,101,102,103,104,105,111,112,115,117,118,119,120,123,124,127,129,130,131,132,133,136,137,138,139,140,141,142,145.